UNIVERSITÉ DE MONTRÉAL

A DYNAMIC METABOLOMIC STUDY OF LIPID PRODUCTION IN CHLORELLA PROTOTHECOIDES

XIAOJIE REN

DÉPARTEMENT DE GÉNIE CHIMIQUE

ÉCOLE POLYTECHNIQUE DE MONTRÉAL

THÈSE PRÉSENTÉE EN VUE DE L'OBTENTION

DU DIPLÔME DE PHILOSOPHIAE DOCTOR

(GÉNIE CHIMIQUE)

MAI 2017

UNIVERSITÉ DE MONTRÉAL

ÉCOLE POLYTECHNIQUE DE MONTRÉAL

Cette thèse intitulée :

A DYNAMIC METABOLOMIC STUDY OF LIPID PRODUCTION IN CHLORELLA PROTOTHECOIDES

présentée par : REN Xiaojie

en vue de l'obtention du diplôme de : Philosophiae Doctor

a été dûment acceptée par le jury d'examen constitué de :

Mme BOFFITO Daria C., Ph. D., présidente

M. JOLICOEUR Mario, Ph. D., membre et directeur de recherche

M. DESCHÊNES Jean-Sébastien, Ph. D., membre et codirecteur de recherche

M. TREMBLAY Réjean, Ph. D., membre et codirecteur de recherche

M. HARVEY Jean-Philippe, Ph. D., membre

M. REHMANN Lars, Ph. D., membre

DEDICATION

To my family whom I love most.

ACKNOWLEDGEMENTS

At the end of my Ph.D reseach, I'd like first to thank you for my Professor Mario Jolicoeur, Jean-Sébastien Deschênes, and Réjean Tremblay to give me the valuable chance to do research in the world top University and such excellent lab. I am also grateful to the "Ressources Aquatiques Québec (RAQ)", the "Fonds de recherche du Québec – Nature et technologies (FQRNT)" and National Science and Engineering Council of Canada for the financial support to this project.

During the research life here, there are so many significant people I want to thank, especially my dear supervisor Mario Jolicoeur. During my research process, you have always been patient to guide my work, gave me thoughtful advices, with continuous encouragement and various support. Your affirmation, praise and encouragement helped me find the courage to overcome difficulties. Meanwhile, I am also very grateful for your help in my academic publications, from writing to modifying, each of my articles filled with your great effort. You are my supervisor, but also like a father, you can feel every little thing in both my research and life, and give me meticulous care and help. From you, I learned patience, persistence, being principle and positive, which I may not have deep experience from my previous research life. These excellent characters will affect my whole life. You took me overcome obstacles one after another, and helped my self-confidence grow constantly strong, so the research process is not only the process of creating knowledge, but also the growth process of my personal character. Indeed, you are really a great professor, it's a wealth to meet you in my life.

At the same time I would also like to thank my co-supervisors, thank you for your guidance to carry out my project. Thank you to provide experimental platform for my training; to provide a variety of literature and books concerned about my research, thank you for the valuable advice and help in each of my research project as well as in my essay writing. It's your support and encouragement make my subject progress so smoothly.

I would also like to thank Jinkui Chen, thank you for your great help in my analysis work, from recognizing the new research objective/material to the development of new analysis method, none of these could separable from your help and experienced guidance. Thank you for your great contribution for all of the precise analysis. I would also thank François Turcotte from the "Université du Québec à Rimouski (UQAR)" for his help and contribution on the analysis of fatty acids. Thank you Julien, Benoit, thank you for your great help in the modeling process. My success is relevant to all your help and support.

Specially, I would like to thank my family, especially my husband, with the deepest love. I am so lucky to have you. You are my lover and my comrades as college. You helped me with your most selfless love with no reservations. You accompanied with me the entire research journey, and gave me valuable advice and endless help in each of my research project. Doing things with you make me understand that we must keep a flexible attitude to research and an optimistic attitude to life, so that both of them could be beautiful. You are always thriving in front of me to clear obstacles, and like a powerful engine, dragging me across variety of muddy and swamp! Meanwhile, I would also like to thank my dearest daughter, your bright smile make the life full of sunshine. At the same time, I want to thank my mother in law, who took care of my life during my pregnancy. I am also grateful for my dearest mothers' help in the past one year to take care of Mindy and release me to concentrate on my research. And my dear daddy, thank you for the courage you give me. And my sister and brother, thank you for taking care of daddy for me in China, with your support, I go higher and look further.

Finally warmly thank all my colleagues in the lab, especially Eric Karengera, Chi-yuan Chang, Prajwal Kumar, Zhihui Yi, Irina Valitova and Edwige Arnold.

RÉSUMÉ

De nombreuses espèces d'algues se sont révélées se développer rapidement et produire des quantités substantielles de lipides. Ainsi, identifiées comme des algues oléagineuses, on a longtemps proposé que les algues pourraient être utilisées comme une usine cellulaire de production de lipides pour l'industrie des biodiesels. Cependant, la faible production de lipides, due à un métabolisme des lipides fortement interconnecté, ainsi qu'un rendement relativement faible des procédés d'extraction ont représenté des obstacles majeurs à l'industrialisation des technologies de production de lipides d'algues. Algues d'eau douce *Chlorella protothecoides* était l'espèce la plus métabolique diverse et robuste trouvée dans les littératures. Il pourrait appliquer trois modes de culture différents, qui sont autotrophes sur le CO_2, l'alimentation mixotrophique sur le CO_2 et le glucose, et l'hétérotrophie avec le glucose uniquement. Dans cette espèce, la teneur en lipides et le rendement en biomasse étaient beaucoup plus élevés en mode de culture hétérotrophique par rapport au mode de culture autotrophique. Bien que les recherches montrent que le glucose pourrait inhiber l'affinité du CO_2 dans le système de fixation du CO_2 et avoir un fort effet inhibiteur sur les enzymes du cycle de Calvin ainsi que sur les protéines de collecte de lumière, l'impact de la régulation du glucose sur le niveau métabolique n'était pas clair. L'objectif principal du travail était d'améliorer le rendement lipidique des algues, en mettant l'accent sur l'ingénierie métabolique basée sur l'étude métabolomique et une modélisation cinétique, ainsi que sur l'exploration de nouvelles approches et de méthodes efficaces d'extraction des lipides, afin d'améliorer la cellule d'algues comme plate-forme d'accumulation de lipides pour la production de biodiesel.

Dans la première partie, nous avons étudié différents modes de culture à base de carbone, tels que autotrophes, mixotrophes et hétérotrophes sous un faible pouvoir azoté. Sous un faible taux d'azote, les lipides pourraient être évidemment accumulés; Pendant ce temps, la différence de métabolisme cellulaire pourrait être clairement observée à cause de l'impact du glucose. L'objectif était de démêler les liens et la régulation entre le métabolisme du carbone des algues et la production de lipides. Dans cet article, nous nous concentrons profondément sur l'étude du métabolisme et de la régulation de la production de lipides dans la plate-forme d'algues et apporte une nouvelle connaissance de la régulation dans le métabolisme des lipides d'algues. Surtout, c'est la première fois que l'on étudie la dynamique de l'énergie dans les algues et que l'on retrouve la capacité de

rotation de l'énergie dans les modes de culture hétérotrophes et mixotrophes pour une forte accumulation de lipides.

La deuxième partie de ce travail a porté sur le développement d'un modèle métabolique cinétique décrivant le métabolisme central du carbone de *Chlorella protothecoides* cultivé dans des conditions hétérotrophes. Le modèle comprend la plupart des principales voies du métabolisme cellulaire. On a montré que les simulations de modèles concordaient avec les données expérimentales, ce qui suggère que la structure de modèle proposée fait face à la biologie des cellules de *Chlorella protothecoides*. Le modèle a permis d'effectuer une analyse dynamique du flux métabolique et nous a permis de démontrer que le rendement lipidique élevé s'accompagne d'un flux lipidique élevé et d'une faible activité TCA. Pendant ce temps, la distribution du flux dynamique suggère également un métabolisme stable et robuste dans *Chlorella protothecoides* avec un rapport relativement constant de la distribution du glucose. Ce modèle est un premier modèle métabolique cinétique dans les plates-formes d'algues et a jeté une base de base pour servir d'outil pour prédire l'ingénierie génétique ainsi que la stratégie de culture de conception pour une production optimisée de lipides en la définissant comme fonction objective.

Dans la troisième et dernière partie, nous avons travaillé à améliorer les protocoles d'extraction des lipides actuels, afin de maximiser le rendement de l'extraction des lipides. Une étape de traitement de l'eau a été ajoutée et adaptée aux protocoles d'extraction actuels, entre les deux extractions de solvant organique. Les résultats ont montré que le traitement de l'eau de la biomasse après la première étape d'extraction du solvant aide à la libération des lipides intracellulaires dans la deuxième étape d'extraction, améliorant ainsi le rendement final d'extraction des lipides. Le nouveau procédé fournit donc un moyen efficace d'améliorer le rendement en extraction des lipides des méthodes existantes, ainsi que de favoriser le TAG, un lipide présentant le plus grand intérêt pour la production de biodiesel.

En résumé, ce travail a permis de décrire le comportement métabolique de la production de lipides chez *Chlorella protothecoides.* La combinaison d'un outil d'ingénierie métabolique en amont et d'une approche optimisée de l'extraction des lipides en aval a clairement contribué à améliorer la faisabilité commerciale du bioprocessage de la production de lipides à base de microalgues.

ABSTRACT

Many algal species have been found to grow rapidly and produce substantial amounts of lipid. These microalgae are identified as oleaginous algae and it has long been proposed that algae could be employed as a cell factory to produce lipids for biodiesel. However, low lipid production level, because of a highly regulated lipid metabolism as well as relatively low lipid extraction yields, have been major barriers to the practical application of algae lipid technologies industrially. Fresh water algae *Chlorella protothecoides* was the most metabolic diverse and robust species found in literatures. It could apply three different culture modes, which are autotrophic on CO_2, mixotrophic feeding on CO_2 and glucose, and heterotrophic with glucose only. In this species, lipid content and biomass yield were much higher under heterotrophic culture mode compared with autotrophic culture mode. Although researches found glucose could inhibit the affinity of CO_2 in the CO_2 fixation system, and have strong inhibitory effect on Calvin cycle enzymes as well as on light gathering proteins, the impact of glucose regulation on metabolic level were not clear. The main objective of this thesis was thus to improve the algae lipid yield, with a special emphasis on a metabolic engineering approach based on a metabolomics study, kinetic modeling as well as on exploring new approaches of efficient lipid extraction methods, in order to improve algae cell as a lipid accumulation platform for biodiesel production.

In the first part, we studied different carbon-based culture modes, such as autotrophic, mixotrophic, and heterotrophic under a low nitrogen medium condition. Under low nitrogen condition, lipid could be obviously accumulated; meanwhile the difference of cell metabolism could be clearly seen from glucose impact. The aim was to unravel the links and regulation between algae carbon metabolism and lipid production. In this article, we deeply focus on the metabolism and regulation study of lipid production in algae platform and it brings novel knowledge of regulation in algae lipid metabolism. Especially it's the first time to investigate the energy dynamic in algae and found energy turn over capacity in heterotrophic and mixotrophic culture modes for high lipid accumulation.

The second part of this work focused on the development of a kinetic metabolic model describing *Chlorella protothecoides* central carbon metabolism grown under heterotrophic condition. The model includes most of the major pathways of the cell metabolism. Model simulations were shown to agree with experimental data, which is suggesting that the proposed model structure copes with

Chlorella protothecoides cells' biology. The model enabled performing a dynamic metabolic flux analysis, and enabled us to demonstrate that high lipid yield is accompanied with high lipid flux and low TCA activity. Meanwhile, the dynamic flux distribution also suggests a robust and stable metabolism in *Chlorella protothecoides* with relatively constant ratio of glucose distribution. This model is a first kinetic metabolic model in algae platforms and laid a basic foundation to serve as a tool in predicting genetic engineering as well as design culture strategy for optimized lipid production by defining it as objective function.

In the third and final part, we worked at improving current lipid extraction protocols, to maximize lipid extraction yield. A water treatment step was added and adapted to current extraction protocols, between the two organic solvent extractions. Results showed water treatment of biomass after the first solvent extraction step helps the release of intracellular lipids in the second extraction step, thus improving the final lipids extraction yield. The novel method thus provides an efficient way to improve lipid extraction yield of existing methods, as well as favoring TAG, a lipid of the highest interest for biodiesel production.

In conclusion, this thesis allowed ameliorating our understanding of the links between cell metabolomic behavior and lipid production in *Chlorella protothecoides*. The combination of an upstream metabolic engineering tool and an optimized downstream lipid extraction approach has clearly contributed to ameliorate the commercial feasibility of lipids production bioprocess based on microalgae.

TABLE OF CONTENTS

LIST OF TABLES

LIST OF FIGURES

LIST OF SYMBOLS AND ABBREVIATIONS

Symbols	Description
3PG	3 - glyceric acid phosphate
A	Autotrophy/autotrophic
AA	Amino acids
AcCOA	Acetyl - coenzyme A
ADP	Adenosine diphosphate
ADPG	Adenosine diphosphate glucose-starch glucosyltransferase
AK	Adenylate kinase
AKG/α- KG	α - Ketoglutarate
AKGDH	Oxoglutarate dehydrogenase
AMPL	Acetone mobile polar lipids
AP	Amylase
ATP	Adenosine triphosphate
CHL	Chlorophyll
Chl/Met	Chloroform/methanol
Chl/Met/H_2O	Chloroform/methanol/H_2O
CIT	Citrate
CK	Creatine kinase
CO_2	Carbon dioxide
CS	Citrate synthase
DHAP	Dihydroxy acetone phosphate
Dic/Met	Dichloromethane/methanol
DCW	Dry cell weight
dFBA	Dynamic flux balance analysis
E4P	Erythrose - 4 - phosphate
EGLC	Extracellular glucose
ER	Endoplasmic reticulum
F6P	Fructose 6 - phosphate
FAMEs	Fatty acid methyl esters
FASN	Fatty acid synthase

FBPase	Fructose biphosphate aldolase
FFA	Free fatty acids
FH	Fumarate hydratase
FUM	Fumarate
G1P	Glucose - 1 - phosphate
G6P	Glucose - 6 - phosphate
G6PDH	Glucose 6 phosphate 1 dehydrogenase
GA3P	Glycerol dehyde - 3 - Phosphate
GAPDH	Glyceraldehyde 3 - phosphate dehydrogenase
GD	Glyceraldehyde 3 - phosphate & Dihydroxyacetone phosphate
GHMT	Glycine hydroxymethyltransferase
GLDH	Glutamate dehydrogenase
GLU	Glutamate
GLY	Glycine
GlyP	Glycerone - phosphate
GPAT	Glycerol - 3 - phosphate acyltransferases
GPI	Glucose 6 phosphate isomerase
growth	Biomass synthesis
H	Heterotrophy/heterotrophic
HC	Hydrocarbons
HK	Hexokinase
ISOD	Isocitrate dehydrogenase
Lipase	Lipase
Lipid	Lipid
M	Mixotrophy/mixotrophic
MAL	Malate
ME	Malic Enzyme
MFA	Metabolic flux analysis
MLD	Malate dehydrogenase
NL	Neutual lipid
PDH	Pyruvate dehydrogenase

PEP	Phosphoenolpyruvate
PFK	6 phosphofructokinase
PGA	3 - phosphoglycerate
PGK	Phosphoglycerate kinase
PGM	Phosphoglucomutase
PK	Pyruvate kinase
PL	Phospholipids
PPP	Pentose phosphate pathway
PPRiBP	Phosphoribosyl - diphosphate synthetase
PYR	Pyruvate
q_{lipid}	Lipid productivity
R5P	Ribose 5 - phosphate
Ru5P	Ribulose - 5- phosphate
RX	Ribose 5 - phosphate & Xylose - 5 - phosphate
SCOA	Succinyl - coA
SCOAS	Succinyl CoA ligase
SDH	Succinate dehydrogenase
ST	Sterols
Starch	Starch
SUCC	Succinate
TAG	Triacylglycerols
TCA	Tricarboxylic acid cycle
TK	Transketolase
TPI	Triosephosphate isomerase
X (x)	Biomass
X5P	Xylose - 5 - phosphate
μ	Specific growth rate
$Y_{lipid/biomass}$	Lipid yield on biomass

LIST OF APPENDICES

CHAPTER 1 INTRODUCTION

1.1 Background

Microalgae are rich in protein, fat, sugar, amino acids, polyunsaturated fatty acids and other biologically active substances. It is a golden key for human to obtain food, pharmaceutical, fine chemical products, and other important materials from the ocean. Microalgae are easy to culture, and have high photosynthetic efficiency, zero net carbon values, short growth cycle (10 ~ 60 days) compared with plants and high lipid content (25-70 %). They do not compete nor hijack farming; do not compete with food and do not affect the global energy distribution.

Two oil crises during the 1970's stimulated a vigorous search for alternative energy sources and microalgae are among the top priority candidates (Georgianna & Mayfield, 2012; Quintana et al., 2011a). The capability of lipid accumulation in different microalgae varies from 20 % - 50 % (cell dry weight) with some that can even reach 70 %. In most cases, only the neutral lipids will be used for biodiesel production as transesterification yields from polar lipids require more expensive catalysts, longer reaction times, and higher reaction temperatures (Orr & Rehmann, 2016; Hidalgo et al., 2013). Meanwhile, although TAG and FFA are all neutral lipid classes, in our work, TAG is a more favorable component. As from our result, TAG account for 50-60% of the total lipids while FFAs are only around 1% of total lipids. Meanwhile, TAG has suitable fatty acids composition of C16 and C18 chains with saturated or mono-unsaturated fatty acids, which are the most suitable components for biodiesel production (Xu et al., 2006). So, microalgae lipid production is now one of the hottest topics around the world. In 1973, Japan launched the first "Sunshine project", and then followed the "Microalgae diesel research program" and declared to be a biodiesel exporter in 2025. The United States started Aquatic Species Program (ASP) in 1978 and completed high-oil algae species selection and improvement in the two following decades (Yu et al., 2011b). Then in 2006, they launched a "Mini-Manhattan Project", which did plan to realize microalgae diesel industrialization in four years. Meanwhile, the UK "Carbon Trust", U.S. "Solix Biofuel" and "Green Fuels Technology", Canada "International energy" and New Zealand "Aquaflow bionomic" are all committed to large-scale cultivation of microalgae and biodiesel research and development, setting off a global wave of biodiesel production and research by engineered microalgae (Bollinger, 2011; Greenwell et al., 2010a; Maia, 2010; Senne, 2012; Thurman, 1997).

1.2 Microalgae application in lipid production

A microalgae cell contains water at about 60-80 % by weight and approximately 98 % of the dry weight is composed of organic molecules and the remaining 2 % is composed of inorganic molecules. The organic molecules present are predominantly proteins, carbohydrates and lipids, which total constitutes about 90 %, while other organics like DNA, RNA and ATP are found in lesser amounts of about 10-12 % (Bumbak et al., 2011; Sivakaminathan, 2012).

Many algal species have been found to grow rapidly and produce substantial amounts of triacylglycerol (TAG) or oil, so they are referred to as oleaginous algae. It has long been postulated that algae could be employed as a cell factories to produce oils and other lipids for biofuels and other biomaterials (Borowitzka, 1988; Nan et al., 2015). The advantages of algae as feedstock for biofuels and biomaterials include:

a) They can synthesize and accumulate large quantities of neutral lipids/oil (20–50 % DCW), and grow at high rates (0.1-1.6 day^{-1}) (Duong et al., 2015; Welter et al., 2013),

b) They can grow in saline, coastal seawater where there are few competing stress,

c) They can be grown in pounds on marginal lands (e.g. desert, arid- and semi-arid lands), so they do not compete with farmlands,

d) They can fix carbon dioxide from flue gases emitted from fossil fuel-fired power plants and other sources, thereby reducing emissions of a major greenhouse gas,

e) Meanwhile, they can produce various value-added co-products such as biopolymers, proteins, polysaccharides, pigments, animal feed, fertilizer and H_2,

Based upon the photosynthetic efficiency and growth potential of algae, theoretical calculations indicate that annual oil production of >30 000t of algal oil per hectare of land may be achievable in mass culture of oleaginous algae, which is 100-fold greater than that of soybeans, a major feedstock currently being used for biodiesel in the USA (Hu et al., 2008). Also because of its extremely high lipid content, it is attractive as a second-generation alternative fuel and was widely studied and investigated.

1.3 Microalgae characteristics and classification

Microalgae includes a wide range of organisms differing in size, shape, color and structure. However, they have a common property having a photosynthetic system, capturing carbon dioxide and assimilating it as a part of their central metabolism. Their photosynthetic system is highly similar to that in plants, but they have a much simpler whole organism organization level (uni-cellular species). So unlike plant cells, in which lipids were not only trapped in the cell walls and membranes but also only in certain tissue/organization. Meanwhile they also have higher reproduction capabilities, the growth cycle of microalgae is around 10 ~ 60 days compared with that of 1 year for soybeans (Sivakaminathan, 2012).

Based on their color (pigment type), size (cell structure) and their life cycle, microalgae are divided into nine categories (Khan & Rashmi, 2009) namely: *Chlorophyta, Chlorarachniophyta, Cryptophyta, Dinophyta, Euglenophyta, Glaucophyta, Haptophyta, Heterokontophyta* and *Rhodophyta,* and two prokaryotic divisions: *Cyanophyta* and *Prochlorophyta* (Mutanda et al., 2011; Sivakaminathan, 2012).

1.3.1 Oleaginous algae strains

In 1998, 3,000 microalgae species were screened by the U.S. Department of Energy's Aquatic Species Program with the aim to identify species with high lipid and fatty acid content (Georgianna & Mayfield, 2012). After almost two decades of the ASP program, thousands of algae strains were isolated and screened for their lipid and fatty acid content. Algae were classified in categories based on their lipid content (Sheehan, 1998). For instance, diatoms are among the most common and widely distributed group of algae. They store energetic molecules primarily in the form of lipids (TAGs), and the average lipid content of oleaginous diatoms has been reported at 22.7 % dry-cell weight (DCW) under normal growth conditions and up to 44.6 % DCW under stress conditions (Hu et al., 2008). *Chlorella* and *Nannochloropsis* are categorized as the most potential oil producing species. *Nannochloropsis sp*. bears a high lipid content (60 % DCW), especially with eicosapentaenoic acid (EPA) component (4 % DCW) (Maia, 2010), which makes this algae species the only that has been used for industrial EPA production (Sakthivel & Elumalai, 2011; Sivakaminathan, 2012). *Chlorella* mainly includes *Chlorella vulgaris*， *Chlorella pyrenoidosa* and *Chlorella protothecoides*. Although the lipid content for the first two species is not high (13 %-20

%), a relatively short (10-19h) doubling time compared to 1-5 day normally observed (Bollinger, 2011; Duong et al., 2015) leads to a higher lipid productivity level. Since *Chlorella protothecoides* can use organic carbon source such as glucose, glycerol, starch, *etc*., to live a heterotrophic life, it results in a higher cell culture density and lipid content compared to autotrophic growth. Miao *et al*. applied cell engineering techniques to reach a high lipid content in heterotrophic *Chlorella* cells, with 55 % of the dry cell weight, corresponding a 4-fold that in autotrophic algae cells (Miao & Wu, 2006b). Moreover, *Salina* and *Phaeodactylum* are high oil content seawater algae.

Table 1. 1 Lipid content of the major microalgae species

Microalgae	**lipid content (% dry wt)**
Botryoccus braunii	25-75
Chlorella sp.	28-32
Chlorella protothecoides (autotrophic/heterotrophic)	15-55
Dunaliella. tertiolecta	36-42
Nannochloropsis sp.	31-68
Nannochlosis sp.	15-32
Crypthecodinium cohnii	20
cylindrotheca sp.	16-37
Dunaliella primolecta	23
Neochloris oleoabundans	35-54
Nitzschia sp.	45-47
phaeodactylum tricornutum	20-30
Schizochytrium sp.	50-77
Tetraselmis sueica	15-23

Among eukaryotic microalgae, *Chlamydomonas reinhardtii* has arisen as the hallmark model organism, with its genome been sequenced and annotated, although having a low lipid content (Merchant et al., 2007). *C. reinhardtii* has been widely used to study photosynthesis, cell motility and phototaxis, cell wall biogenesis, and other fundamental cellular processes (Harris, 2001). These studies laid a foundation framework for researches on other species. (Shah, 2010) listed major lipid-producing strains.

Up to date, published biofuel studies have focused on less than 20 species taken from culture collections (Figure 1.1), and of these publications, *Chlamydomonas reinharditii, Synechocystis sp.* and *Chlorella sp.* are top 3 intensive species studied (Larkum, 2012).

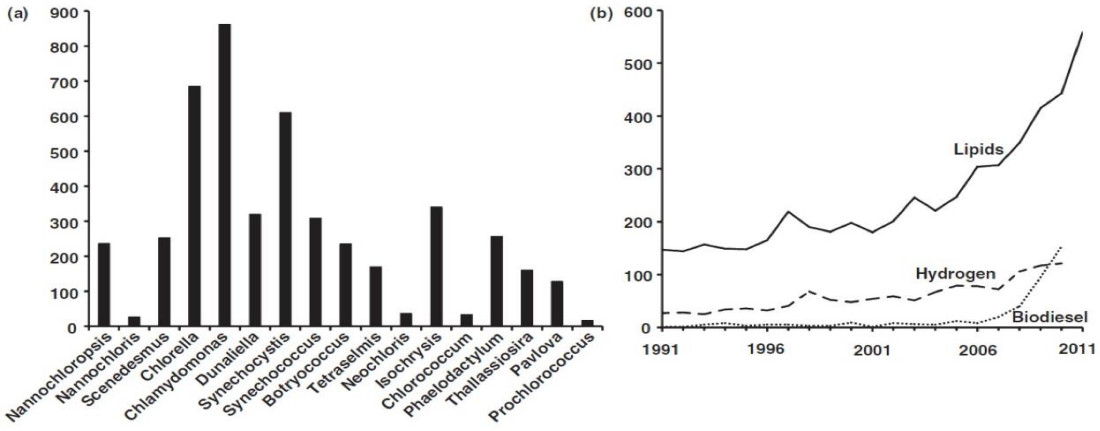

Figure 1. 1 (a) Microalgae strain-specific publications related to biofuels published in Web of Science since 1991. The references presented capture 70 % of all microalgal biofuel publications. (b) Number of publications per year for microalgae biofuel publications referring to biodiesel, hydrogen and lipids (Larkum, 2012).

1.3.2 **Algae lipid classes**

Algal lipids fall under two broad categories: non polar lipids and polar/membrane lipids (Bumbak et al., 2011). Most of the algal lipids are glycerinated membrane lipids (polar lipids), with minor contributions to overall lipid content from TAG, wax esters, hydrocarbons, sterols, and prenyl derivatives (non-polar lipids) (Hu et al., 2008).

Under optimal growth conditions, algae synthesize fatty acids principally for esterification into glycerol-based membrane lipids, which constitute about 5–20 % of their dry cell weight (DCW). Fatty acids include medium-chain (C10–C14), long-chain (C16–18) and very-long-chain (≥C20)

species and fatty acid derivatives. The major membrane lipids are the glycosylglycerides (e.g. monogalactosyldiacylglycerol, digalactosyldiacylglycerol and sulfoquinovosyldiacylglycerol), which are enriched in the chloroplast together with significant amounts of phosphoglycerides (e.g. phosphatidylethanolamine (PE) and phosphatidylglycerol (PG)), which mainly reside in the plasma membrane and many endoplasmic membrane systems (Murata, 2007). The major constituents of the membrane glycerolipids are various kinds of fatty acids that are polyunsaturated and derived through aerobic desaturation and chain elongation from the "precursor" fatty acids palmitic (16:0) and oleic (18:1ω9) acids (Erwin, 1973).

Under unfavorable environmental or stressful conditions for growth, however, many algae alter their lipid biosynthetic pathways towards the formation and accumulation of neutral lipids (non-polar lipids) (20–50 % DCW), mainly in the form of triacylglycerol (TAG). Unlike the glycerolipids found in membranes, TAGs do not have a structural role but, instead, serve primarily as a storage form of carbon and energy. However, there is some evidence suggesting that, in algae, the TAG biosynthesis pathway may play a more active role in the stress response, in addition to being a carbon and energy storage under environmental stress conditions. Unlike higher plants, where individual classes of lipid may be synthesized and localized in a specific cell, tissue or organ, many of these different types of lipids may be produced in a single algal cell. After being synthesized, TAGs are deposited in densely packed lipid bodies located in the cytoplasm of the algal cell. The transesterification reaction from TAG to biodiesel is shown in Figure 1.2.

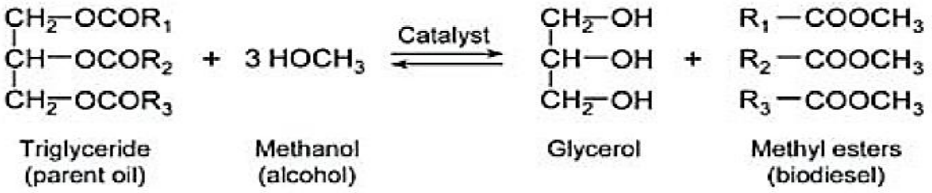

Figure 1. 2 Transesterification process for the conversion of oil to biodiesel. R1, R2, R3 are hydrocarbon groups (Sivakaminathan, 2012).

1.4 **Challenges of industrial lipid production**

Although microalgae metabolism has been described in various species (Radakovits et al., 2010), we still have sparse details on metabolic flux distribution and regulation in lipid production bioprocesses. For instance, it becomes crucial, while developing lipid production bioprocesses, to

better understand metabolic flux regulation favouring cell lipid storage accumulation or algae growth acceleration, for determining optimal culture conditions maximizing total lipid productivity (i.e. q_{lipid} or $\mu \times Y_{lipid/biomass}$). For instance, diatoms are known for their high lipid content but a low growth rate limits their use at large scale. Indeed, it is quite common to observe a reduced biomass yield when reaching high cell lipid content. The field thus seems attractive for improvement looking at a better control of cell lipid productivity, and acquiring fundamental knowledge on algae cell metabolism can result in tips for identifying efficient strategies to favor a specific cell behavior. Moreover, significant amounts of lipids are trapped in the cytoplasm by the cell walls and various organelles membrane, so the lipid extraction efficiency can greatly impact the final extracted lipid yield, another major bottleneck of commercial-scale biodiesel production (Guldhe et al. 2016).

1.5 Research problems

1.5.1 Carbon and nitrogen nutrition: a key to control microalgae lipid metabolism

As mentioned previously, one of the major bottlenecks for algae lipid industrialization relies in the metabolic conflict between lipid accumulation and biomass growth. Previous studies have clearly shown that lipid content of a unit microalgae cell evolves along with the growth stages, culture conditions and nutritional states. Lipid productivity is thus seen as quite unstable since a slight perturbation of bioprocess culture conditions can either result in an increase or a decrease of the cell lipid content. In the recent years, heterotrophic algae culture have gained in interest for lipid production, since high biomass and lipid content (55 % of the dry weight) can be reached while feeding sugar-rich waste streams (Miao and Wu 2006) or other agricultural stocks (Gao et al., 2009). It is thus expected that feeding an organic carbon source would make a bioprocess more productive but it is not known if it could be more efficient in stimulating lipid accumulation. It is known that most of microalgae strains accumulate lipids when the cell division is blocked or inhibited such as from nitrogen shortage stress conditions, while carbon continued being fixed (i.e. CO_2 in autotrophic) or consumed (i.e. organic carbon source in heterotrophic) (Georgianna & Mayfield, 2012; Quintana et al., 2011b).

Nitrogen is an essential nutrient factor for algae growth, as well as for any other biosystem. It is the essential element structurally formatting amino acids, purines, pyrimidines, amino sugars and

amine compounds. Nitrogen (N) is also a component of chlorophyll, so it is essential in photosynthesis. Therefore, under insufficient N conditions, chlorophyll amount in algal cells is reduced, and the cell photosynthesis capacity from light intensity and CO_2 concentration reduces accordingly, leading to weakened photosynthesis and respiration (Yang, 2012). Furthermore, under limited N condition, protein and nucleic acid synthesis slow down so cell division and growth are restricted, and most assimilated carbon molecules go into the production of storage and stress-resistant materials such as lipid, starch and beta-carotene. A detailed cell response for the carbon metabolism reprogramming under N limitation is illustrated below (Figure 1.3) in which the red color represents enhanced pathways and the green ones reduced metabolic activity.

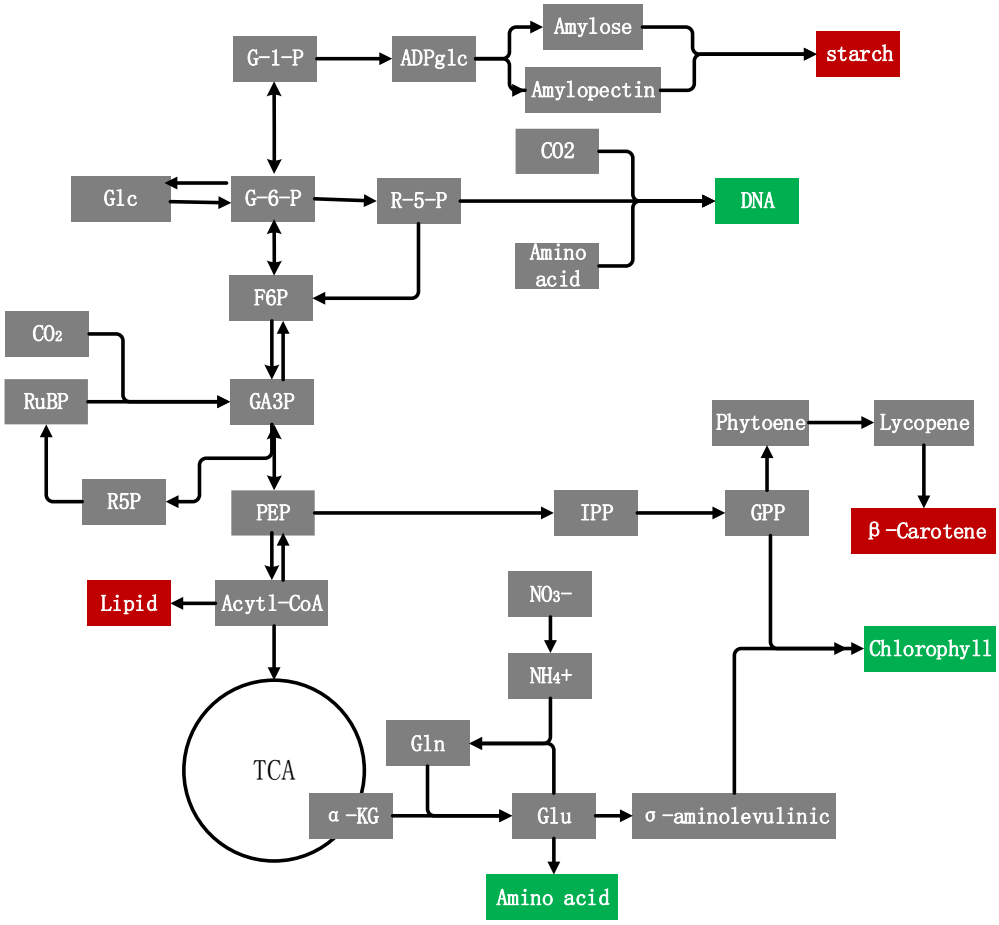

Figure 1. 3 Carbon metabolism reprogramming in N limitation. The red color represents enhanced pathways and the green ones reduced metabolic activity

Nitrogen metabolism is thus tightly linked to carbon metabolism with, for instance, the uptake and assimilation of nitrogenous compounds requiring organic acids such as 2-oxoglutarate, which is

the primary carbon acceptor for ammonium; and malate which prevents alkalinization during nitrate assimilation (Stitt, 2002). Therefore, in presence of nitrogenous compounds the synthesis of organic acids requires the re-direction of the carbon influx that would go to carbohydrate synthesis. Of interest, nitrate represses ADP-glucose pyrophosphorylase (a key enzyme in the starch synthesis pathway) activity, which lead to a marked starch depletion (Scheible & Gonzales, 1997). However, under nitrogen deficiency, this pathway repression phenomenon is removed and the competing pathway of organic acid synthesis is under-expressed (TCA cylcle), and starch accumulates intracellularly. Takuro Ito and Miho Tanaka (Ito & Tanaka, 2012) have specifically studied the metabolic profile of microalgae cells in N-limited conditions and they found that within the starch-sucrose and the glycolysis/gluconeogenesis metabolisms, four out of eight metabolites are increasing, phenomena correlating with the intracellular accumulation of starch granules.

Except for the competition and repression effects in carbon metabolism, N is also a resource for amino acid synthesis, as previously discussed and shown in Figure 1.3. Nitrate is assimilated and converted to ammonium, entering the glutamate synthase or GS-GOGAT (glutamine synthetase-oxoglutarate amidotransferase) pathway. So under deficient N conditions, the influx of carbon to the amino acid synthesis pathway is reduced, and the limitation of amino acid supply results in the reduction to the cessation of net protein synthesis, which slows down algae cell division and growth (Levy & Gantt, 1990; Lewitus & Caron, 1990). In Takuro Ito and Miho Tanaka's study (Ito & Tanaka, 2012), amino acids in nitrogen assimilation and N-transport metabolisms under N-limited conditions were decreased to $1/20^{th}$ of that under normal N condition. (Coleman et al., 1988a) also reported that the exposure of algae cells to N-deficient conditions resulted in the level decrease of 37 proteins identified of the chloroplast.

Nitrogen is the major elements of chlorophyll; the synthesis of chlorophyll requiring N to form δ-aminolevulinic acid, a chlorophyll precursor. Net mass balance of chlorophyll concentration in the cell is the sum of its synthesis and photooxidation rates. Photooxidation of chlorophyll occurs constantly under light excitation, and the synthesis of new chlorophyll molecules also occurs to replace degraded molecules (i.e. a maintenance phenomenon). However, under N-limited levels, new chlorophyll cannot be produced and the quantity of chlorophyll thus reduces per cell with time. Indeed, it has been widely reported that growth of algae under N-deficient conditions results in a significant loss of chlorophyll molecules. In *Nannochloropsis*, cells grown under N-deficient conditions resulted in increased levels of storage products per cell such as lipid and carbohydrate

(starch), while the level of chlorophyll declined rapidly. Thus, N depletion would also presumably decrease photosynthetic efficiency and the availability of carbon-based substrates synthesized through CO_2 fixation pathway (i.e. Calvin-Benson cycle) (Sheehan, 1998). Similar results were also reported in other oil-rich green algae grown under N-limited conditions, with increased cell content in oil bodies and starch granules and decreasing chlorophyll cell content (Coleman et al., 1988a; Hu & Sommerfeld, 2008; Shifrin & Chisholm, 1981).

The *de novo* nucleotides synthesis requires metabolic intermediates such as ribose phosphate (i.e. within PPP pathway), amino acids and CO_2. Insufficient concentrations in amino acids, as mentioned previously, is limiting the carbon integration in nucleic acids molecules, so the carbon flowing in extra is then thought being re-oriented feeding other synthetic pathways such as those leading to lipid and starch.

In addition to the metabolic variations in macromolecules such as proteins, nuclear acids, carbohydrates and lipids, there is also an increase in the ratio of carotenoid to chlorophyll. N depletion induces the accumulation of antioxidative beta-carotenoids (e.g. carotene), which may play a role in the cell resistance under stressed conditions. The carbon flow to carotene is shown in Figure 1.3, where pyruvic acid and phosphoglyceraldehyde are combined for the synthesis of IPP (isoprenyl pyrophosphate), which first leads to GPP (geranyl pyrophosphate) and further to beta-carotene. As we can see, beta-carotene and chlorophyll are also competitive pathways, which means when chlorophyll synthesis flux is reduced, the synthesis flux of beta-carotene is enhanced. Jianxin etc. (Jianxin & Jue, 2003) reported a beta-carotene content two times that in the high N condition, when growing microalgae cells under nitrogen deficiency conditions .

So in summary, lipid synthesis includes a complex network of metabolic reactions that are highly interconnected to carbon and nitrogen metabolisms. Nitrogen deficiency conditions thus reprogram the cell carbon metabolism favoring carbon flow toward carbon-storage molecules (e.g. starch, lipids) and anti-stress components (beta-carotene). N-based carbon fluxes to synthetic pathways for proteins, nucleic acids and chlorophyll molecules are then reduced, resulting in a slow specific growth rate and low final biomass levels. Indeed, the two effects seem being tightly regulated as mutually exclusive. It is thus of high interest to find ways balancing the global metabolism to minimize these metabolic conflicts and optimize lipid productivity of microalgae, i.e. maximizing μ, x, $Y_{lipid/biomass}$.

1.5.2 The metabolic engineering of lipid production is a multifactorial problem

Metabolic modeling (modeling in America and modelling in Europe) is a systematic way to describe cell metabolism and predict cell behavior, ultimately. It can serve as a tool to guide the development of control strategies for maximizing bioprocess output in biomolecules of interest. A model allows performing a series of computer simulations to assess hypotheses of various types, either on culture strategies or on cell interaction with its environment. Conclusions can thus be drawn faster than performing successive comprehensive experimental operations, or even guide their planning and objectives. Multiple culture conditions can then be rapidly covered and the more the model describes finely cellular processes the more reliable are expected to be the output results. A cell-mirror model, which can be highly complex to develop and to handle, is thus expected to allow predictive model simulations, i.e. exploring outside the experimental space covered to generate experimental data used to develop a model. However, optimising complex biosystems such as microalgae for lipid production may require complex accurate mathematical models.

Different models have shown great efficiencies for process control while providing complementary knowledge on microalgae nutrition, culture condition (macroscopic models; (Deschênes & Wouwer, 2015; Mairet et al., 2013; Packer et al., 2011; Yang et al., 2011)) and metabolism (microscopic; (Kliphuis et al., 2012; Quintana et al., 2011a; Sweetlove et al., 2013)). Among macroscopical dynamic models developed to optimize operating conditions of bioprocesses using microalgae for lipid production, Bernard nutrition-based models (Oliver Bernard 2005) modified from Droop model (Droop, 1983b; Droop, 1968b) shown being highly efficient and reliable. For instance, a model was developed and used for neutral lipid production by the microalgae *Isochrysis aff. galbana* under nitrogen limitation (Oliver Bernard 2011). Temperature effect on microalgae was also included in a model (Olivier Bernard 2013), as well as accounting for light and temperature effects (Oliver Bernard 2012). Several kinetic models dealing with photosynthesis have then been proposed, effect of light, photoinhibition by light excess (J.C.H. Peeters, P. Eilers 2007). So based on the predicted optimized conditions, the production process are oriented controlled.

Various microscopic models have also been developed for describing cell metabolism. For instance, to quantify the effect of the O_2-to-CO_2 ratio on the metabolism of *C. reinhardtii*, Kliphuis developed a metabolic model to estimate the metabolic flux distribution at different steady states

for *Chlamydomonas reinhardtii*, performing a metabolic flux analysis (MFA). The metabolic network included 18 pathways, 159 reactions and 326 metabolites (Kliphuis et al., 2011), making that work the more detailed flux analysis in the algae platform. Muthuraj also performed a steady state metabolic flux analysis (a stoichiometric study) to study the behavior of *Chlorella sp.* FC2 IITG under different conditions. A shift of the intracellular flux distribution was identified at the transition from the nutrient sufficient to nutrient starvation growth phases. This author also applied their approach to perform a dynamic flux balance analysis (dFBA) to evaluate the bio-reaction velocity change and predict cyclic metabolism behavior of microalgae grown under a light–dark cycle (Muthuraj et al., 2013). In that work, the author considered CO_2, nitrate, phosphate and inoculated biomass as input variables, and intracellular fluxes were estimated by validating known cell contents in protein, carbohydrate, neutral lipid as well as biomass yield value. Therefore, metabolic modeling opens the black box of intracellular metabolism. It can describe every metabolic reaction of a network and integrate multifactorial approach, which can comprehensively help to identify key metabolic processes and improve cell productivity in an end-product of interest including growth. However, current metabolic models mostly considers every reaction rate as constant and do not consider flux enzymatic reality (enzyme kinetics). However, a cell culture is necessarily a dynamic process and steady state models can only partially predict a culture behavior, from time point to time point. In addition, such MFA and FBA approaches do not implicitly consider flux regulation mechanisms, which need being defined as objective criteria for the system resolution. More recently, dynamic modeling approaches, allowing to perform time-continuous simulations of a cell population behaviour, were proposed. Such models, also called kinetic metabolic models, can describe flux kinetics and regulation, time-based perturbations and complex enzymatic and gene interactions (Cloutier et al., 2009; Cloutier et al., 2007; Ghorbaniaghdam et al., 2013; Leduc et al., 2006). Some models consider both cell inorganic nutrition and metabolism, aiming at identifying a balanced nutritional strategy to optimize culture conditions favoring a specific metabolic end-product (Cloutier et al., 2009). However, kinetic models require the identification of a large amount of parameter values, which can be hardly found in literature such as for the microalgae biosystem (Surendhiran & Sirajunnisa, 2015). From all the above, it is thus clear that the microalgae biosystem is highly regulated with complex non-linear interactions among metabolic pathways. Therefore, we think that only a modeling approach having the capacity to describe such regulation mechanisms linking metabolic pathways, can provide a tool allowing,

ultimately, to identify the key culture parameters enabling the modulation of the cell metabolism for maximizing cell lipid productivity.

1.6 **Research objectives**

The overall purpose of the research presented in this thesis was to improve algae lipid yield by using metabolic engineering approaches. To this end, we have followed three sub-objectives:

1- At the upstream of microalgae bioprocess, we worked at the enhancement of fundamental understanding of microalgae cell behavior, performing a metabolomic study to identify differences in cell metabolic behavior under autotrophic, mixotrophic and heterotrophic culture conditions.

2- This metabolomics knowledge has then enabled developing a kinetic metabolic model which was asked to describe, as a first attempt, heterotrophic culture condition.

3- Finally, working at the downstream of microalgae bioprocess, we have contributed to the enhancement of the yield for current lipid extraction methods by a slight but efficient modification of the protocols.

First, we characterized the effect of different carbon feeding strategies, comparing autotrophic (i.e. with CO_2 only), mixotrophic (i.e. with CO_2 and glucose) and heterotrophic (i.e. with glucose only) culture modes, on *Chlorella protothecoides* metabolic behavior. All cultures were performed at low initial concentration in nitrogenous nutrients (1.32 mmol L^{-1} glycine plus 1.6 mmol L^{-1} amino acids) to better understand lipid metabolism for the three culture strategies. To achieve this goal, an algae species with a flexible metabolism, *Chlorella protothecoides*, was studied. Algae cells quantitative metabolomics was determined performing analysis of the culture media as well as of intracellular metabolites from cell extracts. Carbon flux distribution within glycolysis, PPP and TCA cycle, cell energetics fluctuation, and extra- and intracellular metabolites concentration variation were determined. Experimental data helped building a simplified metabolic network of the microalgae, and helped to understand the complex interplay between carbon utilization, energy regulation, and biosynthetic pathways, from the carbon substrate uptake to carbon storages (i.e. starch and lipid) metabolism. This metabolomics study is the more complete published to date.

Second, we developed a kinetic metabolic model, based on the laboratory modeling approach as well as on the metabolomics experimental data previously described, to better characterize the

algae platform, and to develop an *in silico* simulation platform of the microalgae biosystem. To realize this objective, we developed a kinetic metabolic model based on a simplified network stoichiometry, Michaelis-Menten kinetic equation and mass balances on cell metabolites (intracellular and extracellular) quantified previously, covering central and secondary metabolic pathways in the microalgae *Chlorella protothecoides*. The final model included 7 pathways, 30 metabolic reactions for carbon, nitrogen and lipid metabolisms. Cell growth, lipid production and 25 metabolic intermediates were simulated. So the model included most of the main characters of the cell metabolism. The model structure and parameter values were calibrated using experimental data of previously described heterotrophic culture, and then the model was used to perform a dynamic metabolic flux analysis to further understand cell behavior. To the best of our knowledge, this is the first metabolic kinetic model proposed to describe microalgae cell behavior.

Finally, after performing the metabolomic study, we tested different hypotheses and finally confirmed that a water treatment step added to current extraction protocols, between the two organic solvent extraction steps, would perturb cell integrity and increase cell material disruptions with an enhancement of lipid release from the cell. We have thus ameliorated currently used lipid extraction protocols, which will ultimately improve lipid extraction yield, at the lab and industrial scale.

1.7 Organization of the thesis

The thesis contains nine chapters. Chapter one is a brief introduction which describes the thesis background, context, research problems and objectives. The status of oleaginous algae application in lipid production and challenges of microalgae lipid industrial production were introduced. In chapter two, we reviewed the physical characteristic of the microalgae platform, and its metabolic engineering from a deep overview of metabolism and regulatory interactions. Mathematical modelling of cell behaviour, as a method to study and control the bioprocess were finally reviewed. In the third chapter, the general methodology used in this work is presented. In chapter four, a metabolomics study of *Chlorella protothecoides* under different carbon-based culture modes with a low nitrogen medium condition was investigated to unravel the links between algae metabolism and lipid production. In chapter five, a kinetic metabolic model is developed to describe *Chlorella protothecoides* central carbon metabolism grown under heterotrophic condition. This is the first kinetic metabolic model in microalgae platform. The model is adapted from a kinetic model from

mammalian cell, Chinese hamster ovary cell (CHO) and developed based on the biochemical information of metabolic pathways and calibrated according to the dynamic metabolic data obtained from heterotrophic culture mode. In chapter six, we explored an efficient way to improve lipid extraction yield of existing methods by simply adding a water treatment step to current extraction protocols between the two organic solvent extractions. In chapter seven, we present the general discussion, in chapter eight, we draw the main conclusions of this thesis and in chapter nine finally recommended the future works.

CHAPTER 2 LITERATURE REVIEW

2.1 Physiological factors affecting lipid production

While the 'algae-for-fuel' concept has been explored in the USA and in many other countries over the past few decades, interest and funding levels are growing and waning according to fluctuations of the world petroleum oil market. The lipid yields obtained from algal mass culture efforts performed to date fall short of the theoretical maximum yield (at least 10–20 times lower), and have historically made algal oil production technology prohibitively expensive (Sheehan, 1998).

Researchers found that even neutral lipid content of unit microalgae biomass greatly differs between different strains within the same species, indicating the accumulation of neutral lipids is microalgae species dependant, culture condition and growth stage. Therefore, the effect of nutrient and culture conditions on lipid production was studied discriminating among defined species. For example, studies clearly showed that the cultivation mode greatly affects lipid accumulation in microalgae. Heterotrophic grown microalgae usually accumulate more lipids than those cultivated under photoautotrophic condition (Miao & Wu, 2006b). Indeed, the heterotrophic mode offers several advantages over phototrophic including the elimination of light requirement, a more direct control of the cultivation process controlling the organic carbon source concentration in the liquid medium, and lowered costs of lipid harvesting because of higher cell densities normally obtained in heterotrophic culture (Chen, 1996). Heterotrophic growth of *C. protothecoides* using acetate, glucose, or other organic compounds as carbon source results in much higher biomass as well as lipid content in cells (Liu et al., 1999). These authors have compared several carbon sources and concluded that glucose leads to the highest yields in both biomass and lipid. Jiang 2000, Chen 2008 (Guanqun Chen, 2008; Yue Jiang, 2000) studied the effect of glucose, salinity, pH, and of dissolved O_2 on the behavior of microalgae, and they concluded that low glucose concentrations (5g L^{-1}) and medium pH (7.2) enhanced the degree of fatty acid unsaturation and DHA formation in *Crypthecodinium cohnii*. High salt stress (20g L^{-1}) also lead to highest contents of total fatty acids, EPA, and polar lipids as well as enhance the degree of fatty acid unsaturation. Other studies also focusing on the light parameter confirmed that a strategic light photoperiod management can lead to high cell densities as it is critical for cell growth and lipid production (Zhiyou Wen, 2003), while excessive light can rather induce the "photoinhibition" phenomenon which will affect and limit a bioprocess productivity (Jack Myers, 1940). Of interest, previous studies have shown that most

microalgae strains accumulate lipids when the cell division is blocked or inhibited, as far as carbon continue to being fixed (e.g. such as from nitrogen shortage stress conditions) (Georgianna & Mayfield, 2012; Quintana et al., 2011b). It was observed that cell growth continued even after medium depletion in external nitrogenenous nutrients pool, while hypothetically supported by anabolic reactions of intracellular macromolecular nitrogenenous pools such as chlorophyll molecules. The relationship between nitrate depletion, cell growth, lipid cell content, and cell chlorophyll content was investigated by Yanqun Li et al. (Li et al., 2008), and Chen and Johns (Feng Chen, 1991) focused on the effect of the C-to-N ratio and of aeration on the fatty acid composition of heterotrophic *Chlorella sorokiniana.* At a C-to-N ratio (C/N) of approximately 20, cell lipid content was at a minimum, but it increased at either higher or lower C/N values. However, culture management strategies only based on physiological parameters cannot fundamentally solve the conflict between cell growth and lipid accumulation. Consequently, the community started seeking solutions looking at metabolic and genetic approaches.

2.2 Lipid metabolism and genetic engineering

Lipid biosynthesis and catabolism, as well as pathways that modify the length and saturation level of fatty acids, have not been as thoroughly investigated for algae as they have for terrestrial plants. However, many of the genes involved in lipid metabolism in terrestrial plants have homologs in the sequenced microalgae genomes. The following figure 2.1 is a simplification of lipid synthesis pathways in microalgae (Radakovits et al., 2010). Although TAG and FFA are all neutral lipid classes, in our work, TAG is a more favorable component. As from our result, TAG account for 50-60% of the total lipids while FFAs are only around 1% of total lipids. Meanwhile, TAG has suitable fatty acids composition of C16 and C18 chains with saturated or mono-unsaturated fatty acids, which are the most suitable components for biodiesel production. Transformation of TAG to biodiesel is also with lower cost compare with PL and FFAs. As a more comprehensive model of cell metabolism, under mixtrophic conditions, cells use concurrently both CO_2, which is fixed from photosynthesis, and organic carbon source in the medium, and the key metabolic nodes in the mixtrophic metabolism include the following.

First, GA3P (glyceraldehyde-3-phosphate), where Calvin cycle enters glycolysis and alternatively leads to Ru5P regeneration through reversed PPP pathway (Figure 2.2). It is also a very important

precursor for various organic molecules. Therefore, it is an important metabolic node in mixotrophic algae cell.

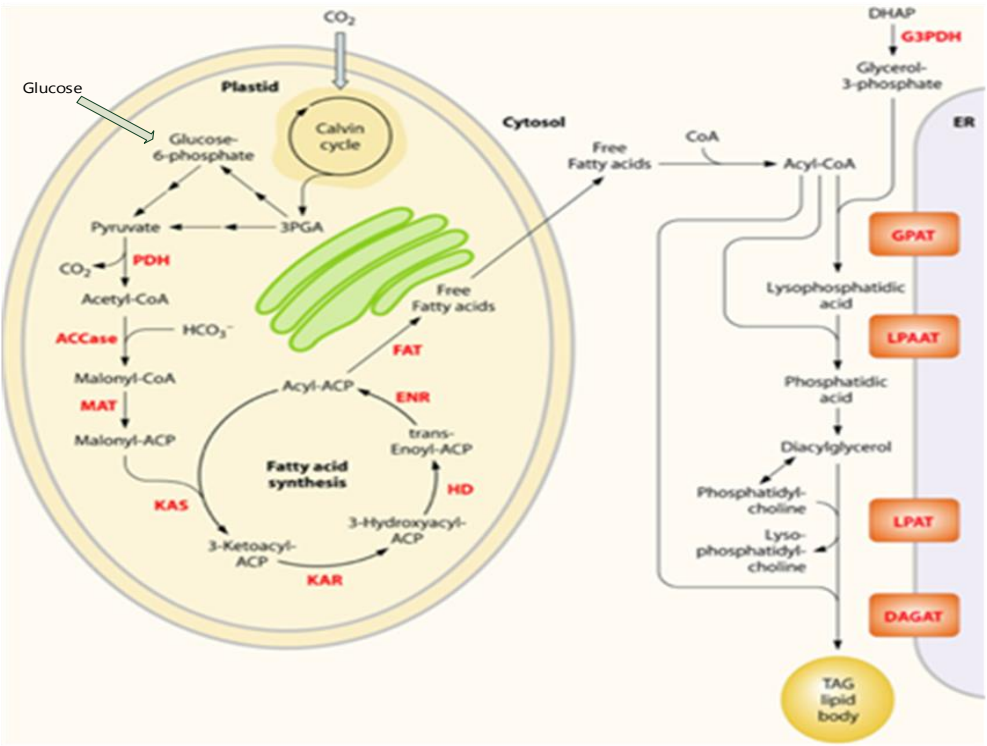

Figure 2. 1 Simplified overview of the metabolites and representative pathways in microalgae. Lipid biosynthesis shown in black and enzymes shown in red. Free fatty acids are synthesized in the chloroplast, while TAGs may be assembled at the ER. ACCase, acetyl-CoA carboxylase; ACP, acyl carrier protein; CoA, coenzyme A; DAGAT, diacylglycerol acyltransferase; DHAP, dihydroxyacetone phosphate; ENR, enoyl-ACP reductase; FAT, fatty acyl-ACP thioesterase; G3PDH, gycerol-3-phosphate dehydrogenase; GPAT, glycerol-3-phosphate acyltransferase; HD, 3-hydroxyacyl- ACP dehydratase; KAR, 3-ketoacyl-ACP reductase; KAS, 3-ketoacyl-ACP synthase; LPAAT, lyso-phosphatidic acid acyltransferase; LPAT, lyso-phosphatidylcholine acyltransferase; MAT, malonyl-CoA:ACP transacylase; PDH, pyruvate dehydrogenase complex; TAG, triacylglycerols. Figure cited from (Radakovits et al., 2010)

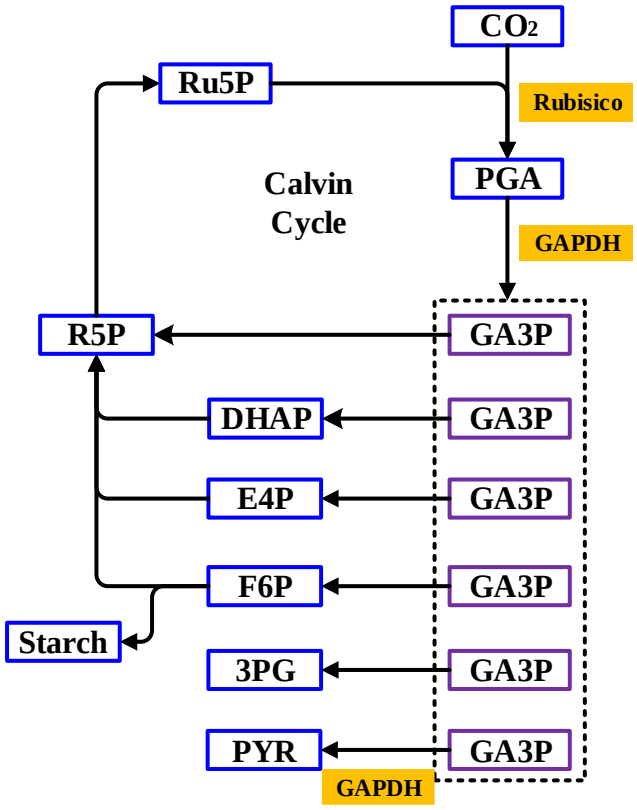

Figure 2. 2 Metabolic division in GA3P node

Calvin cycle is regulated by Rubisco, GAPDH (glyceraldehyde phosphate dehydrogenase), FBPase (fructose-1,6-bisphosphatase), SBPase (sedoheptulose-1,7-bisphosphatase) and Ru5PK (ribulose-5-phosphate kinase). RuBisco is an important carboxylase in C_3 photosynthetic metabolism. It determines carbon assimilation rate. Meanwhile, it is also an indispensable oxygenase in photorespiration. Photorespiration could lead to carbon loss during carbon fixation, which reduces the carbon flow to carbohydrates and lipid pools build-up. Higher concentration of CO_2 under light condition can enhance the carboxylase activity of Rubisco, so as to produce more GA3P and increase the Calvin cycle flux. Rubisco is the key enzyme that can increase the ratio of fixed carbon of the Calvin cycle in mixtrophic algae culture. GAPDH is also a key enzyme for glycolysis and Calvin cycle. GAPDH is located in chloroplasts, and requires NADPH as coenzyme to catalyze the reverse reaction in glycolysis and convert 1,3-diphosphoglycerate to GA3P. This enzyme plays a central role in Calvin cycle. GAPDH is also located in cytoplasts, specifically needing $NAD^+(H)$ as coenzyme, to catalyze GA3P convertion to 1,3-diphosphoglycerate, which is the only redox reaction in glycolysis. The NADPH-to-NADP+ ratio regulates the direction of GAPDH enzymatic catalysis, as well as the flux distribution among the Calvin cycle and glycolysis. Moreover,

GAPDH is a light regulated enzyme; light can increase the enzyme activity and then leading to more GA3P products and higher carbon flux entering glycolysis.

GA3P is also a key point where GA3P is reversed to FBP by FBPase and enters reversed PPP to regenerate Ru5P consumed in the first step of Calvin cycle. This process is regulated by FBPase, SBPase and Ru5PK, since these enzymes are regulated by light.

GA3P can also be converted by triosephosphate isomerase (TPI) to DHAP, which is the precursor of 3- phosphoglycerol, thus preparing carbon skeletons for lipid boosting carbon flux into lipid synthesis pathway.

Secondly, G6P and F6P, where free sugar metabolism branches out (catalyzed by 6-phosphate dehydrogenase) from glycolysis and goes to PPP pathway. PPP pathway is mainly regulated by 6-phosphate dehydrogenase, which catalyzes G6P to Ru5P. It is a rate-limiting enzyme in PPP pathway, and thus determines the carbon flux entering PPP. PPP pathway can generate large amount of NADPH, which is the reducing power necessary for fatty acid synthesis. The NADPH-to-NADP+ ratio regulates specific enzymes activity. High concentrations of NADPH competitively inhibit glucose 6-phosphate dehydrogenase, and thus limit carbon flux access to the PPP. PPP pathway can also generate Ru5P, so when free sugar exists 6-phosphate dehydrogenase can also accelerate the Calvin cycle indirectly by producing more Ru5P as the normal replenishment rate in Calvin cycle.

Glycolysis and gluconeogenesis are also regulated at the G6P and F6P node. In glycolysis, hexokinase and 6-phosphofructokinase (PFK) catalyze glucose to FBP. But in gluconeogenesis, the reverse steps are catalyzed instead by fructose bisphosphatase and glucose-6-phosphatase. Hexokinase is allosterically inhibited by its product G6P. Therefore, large G6P accumulation cause the inhibition of PFK enzyme activity, thus inhibiting the glycolytic pathway global flux. Phosphofructokinase (PFK) is regulated by the allosteric activation of ADP and AMP, while it is inhibited by ATP. In addition, citric acid is also an allosteric inhibitor of PFK enzyme. However, opposite regulation mechanisms will affect the gluconeogenesis pathway. Indeed, when TCA cycle goes too fast, the excessive ATP and citric acid generated will inhibit PFK, but activate the fructose bisphosphatase and glucose-6-phosphatase enzymes, which finally reverse the glycolysis to gluconeogenesis pathway.

Third, acetyl-CoA (Acetyl coenzyme A), which is a very critical metabolic node, is regulated to act on flux distribution to gluconeogenesis, TCA cycle, fatty acids and amino acids synthesis. Acetyl coenzyme A carboxylase（ACCase）is a key rate-limiting enzyme in the fatty acid biosynthetic pathway. Early in 1988, Roessler discovered that nutritional limitation could induce ACCase gene expression, thus contributing to the accumulation of fatty acid (Roessler 1988). PEPC (pyruvate dehydrogenase complex) is also a critical enzyme leading glycolytic flux to TCA cycle, thus diverging fluxes toward non-lipid synthesis direction. PEPC is regulated by an allosteric control and chemical modification, and its catalytic products ATP, NADH and acetyl-coA potently inhibit the enzyme activity. Indeed, such allosteric inhibition can be enhanced by long chain fatty acids, and when reduced acetyl-CoA enters TCA cycle, AMP, CoA and NAD^+ accumulate in the cell and the enzyme complex will be activated again.

ACCase and PEPC relative activities affects lipid metabolism direction. ACCase catalyzes acetyl-CoA into fatty acid synthesis pathway. Accumulation of acetyl-CoA can activate PEPC, which catalyzes pyruvate to oxalic acid and enters the amino acid biosynthetic pathway. Therefore, inhibition of PEPC activity is thought to stimulate ACCase catalyze its substrate into fatty acids pathway.

Moreover, at the acetyl-CoA node, citrate synthase and isocitrate dehydrogenase regulates acetyl-CoA entering the TCA cycle. The reaction regulation is mainly achieved through product feedback inhibition. TCA cycle is the main energy producing pathway in the metabolic network. Therefore, the ATP-to-ADP and NADH-to-NAD^+ ratios are main regulators of TCA as well as the energetic metabolism. When ATP-to-ADP ratio increases, citrate synthase and isocitrate dehydrogenase are inhibited, whereas reduction of ATP-to-ADP ratio is activating these two enzymes. An NADH-to-NAD+ ratio increase can also inhibit citrate synthase activity, thereby reducing the carbon flux entering the TCA cycle.

Acetyl-CoA concentration also affects gluconeogenesis since it determines the direction of pyruvate metabolism. When fatty acids are oxygenolyzed, large quantity of acetyl-CoA products can inhibit pyruvate dehydrogenase and makes pyruvate accumulating, which on the one hand provides raw materials for gluconeogenesis, and on the other hand activates the pyruvate carboxylase and thus enhancing gluconeogenesis.

Furthermore, Kozaki proposed that light can also activate plastids ACCase though ferredoxin and thioredoxin intermediate signal transduction, thus inducing the carbon flux to fatty acid synthesis. Under dark condition, ACCase is inactive as an oxidized state. It is this oxidation-reduction cascade system that makes photosynthesis and fatty acid synthesis coupled together, and results in synergy effects of these two physiological responses (Kozaki et al., 2000).

Based on recent information on metabolism and its regulation, applying genetic engineering strategies has become attractive to improve the microalgae lipid content. The U.S. National Renewable Energy Laboratory (NREL) launched the High oil microalgae genetic engineering project in 1991. From this initiative, the role of acetyl CoA carboxylase (ACCase) in the regulation of fatty acids production in microalgae has been clearly identified as a major bottleneck (Bao & Ohlrogge, 1999; Post-Beittenmiller & Roughan, 1992).

However, intuitively, increasing ACCase activity may push an excess of substrate, malonyl-CoA, into the lipid biosynthesis pathway. In 1995 acetyl-CoA carboxylase (ACC) was first isolated from the microalga *Cyclotella cryptica* by Roessler (Roessler & Ohlrogge, 1993) and then successfully transformed by Dunahay *et al*. (Dunahay et al., 1995) into the diatoms *C. cryptica* and *Navicula saprophila*. The ACC gene, *acc*1, was overexpressed with the enzyme activity enhanced by 2–3-folds. This was the first time an exogenous gene transformation system was reported in the algae platform. However, these experiments demonstrated that although ACCase could be transformed efficiently into microalgae, there was no significant increase of lipid accumulation observed in the transgenic diatoms (Dunahay et al., 1995). This negative result suggested that overexpression of the ACCase enzyme alone might not be sufficient to enhance the whole lipid biosynthesis pathway.

Fatty acid synthase (FAS) has been suggested to be another rate-limiting regulator of lipid production, and several studies have been performed where a single enzyme of the FAS complex was selectively overexpressed, however, results show a reduced rate of lipid synthesis when overexpressing 3-ketoacyl-acyl-carrier protein synthase IIIs in plants (Dehesh et al., 2001). While demonstration of protein-protein interactions between the fatty acid acyl carrier protein (ACP) and thioesterase (TE) govern fatty acid hydrolysis within the algal chloroplast, which provide another way to manipulate fatty acid biosynthesis (Blatti et al., 2012). Another successful example of genetic strategies for increasing plant oil levels have come by altering the acyltransferases of TAGs biosynthesis pathway (Jain et al., 2000).

Indeed, with the development of more precise and powerful molecular biology techniques significant advances in microalgae genomics have been achieved during the last decade. Several nuclear genome-sequencing projects have now been completed, including those for *C. reinhardtii* (Merchant et al., 2007), *Phaeodactylum tricornutum* (Bowler et al., 2008), *Thalassiosira pseudonana* (Armbrust et al., 2004), *Ostreococcus lucimarinus* (Palenik et al., 2007), *Ostreococcus tauri* (Derelle et al., 2006), and *Micromonas pusilla* (Worden, 2009). These tools and knowledge have definitely stimulated researchers to progress characterizing the genetic regulation mechanisms of lipid accumulation metabolism and to develop genetic manipulation platforms. Significant achievements in the development of genetic manipulation tools have recently been reported for the microalgal model system (Radakovits et al., 2010), such as intrinsic algal gene silencing mechanisms; albeit repressive histone H3 lysine methylation, DNA cytosine methylation, RNA interference and microRNA-mediated gene regulation for instable foreign transcript or protein degradation (Guihéneuf et al., 2016). However, lipid synthesis pathways is highly regulated in microalgae, which may explain there is so little improvements that have come out of modifying enzymes activity levels. For this reason, it is hypothesized that the use of metabolic models can help understanding how flux regulation limits lipid production increase as well as guiding research to the identification of efficient strategies to perform genetic manipulation (Yu et al., 2011b).

2.3 Mathematical model application in the microalgae cell factory

Predicting the behaviour of microalgae based processes is delicate because of the strong interaction between biology and environmental factors. For example, photosynthesis activity greatly depends on the light accessibility of an algae population, and on the pigment concentration which varies along nutrition states. However, the algae metabolism is quite flexible as it is used to cope with evolving natural environment with light cycle and temperature variations. Therefore, modeling microalgae behavior has to account for its physiology. In this section, mathematical models in algae platform were reviewed. The symbols appeared in different literatures' equations with the same meaning were unified to the same style for the convenience of understanding.

2.3.1 Microalgae growth models

The first models describing microalgae growth in continuous culture was proposed using Jacques Monod kinetics (Monod, 1942), which is based on the assumption that the microorganisms growth

rate is proportional to their consumption rate of an extracellular limiting nutrient (Bernard, 2005). However, it was observed that in microalgae platform cell growth continued after the exhaustion of external nitrogen pool, hypothetically supported by the consumption of intracellular nitrogen pools such as chlorophyll molecules. Therefore, algae cell growth cannot be taken as being proportional to the extracellular medium nutrients content. This phenomenon was first described by Droop (Droop, 1983b; Droop, 1968b). He assumed that unicellular algae growth on a limiting nutrient is ruled by a two-step phenomenon: first, uptake of the nutrient in the cell and then, use of the intracellular nutrient to support cells growth. So, based on this hypothesis, microalgae have the ability to store nutrients into a so-called internal quota "q_n", which is further used for biomass growth. Nitrogen uptake rate ρ(s) can be described by a Michaelis-Menten type kinetics (equation 2.1):

$$\mu(q_n) = \mu_{max}\left(1 - \frac{Q_0}{q_n}\right) \qquad \text{Equation 2.1}$$

$$\rho(s) = \rho_{\max}\frac{s}{K_S + s} \qquad \text{Equation 2.2}$$

whereas the growth rate $\mu(q_n)$ (d^{-1}) can be modelled by Droop kinetics: equation 2.1, (Droop, 1968b). In these expressions, μ_{max} (d^{-1}) is the maximum growth rate, Q_0 (mgN mgC^{-1}) is the quota threshold below which no growth is possible, q_n (mgN mgC^{-1}) is the intracellular nitrogen concentration. Then the nutrition uptake rate $\rho_{(S)}$ is expressed by equation 2.2, where ρ_{max} (mgN mgC^{-1} d^{-1}) is the maximum uptake rates, K_S is a half-saturation constant (mgN mm^{-3}) and S (mgN mm^{-3}) is the concentration of nutrition in cell medium. The Droop model has been widely validated (Bernard & Gouzé, 1999; Droop, 1983b; Sciandra & Ramani, 1994) for its aptitude to predict both biomass and remaining inorganic nitrogen, and a similar approach has also been developed for plant cells (Cloutier, et al. 2009).

2.3.2 Macroscopic model on algae physiology

Microalgae models dealing with nutrition effects

Droop model is a growth model for microalgae, and it was improved by adding nutrient and product terms such as neutral lipids, to predict the lipid production under certain nutritional states and identify optimization strategy between cell growth and lipid accumulation (Mairet et al., 2011b).

Indeed, a dynamical model based on Droop's was developed to predict neutral lipid productivity under nitrogen stress in order to propose an optimization strategy (Mairet et al., 2011b). In this model (Figure 2.3), nitrogen is considered as a part of the internal nitrogen quota (q_n) of nutrient as defined by Droop, and the microalgae specific growth rate is as in equation 2.2.

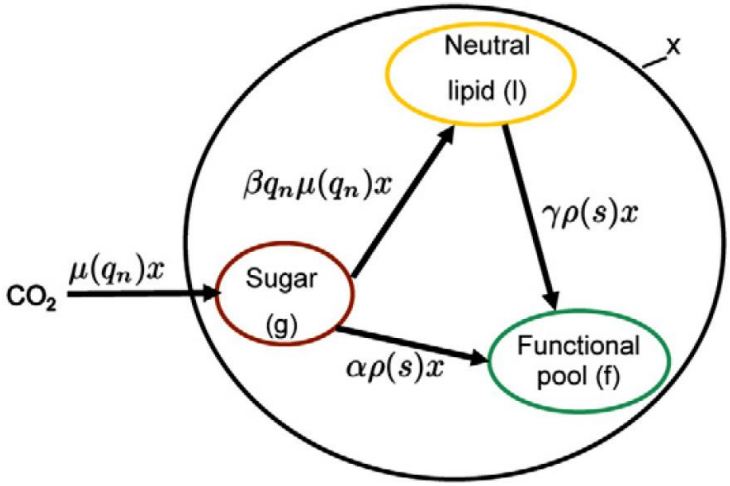

Figure 2. 3 Carbon pools and fluxes hypothesised in the model structure, figure cited from (Mairet et al., 2011b)

The biomass is assumed as the sum of three carbon pools in the cell: functional pool-(f), sugar-(g), and neutral lipid pool-(l) (Figure 2.3). Various intracellular carbon fluxes between these pools are proportional to the nitrogen assimilation rate $\rho(s)$ or the internal nitrogen quota (q_n) as well as the specific growth rate $\mu_{(qn)}$ (Figure 2.3). Therefore, the model structure illustrated in Figure 2.3 can then be written as a system of ordinary differential equations (equations 2.3 (Mairet et al., 2011b)):

$$\begin{cases} \dot{s} = Ds_{in} - \rho(s)x - Ds \\ \dot{q}_n = \rho(s) - \mu(q_n)q_n \\ \dot{x} = \mu(q_n)x - Dx \\ \dot{q}_l = (\beta q_n - q_l)\mu(q_n) - \gamma\rho(s) \\ \dot{q}_f = -q_f\mu(q_n) + (\alpha+\gamma)\rho(s) \end{cases}$$

Equations 2.3

Where D is the dilution rate (d^{-1}), S is the extra-cellular nutrition concentration (mg L^{-1}), "χ" (mg C L^{-1}) is the biomass. The first three equations of this system are exactly those of Droop model (Droop, 1968, 1983), while the dynamics of neutral lipid quota $\dot{q}_l$ (gC gC^{-1} d^{-1}) and functional lipid

quota $\dot{q}_f$ (gC gC^{-1} d^{-1}) were validated by the authors' more recent work; where α (g[C] $g[N]^{-1}$) is the protein synthesis coefficient, β (g[C] $g[N]^{-1}$) is the fatty acid synthesis coefficient, γ (g[C] $g[N]^{-1}$) is the fatty acid mobilisation coefficient. The model connects the lipid production and biomass accumulation as a response of nitrogen states, and predicts an optimal lipid productivity obtained when the specific growth rate was kept at (0.95 d^{-1}). Nitrogen-limited continuous cultures, which allow the control of the cell growth by maintaining a suboptimal nitrogen level (Falkowski & Raven, 2007), could then be used to control the lipid production process, calculating nitrogenous nutrient feed using the authors' nutritional model. However, cell metabolism is not simply pools of products, complex non-linear interactions among metabolic pathways directly affect the final product, and thus such products pool model could not ultimate enable the modulation of the cell metabolism for maximizing cell lipid productivity.

Microalgae models dealing with light effects

The Droop model was further developed by adding other environmental factors such as light and temperature effects. In Droop plus light model, the growth is regulated not only by nitrogen but also by light condition. It was gradually developed to predict biomass, carbohydrate and neutral lipid cell productivities (Mairet et al., 2011a). To introduce the light effect, cell chlorophyll content was related to the nitrogen quota, and its contribution to growth rate was added, meanwhile, photo-inhibition phenomenon and light distribution intensity inside the photobioreactor was also considered. The model kinetics was as follow (Mairet et al., 2011a):

$$\mu(q_n, I) = \bar{\mu}(I)(1 - \frac{Q_0}{q_n})$$

Equation 2.4

$$\bar{\mu}(I) = \tilde{\mu}\frac{I}{I + K_{sI} + \frac{I^2}{K_{iI}}}$$

Equation 2.5

In the light related specific growth rate $\bar{\mu}(I)$ term (d^{-1}) (Equation 2.5), μ̃ is the maximum light related specific growth rate (d^{-1}), *KsI* is the light half saturated coefficient (μmol m^{-2} s^{-1}), *I* is light intensity (μmol m^{-2} s^{-1}) and *KiI* is the light inhibition constant (μmol m^{-2} s^{-1}). The light dynamic effect is related to chlorophyll cell content, which is related to the nitrogen quota. This model has then been successfully used in a "raceway" algae culture pond experiment to optimize the biomass yield, resulting in enhanced biomass and lipid productivities of *Isochrysis aff. galbana* at a 0.5 d^{-1} dilution rate and an inlet feed at a nitrogen concentration over 15 gN m^3.

Different from Barnard's model structure, Packer proposed describing from another mechanism (Packer et al., 2011) in which nitrogen depletion uncouples photosynthesis and growth (Frank & Dubinsky, 1999), thus resulting in the synthesis and accumulation of neutral lipids. In their model, total biomass was divided into two parts as non-neutral lipid biomass (χ) and neutral lipids part (L). Neutral lipid synthesis resulted from an excess of carbon fixation in top of reduced carbon requirements for biomass synthesis. Therefore, when the nitrogen quota (q_n) was consumed to minimum quota (q_0) required for χ, with the increase in total biomass now due to de novo neutral lipids synthesis. This model is described as follow:

$$\mu(x, L, H, S) = \min\left\{\mu_{max}\left(1 - \frac{q_0}{q_n(t)}\right), \frac{p(x,L,H,S)}{c}\right\} \quad \text{Equation 2.6}$$

$$\mathrm{p}(x, \mathrm{L}, \mathrm{H}, \mathrm{S}) = \mathrm{H(t)} p_m(x, L, S)\left(1 - \exp\left(\frac{-a\varphi I(x,H)}{p_m(x,L,S)}\right)\right) \quad \text{Equation 2.7}$$

$$\frac{dx(t)}{dt} = \mu(x, L, H, S)x(t) \quad \text{Equation 2.8}$$

$$\frac{dL(t)}{dt} = [p(x, L, H, S) - c\mu(x, L, H, S]x(t) \quad \text{Equation 2.9}$$

In which χ is the algal biomass concentration excluding neutral lipids (g dw m^{-3}); L is the neutral lipid concentration (g NL m^{-3}); H is the chlorophyll content (g chl g^{-1} dw); S is the extracellular nitrogen concentration (g N m^{-3}). The cell specific growth rate $\mu(x, L, H, S)$ (day^{-1}) is for the non-lipid biomass χ and is constrained from nitrogen or light source (Equation 2.6). Nitrogen limitation condition is described by the Droop model, but when light is limited the growth rate is limited to the "p/c" term (as shown in Equation 2.6 where p (gC $g^{-}d^{-1}$) is the photosynthesis rate in Equation 2.9; c (gC g^{-1}dw) is a fixed proportion of accumulated carbon that contribute to the non-lipid biomass. This model assumption breaks away from Droop's representation of a cell-quota model. The model was validated on experimental data for both biomass (χ +L), neutral lipids (L) as well as the intracellular nitrogen quota (q_n).

More accurate models, which are presented below, have been proposed to deal with the coupling between nitrogen and carbon assimilation under various light conditions (Faugeras et al., 2004; Geider et al., 1998; Pahlow, 2005) (Armstrong, 2006 ; Flynn, 2001; Ross & Geider, 2009), but none of them describes the lipid fraction.

Microalgae models dealing with temperature effects

Light irradiance could induce high temperatures especially in photobioreactors, which could strongly reduce the growth rate. Meanwhile, temperature is also an important factor related to growth and the rate of metabolic reactions. Therefore, a model accounting for the combined effect of light and temperature on algae growth was also developed (Equation 2.10) (Bernard & Rémond, 2012). It is based on a "cardinal temperature model with inflexion" (CTMI) (Rosso et al., 1993), and predicts the growth rate between a temperature (T) range delimited by T_{min} and T_{max} (Equation 2.12), where μopt is the optimal specific growth rate that can be reached at optimum temperature T_{opt} for a light intensity I, and is the function of temperature through the CTMI $\phi(T)$ term (Equation 2.13).

$$\mu(T,I) = \mu_{\text{opt}}(I) \cdot \phi(T)$$ Equation 2.10

$$\mu_{\text{opt}}(I) = \mu_{\text{max}} \frac{I}{I + \frac{\mu_{\text{max}}}{\alpha}\left(\frac{I}{I_{\text{opt}}} - 1\right)^2}$$ Equation 2.11

$$\mu_{\text{max}} = \begin{cases} 0 \text{ for } T < T_{\text{min}} \\ \mu_{\text{opt}} \cdot \phi(T) \text{ for } T_{\text{min}} < T < T_{\text{max}}, \\ 0 \text{ for } T > T_{\text{max}}, \end{cases}$$ Equation 2.12

$$\phi(T) = \frac{(T - T_{\text{max}})(T - T_{\text{min}})^2}{(T_{\text{opt}} - T_{\text{min}})[(T_{\text{opt}} - T_{\text{min}})(T - T_{\text{opt}}) - (T_{\text{opt}} - T_{\text{max}})(T_{\text{opt}} + T_{\text{min}} - 2T)]}$$ Equation 2.13

The optimal specific growth rate can then be determined using the model and at selected culture temperatures, such as illustrated below:

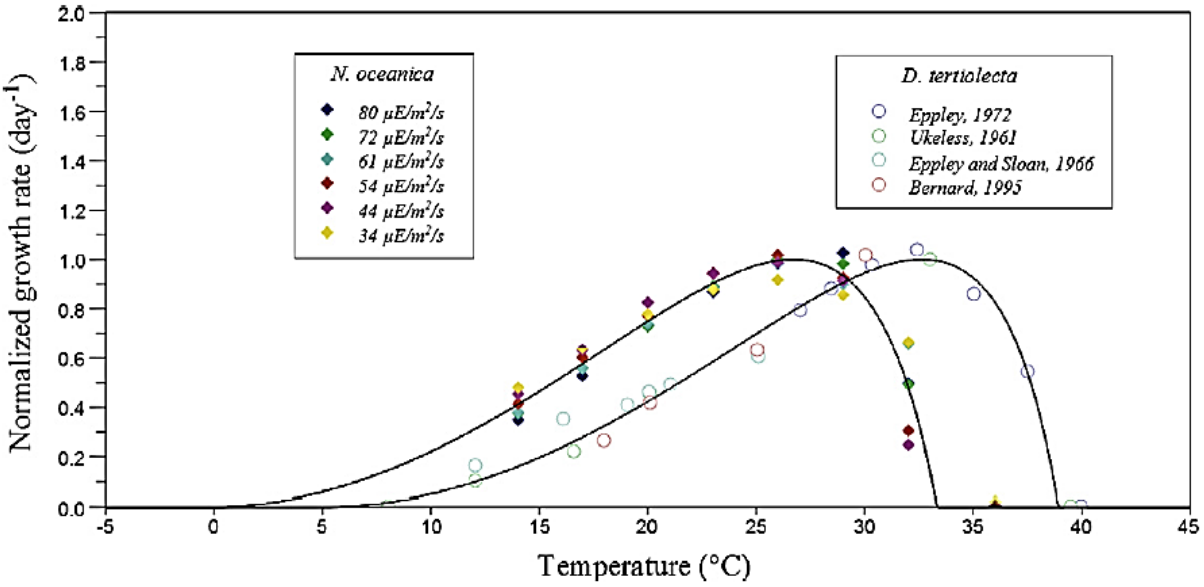

Figure 2. 4 Normalized model predictions (continuous line) for heterogeneous data of D tertiolecta (open circles), in different growth conditions from various authors and *N. oceanica* (diamonds) at different light intensities (Sandnes et al., 2005). This figure is cited from (Bernard & Rémond, 2012).

2.3.3 **Metabolic modelling**

The models discussed so far describe cell behaviour at a general macroscopic level and do not consider precise knowledge on intracellular carbon flux distribution from the carbon substrates to the lipid production. The challenge at developing a model that can describe microalgae cell processing of carbon substrates into desired lipid product relies on the description of the biochemical reactions network involved. However, such as for other cell types, there are peculiarities making microalgae cells tedious to describe at the metabolic level. If the previously discussed carbon flux distribution problem between lipid or cell synthesis pathways may be encountered in other cell biosystems, their metabolic flexibility (autotrophic, mixotrophic, heterotrophic) add a layer of flux regulation complexity.

Although macroscopic physiological models based on cell nutrition management were successful for identifying culture conditions favoring lipid accumulation, they still fail to solve the fundamental conflict between cell growth and lipid accumulation. Therefore, the optimal utilization of microalgae as cell factory for biodiesel production requires a better understanding of the

interaction between the energetic metabolism, carbon fixation and assimilation pathways (Muthuraj et al., 2013). It is thus clear that a deeper understanding of cell metabolic behavior can allow a fine control of microalgae bioprocess, and a biologically reliable mathematical model would be a unique tool to evaluate maximum theoretical product yield and to help developing optimal control strategies (Navarro et al., 2009). Recent genomics, proteomics and metabolomics data that are now more and more available enable exploring novel ways to describe and characterize microalgae biosystem behavior, in complement to the nutritional models. Having in hand data sets on extracellar medium composition with time, a metabolic flux analysis (MFA) method allows studying the topological characteristics (flux distribution) and functional properties (metabolic limitations) of a metabolic network with known stoichiometry. Looking at optimal metabolic flux sets, a flux balance analysis (FBA) (Harris, 1999), which is based on linear programming, can then be performed, where constraints are considered to restrain the resolution of the possible metabolic flux network within a possible space of solution. Both MFA and FBA approaches are based on cells with their intracellular metabolic intermediates at steady-state and allow estimating metabolic flux rate values. The general mass balance equation of a biosystem is as follow:

$$\frac{dx}{dt} = S \cdot v = 0 \qquad \text{Equation 2.14}$$

Where x is the concentration of each metabolite; S represents matrix of the stoichiometric coefficients of the metabolites considered. It has the dimension of (c×r), where c is the number of metabolites and r is the number of reactions. v is the vector of the fluxes through the r bio-chemical reactions. FBA approach is illustrated below: first, it needs a genome-scale metabolic network reconstruction, then the stoichiometric of each biochemical reactions and the constraints for fluxes were represented mathematically, the mass balances of metabolites were defined as a system of linear equations and objective functions were defined to predict the optimum condition (maximum biomass), and finally calculate fluxes that maximize the objective function.

FBA study has been performed in cyanobacteria *Arghrospia platensis* (Cogne et al., 2003) to identify the metabolic network structure and support the existence of a metabolic shunt of PEP to pyruvate through several enzymes to convert $NADH,H^+$ into $NADPH,H^+$. FBA model in *Synechocystis sp*. PCC 6803 (Fu, 2009) was used to predict cell behavior after the insertion of ethanol fermentation pathway, and simulation of cell growth and ethanol production all showed a

satisfactory agreement with experimental data. FBA was also successfully used in higher eukaryote algae *Chlamydomonas reinhardtii* (Boyle & Morgan, 2009; Kliphuis et al., 2012), as well as in *Chlorella sp.*(Muthuraj et al., 2013). For example, Boyle's FBA study of *Chlamydomonas reinhardtii* under three culture conditions (autotrophic, mixtrophic and heterotrophic) included a metabolic network containing 484 metabolic reactions and 458 intracellular metabolites. Except regular carbon metabolism, reactions also included cellular energy production which comes from either photosynthesis or oxidative phosphorylation by consuming organic carbon source. The optimization constraint criteria consisted in finding the flux distribution maximizing biomass at minimum energy usage (light or organic carbon source), it finally predicted the biomass yields ranged from 28.9 g per mole C for autotrophic growth to 15 g per mole C for heterotrophic growth (Boyle and Morgan 2009). FBA approach was also specifically used to characterize CO_2 time-evolution behavior, which reveals that respiration is not always the dominant source of CO_2, and that metabolic processes such as the oxidative pentose phosphate pathway (OPPP) and lipid synthesis can be quantitatively important (Sweetlove et al., 2013). However, as the author indicated, FBA is poor at predicting flux through certain metabolic processes such as the OPPP, which may due to limited number of experimental systems that are suitable for the more tractable steady-state stable isotope FBA approach. Indeed, FBA model only capable of determining fluxes at steady state. Typically, FBA does not account for regulatory effects such as activation of enzymes by protein kinases or regulation of gene expression. Therefore, its predictions may not always be accurate.

Estimation of carbon flux distribution via metabolic flux analysis (MFA) or flux balance analysis (FBA) relies on the pseudo steady state approximation. However, as we previously discussed, microalgae is hardly at steady state. Cells accumulate and reuse energy, carbon and nitrogen along a culture. A model capable to describe transient conditions may then be more biologically reliable. To this end, an improvement of the steady state approaches resides in the dynamic flux analysis (dFBA) approach, which connected two steady states by incorporating the rate of change in flux constraints (Mahadevan et al. 2002). The kinetic of substrate utilization, growth and intracellular biomass composition are require as the input of intracellular flux balance analysis over the exponential growth phase, which manipulations turn the original approach into a time-varying FBA (dFBA). A schematic representation of the approach is illustrated in figure 2.8.

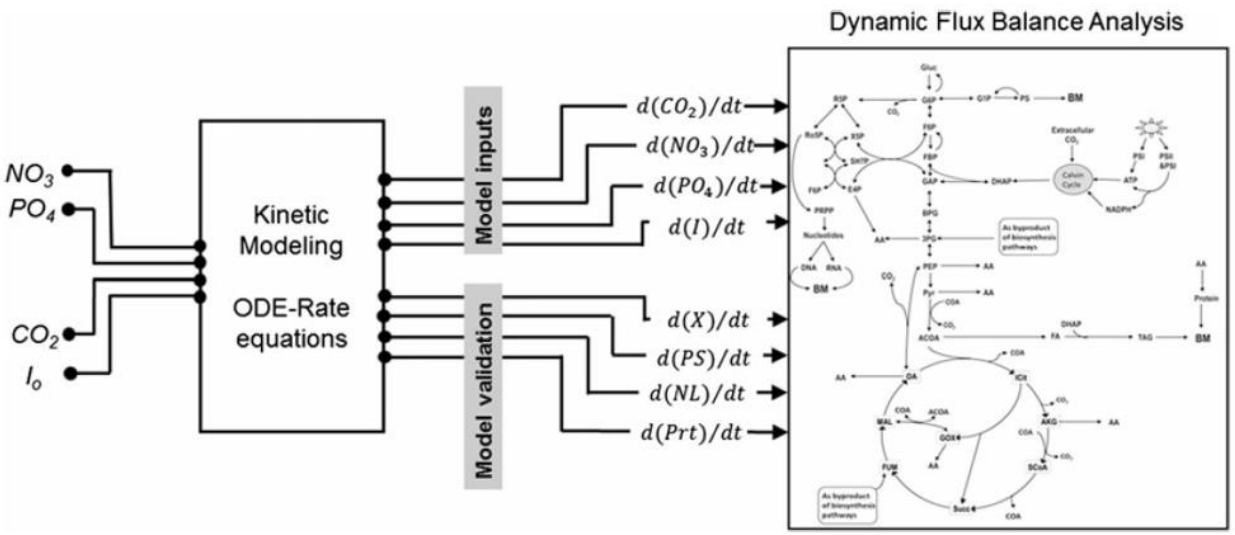

Figure 2. 5 Schematic representation of the steps involved in the dFBA. The dFBA consists of three steps: (i) development of kinetic model to predict dynamic profile of extracellular substrates, growth, and intracellular biomass composition; (ii) estimation of kinetic parameters by fitting simulated dynamic profiles with the corresponding experimental values; and (iii) integrating dynamic reaction rates (fluxes) predicted by kinetic model as inputs for dFBA. This figure is cited from (Muthuraj et al., 2013).

A dynamic flux analysis (dFBA) was carried out to capture light–dark metabolism over discretized pseudo steady state time intervals in *Chlorella* sp (Muthuraj et al., 2013). Results show flux distribution during transition period was toward nongrowth associated (NGA) maintenance energy, oxidative phosphorylation, and photophosphorylation; meanwhile, a shift in the intracellular flux distribution was also predicted during transition from nutrient sufficient phase (72h of cultivation) to nutrient starvation phase (96h of cultivation). However, the steady state based dFBA modelling does not include the true dynamics of the metabolic fluxes, which are represented by kinetic parameters, and thus it cannot predict metabolite concentrations. The addition of kinetic parameters to describe each flux kinetics may allow analyzing complex time-dependent dynamics in microalgae metabolic biosystem.

2.4 Kinetic metabolic modelling

Kinetic modeling (Ghorbaniaghdam et al., 2013; Shinto et al., 2008), however, can make up this shortness, because they can describe time-based perturbations and complex enzymatic and gene interactions. Nowadays, kinetic metabolic modeling opens the black box of internal microbial metabolism (Cloutier et al., 2008; Cloutier et al., 2009; Cloutier et al., 2007), it includes the dynamics of enzymatic reactions, which are time dependent and relies on the enzyme kinetics. It can comprehensively provide the real time metabolic flux fluctuations and provide more precise site of key metabolic processes for genetic manipulation, and in the other hand, provide a preferable but balanced nutritional strategy to optimize the culture conditions favoring aimed products (Cloutier et al., 2009).

However, its application in microalgae is relatively new, since previously few algae have been genome sequenced and annotated (Curtis et al., 2012), the biochemical information such as enzyme kinetic parameters are relatively limited (Surendhiran & Sirajunnisa, 2015). Along with the development of algae biochemistry, genomic information and biochemistry, analysis methods, and kinetic parameters in algae platforms sprung up in the recent years.

So now it's quite urgent that a kinetic model combing metabolomics and biological kinetics can be done; Make the model play its significant role in operating lipid synthesis both in nutrient strategy and potential genetic manipulation strategy. To our best knowledge, the current model in this thesis is the first kinetic metabolic modelling in algae platform. It will be used to provide the real time metabolic flux fluctuation and provide more precise sites for genetic manipulation, and as a tool, provide a preferable but balanced nutritional strategy to optimize the culture conditions favoring lipid production.

2.5 Lipid extraction method greatly impact on the final extraction yield

Amelioration of lipid extraction protocols is a step considered as one of the major bottlenecks for commercial-scale biodiesel production (Guldhe et al., 2016). However, limited attention has been put on this effort (Araujo et al., 2013; Li et al., 2014; Ranjan et al., 2010). Significant amounts of lipids are trapped in the cytoplasm by the cell walls and membranes, so lipid extraction efficiency

greatly depends on cell disruption technique as well as on the polarity of the solvents used to remove lipids from the cell water phase (Burja et al., 2007; Hamilton et al., 1992; Lee et al., 2010; Lewis et al., 2000).

Various methods have been proposed to break down cell wall and release trapped lipids in algae platforms, e.g. Ultrasound was proved to be a very efficient cell wall disruption method (Araujo et al., 2013), with fragmentation efficiency over 90 % after a 12 min ultrasonic treatment (Araujo et al., 2013; Wang et al., 2007). For comparison, a low shear stress approach such as using a hydrocyclone only leads to ~10 % cell lipids extraction efficiency but microalgae cells remain viable (Dommange et al., 2015). "Green solvents" such as 1-butyl-3-methylimidazolium chloride are hydrophilic ionic liquids that were investigated for their ability to dissolve low concentrations of cellulose, which compose about 1 % by mass of the whole algae cell. These solvents are thus capable of lysing microalgae cell walls and microalgae vesicle membranes to form two immiscible layers, one of which consists of the lipids released from the lysed cells (Salvo, 2011a). This method enables to disrupt cell wall and lipid separation in a single step, and currently obtained interest.

Overall, the solvents perform lipid extraction, which also determine the extraction efficiency. A short series of solvent-based methods have been largely used to perform lipid extraction from various biological materials. The Folch method (Folch et al., 1957) consists in using chloroform-methanol (Chl/Met), and then the extracted solvent (chloroform) is washed with water to remove non-lipid substances. Bligh & Dyer then proposed a method based on Folch's combining chloroform, methanol and water (Chl/Met/H_2O), for lipid extraction from a wide range of biological materials (Bligh & Dyer, 1959). More recently, because of concerns on biosafety, a less hazardous solvent mixture of dichloromethane/methanol (Dic/Met) has been proposed by Cequier et al. (Cequier-Sanchez et al., 2008) as a substitute for Bligh & Dyer method. In addition, Drochioiu proposed a fast lipid assay with acetone extraction and turbidimetric reaction with sulfosalicylic acid, which requires only few milligrams of dry samples compared to grams for the above-mentioned methods, which limits their application to pilot and large scale production facilities (Drochioiu, 2005). These methods can be considered as references, or classical, in the field. However, different microalgae species show different extraction efficiency using different extraction systems (Araujo et al., 2013) (Ryckebosch et al., 2012a) (Li et al., 2014) (Grima et al., 1994). As it can be seen, lipid extraction efficiency differs with biomass type as well as with the solvent mixture. Thus specific lipid extraction method could help to increases cell material

disruptions with an enhancement of lipid release from the cell. For example some solvents like ionic liquids could help to hydrolyze cellulose and hemicellulose in the wall.

CHAPTER 3 METHODOLOGY

3.1 Culture species and cultivation methods

The freshwater algae *Chlorella protothecoides* screened from Professor Réjean Tremblay's Lab at Universite du Quebec à Rimouski (UQAR) will be used in this study. Since this algae species can afford three different metabolism, which are autotrophy, mixtrophy and heterotrophy. It is one of the most metabolic diverse and robust species found in literature. The lipid content in *Chlorella protothecoides* can reach up to 40 % of cell dry weight. The major fatty acid components (C16:1, C16:0, C18:1, C18:0) can be a source for biodiesel.

The culture medium was the modified basal medium (Xiong, 2008) containing glycine, yeast extract as nitrogen source, and sufficient amounts of inorganic supplements, including KH_2PO4 (0.7 g/L), K_2HPO4 (0.3 g/L), $MgSO_4 \cdot 7H_2O$ (0.3 g/L), $FeSO_4 \cdot 7H_2O$ (0.003 g/L), H_3BO_3 (0.00286 g/L), $MnCl_2.4H_2O$ (0.00181 g/L), $ZnCl_2$ (0.000105 g/L), Na_2MoO_4 $2H_2O$ (0.000039 g/L), $CuSO_4$ $5H_2O$ (0.000079 g/L), and $CoCl_2$ (0.000030 g/L). Autotrophic, heterotrophic, and mixotrophic flask cultures of *C. protothecoides* were carried out in 2.8L Erlenmeyer flasks containing 1L of the culture medium. And 1 % of glucose (10 g L^{-1}) is added to heterotrophic and mixotrophic culture. Light was provided for autotrophic and mixotrophic cultures with the intense of 60 μmol m^{-2} s^{-1}. 5 % CO_2 was provided to all the cultures. While heterotrophic cells were kept under the dark. The culture medium was always sterilized before the inoculation and then was inoculated exponentially growing microalgae from non-glucose based cultures to reach an original cell density as one million. Cultures were kept at 28 ℃, 150 rpm for 10days. Cell density of culture samples was determined in triplicates by cell counting using a hemocytometer. Culture medium was centrifuged at 4,000 *g* for 10 min., and the collected biomass were vacuumed (remove extra water) and weighed for fresh weight; fresh cell pallets were further freezed dry (VirTis, Advantage Plus EL-85) to determine the dry weight. Cultures were sampled every day and centrifuged, the suspension was kept at -80 ℃ for extracellular analysis and the cell pellets were washed twice with distilled water and then their metabolism was quenched by adding 500 ul 80 % MeOH.

3.2 Metabolomics extraction and analysis

Metabolomics analysis of cell metabolites include metabolic intermediates and energetic and redox nucleotides. The main steps consist in the sampling of the cell suspension, cell separation from the

medium, extraction of metabolites and then the chemical identification and quantification. The nutrient composition and extracellular metabolites in cell medium was obtained after cell separation from the suspension. Cell extraction of metabolites was developed based on the cold methanol method: 10 ml cell culture were harvested by centrifuge at 4℃ for 10 min at 21,000 *g* (Samples suspension were kept for glucose, amino acids and ions analysis) and washed twice by 10 ml of 4 ℃ pre-cold de-ionized (DI) water in centrifuge tube. And separated by 0℃ pre-cold centrifuge at 21,000 *g* for 10 min. Supernatant was drained to the waste tank to keep a small amount of liquid and then removed by 1ml pipette with care. Cell pellets were re-suspended in 0.5 ml DI water and were transferred to 1.5ml micro centrifuge tube, repeating this until all the cells were transferred. Then collect the cell pellets by centrifuge at 21,000 g for 10 min. Supernatant was removed by 1ml pipette with care. After removing medium substrate by the washing steps, 0.5 ml of pre-cold 80% methanol was pipetted onto cell pellet to quench the cell by precipitating enzyme protein. Tube was vigorously homogenized with mini vortexer (Fischer Scientific) for 1-2min. By this step, all the biochemistry reaction was stopped. Then the suspension was put in the ultrasound bath (Crest, 1000 W, 20 kHz) with ice for 30 mins. Then the mixture were centrifuged (Eppendorf centrifuge, maximum speed for 10 min at 4 ℃). The supernatant was transferred into a 1.5 ml centrifuge tube on ice. 0.5 ml 80% cold methanol was added to pellet and vertaxed again. Then the tube was put in the ultrasound bath with ice for 30 mins and centrifuged again. The supernatant was added to the first one. Combined supernatants were passed through 0.2 μm filter (Millipore, Etobicoke, Canada) and stored at -80 ºC for further analysis of nucleotides (analyzed in one shot) and sugar phosphates & organic acids (sugar phosphates and organic acids analysis was carried out in another shot) by UPLC/MS/MS. The cell residue was used to do the starch analysis.

3.2.1 **Glucose analysis**

Samples suspension was used to detect glucose. The analytical method is enzyme-based via oxidization of the analyte by the enzyme immobilized on a membrane. Samples were automatically detected by a dual-channel immobilized oxidase enzyme biochemistry analyzer (YIS 2700 select, YSI Inc. Life Sciences, USA); the analyzer was calibrated with standard glucose when the equipment was started, and then calibrated again for every 6 samples.

3.2.2 Amino acids analysis

Extracellular amino acids analysis was chemical-based method, samples were separated on a solid phase due to different physiochemical properties. Samples suspension was diluted with 70 % MeOH for 200 times, then mix it with ISTD of ratio 1:1. Filter the mixture to a sample vial using 0.22 um filter before analysis, and then 5 µl sample was injected to 1290 UPLC system coupled to a 6460 triple quadruple mass spectrometer in negative ion mode (Agilent Technologies, Santa Clara, CA, USA) (Ghorbaniaghdam et al., 2013). Samples were separated by a 2.1 × 150 mm ZIC^{TM}-Hilic column (3.5 mm, 200 A, PEEK) (Merck SeQuant, Peterborough, Canada) and 2.1 × 20 mm ZIC^{TM}-Hilic guard column (5 mm, 200 A, PEEK) (Merck SeQuant, Peterborough, Canada). The flow rate of mobile phase was set at 0.1 mL min^{-1}. The mobile phase (20 mM NH_4AC at pH 4 in acetonitrile) was linearly decreased from 90% to 35% in the first 19 min, then was increased to 90% in one minute and held at 90% for 15 mins. The mass spectrometer was set at gas temperature 350 ℃, scan time 100 ms, flow rate of 9 L min-1; pressure at 45 PSI and capillary voltage of 3000 V. Internal standard was used for quantification.

3.2.3 Intracellular metabolites analysis

Sugar phosphates and organic acids analysis was done in one shot (Ghorbaniaghdam et al., 2013). Cell extraction of metabolites was injected and analyzed on the UPLC/MS/MS system (Agilent, Montreal, Quebec, Canada) in negative ion mode. And passed through a Hypercarb pre-column (2.1610 mm, 5 mm) and a Hypercarb column (100 × 2.1 mm, 5 mm) (Thermo Fisher, Burlington, Canada). The mobile phase including buffer A: 20 mM ammonium acetate at pH 7.5 and buffer B 10 % v/v menthol/water. The completed separation condition is as follow: 0-5 min with 10 % buffer A. 5-10 min with linear gradient buffer A from 10% to 20%. 10-20 min with linear gradient buffer A from 20% to 100%, 20-30 min with 100% buffer A, 30-32 min with linear gradient buffer A from 100% to 10% and 32-40 min with 10% buffer A. The flow rate was constant at 0.3 mLmin^{-1}. The mass spectrometer was set at gas temperature 300 ℃, scan time 100 ms, flow rate of 7 L min^{-1}; pressure at 35 PSI and capillary voltage of 3500 V. The quantification of the metabolites were compared with standard stock solutions.

Nucleotides were analyzed separately as another shot on the UPLC/MS/MS system (Agilent, Montreal, Quebec, Canada) in positive ion mode. Cell extraction was passed through a symmetry C18 column (150 × 2.1 mm, 3.5 mm) (Waters, Milford, USA). The mobile phase including 10 mM

ammonium acetate (Buffer A), 15 mM DMHA at pH 7.0, 50/50% (v/v), acetonitrile (Buffer B) and 20 mM NH_4Ac at pH 7.0. Flow rate was set at 0.3 mL min^{-1}, with different gradient of mobile phase: 0-10 min with 10% B, 10-20 min at linear gradient of buffer from 10 to 30% B, 20-21 min at linear gradient from 30 to 60% B, 21-26 min at 60% B, 26-27 min at linear gradient from 60 to 10% B and 27-35 min at 10% B (Ghorbaniaghdam et al., 2013). Mass condition was set as the same as mentioned above. External standard curve was used for quantification.

3.2.4 **Ions analysis**

Liquid suspension media was passed through 0.2 µm filter before analysis on the Dionex ion chromatography system in conductivity mode (Dionex Canada Ltd., Oakville, Canada) as previously described (Lamboursain & Jolicoeur, 2005). Anions was separated at 4mm × 250 mm IONPAC AS14A-SC analytical column with mobile phase (2 mM Na_2CO_3 and 1 mM $NaHCO_3$) at 1.0 mL min^{-1} flow rate. Cations were separated using 4mm × 250 mm IONPAC CS-12A column with mobile phase (methanesulfonicsolution 20 mM) flowing at a 0.9 mL min^{-1}. The ion concentrations were calculated by the calibration curve which is the standard ion concentration plotted vs. peak area.

3.2.5 **Starch analysis**

Starch cell content was analyzed by the starch assay kit (Sigma-Aldrich, St. Louis, MO, USA), as previously described (Lamboursain & Jolicoeur, 2005). The cell pellets obtained from intracellular metabolites extraction were re-suspended in 1 mL ddH_2O and sterilized at 121 °C for 15 min. Samples were cooled down at room temperature and the volume was readjusted to 1 mL with ddH_2O. Then it was diluted 1:1 with the amyloglucosidase solution of the starch assay kit and incubated for 30 min in an ultrasound bath at 60 °C. The supernatant was collected and detected by a biochemistry analyzer (YSI Life Science, Yellow Springs, OH, USA).

3.2.6 **Lipid extraction and analysis**

The analysis of total lipid was based on the method developed by Drochioiu Gabi (Drochioiu 2005). 10 mg of dried cells were extracted by 1 ml acetone under ultrasound in ice water for 30 mins; 0.1 ml supernatant of the mixture was introduced into a micro-centrifuge tube containing 0.9 mL 1.5% sulfosalicylic acid; then the absorbance of the mixture was detected at 440 nm by UV-VIS

determination (UNICAM 8625, UV/VIS). A standard curve was constructed using quantity known-raw lipid extracted from the species.

3.2.7 Fatty acids composition analysis

Fatty acids composition was analysed by a multichannel gas chromatograph "Trace GC ultra" (Thermo Scientific) equipped with a mass detector model ITQ900 (Thermo Scientific). An Omega wax 250 (Supelco) capillary column was used for the separation with high purity helium as a carrier gas. The internal standard 19:0 was added to samples and fatty acid methyl esters (FAME) were prepared before injection according to the method using sulphuric acid and methanol (2:98 v/v) at 100°C for 10 min. FAME were identified and quantified using known internal standards (Supelco 37 Component FAME Mix and menhaden oil; Supleco).

3.3 Model development

As the first step in the development of a mathematical model of the cell metabolism, the metabolic network must be known. Nowadays, the genome sequence and annotation have been published for many microalgae. Based on databases that include metabolic reaction pathways such as KEGG, MetaCyc, DiatomCyc, BioCyc, and the established metabolic network model for other microalgae in literature, a metabolic network model was reconstructed specifically for *Chlorella protothecoides*.

The metabolic modelling *in silico* framework already developed in our lab was adapted to cope with microalgae growth and lipid production process. Full kinetic equations were used to describe metabolic reactions and pathways conducting from substrates including CO_2/glucose, to lipids and biomass. Flux kinetics and mass balances were carried out based on stoichiometrics of each reaction, it included kinetic terms of regulation of metabolic reactions. So this tool draws a clear map of the metabolic processes and regulation that helps us understand it well. The modelling *in silico* framework was carried out in Matlab (the MathWorks Inc., Natick, MA, USA), all the model equations will be solved in this platform to get the metabolic fluxes rates.

The original kinetic parameters (Vmax, Km) for each reaction and enzymes in the model were gained from BRANDE. However, during the model modification and validation process, we need to provide abundance of experimental data according to model variables. These analyses were carried out by HPLC-MSMS, Ion-FID etc. in our assay lab. Then these experimental results helped

to adjust parameter values and modify the model to best simulation result. Then sensitivity analysis was used to allow a statistical analysis of estimated model parameters. And the model was validated by estimating the confidence interval of the calibrated parameters. Details of modelling development, model structure calibration, parameter estimation and model validation can be found in Chapter 5 in Material and methods section.

CHAPTER 4 ARTICLE 1: GLUCOSE FEEDING RECALIBRATES CARBON FLUX DISTRIBUTION AND FAVOURS LIPID ACCUMULATION IN CHLORELLA PROTOTHECOIDES THROUGH CELL ENERGETIC MANAGEMENT

Xiaojie Ren[a], Jingkui Chen[a], Jean-Sébastien Deschênes[b], Réjean Tremblay[b], Mario Jolicoeur*[a]

[a] Research Laboratory in Applied Metabolic Engineering, Department of Chemical Engineering, École Polytechnique de Montreal.

[b] Université du Québec à Rimouski, 310 allée des Ursulines, Rimouski, Québec, G5L 3A1, Canada.

(Published in Algal Research -2016, Vol. 14, p: 83–91)

---

*Corresponding author. Address: P.O. Box 6079, Centre-ville Station, Montreal, Quebec, Canada. H3C 3A7; Telephone: 514 340 4711 x4525; fax: 514 340 4159; e-mail: mario.jolicoeur@polymtl.ca

4.1 Abstract

Heterotrophic culture of some algal cells is now known as an efficient avenue for lipids production. However, the mechanism involved is not clearly understood, especially when feeding glucose concurrently to an autotrophic culture. In this work, the time course dynamics of central carbon metabolites of *Chlorella protothecoides* was studied in autotrophic, heterotrophic and mixotrophic culture modes to elucidate the glucose regulation effect. Results show that assimilated CO_2 mainly goes to the synthesis of upstream carbohydrate-based metabolites under autotrophic condition, while supplementing glucose recalibrates the metabolism toward downstream metabolites and lipids, rather than carbohydrates accumulation. The analysis of the lipid class shows, under glucose supplementation, that cells accumulate neutral lipids as storage rather than as membrane polar lipids, while fatty acids composition changes from polyunsaturated to saturated and monosaturated, which shows improving the quality of biodiesel precursors. The metabolic flux rearrangement seemed being regulated by a high cell energetic state that was maintained by a glucose metabolism. A high initial ATP-to-ADP ratio was observed after adding glucose, suggesting cell energetics as a biomarker of a metabolic shift from starch to lipids accumulation. These findings thus bring novel data on the regulation of carbon flow in microalgal cells, and enhance our understanding of microalgae as a lipids production platform.

4.2 Keywords

Chlorella protothecoides; autotrophic; mixotrophic; heterotrophic; carbon metabolism; energy metabolism

4.3 Introduction

Microalgae has received a renewed attention in the recent years for its high potential of lipids production, in the context of biodiesel market, as well as for specific fatty acids of high interest for the cosmeceutical and neutraceutical industry [1]. Algal cells are built to assimilate CO_2 as their sole carbon source under light. However, many microalgae species have the membrane transport systems to uptake and catabolize organic substrates as carbon and energy sources [2].

Chlorella protothecoides is a microalga that can grow either photoautotrophically, mixotrophically or heterotrophically [3]. With the addition of glucose in a fed-batch heterotrophic bioreactor culture, *C. protothecoides* reached 16.8 g L^{-1} of biomass having a crude lipids content of up to 55.2 %. This result represented about four times the lipids level observed in photoautotrophic cultures [4]. *C. protothecoides* has also been cultured mixotrophically when organic carbon as well as CO_2 and light are provided at the same time, and showed a similar growth rate than for heterotrophic culture (0.04 h^{-1}), but which was over 10X higher than under autotrophic mode (0.005 h^{-1}) [3].

Lots of researches have been done on the impact of glucose on algae growth and photosynthetic activities [5, 6]. Glucose was reported to be able to reduce CO_2 apparent affinity in *Chlorella* sp.VJ79 [7] and *C. vulgaris* UAM101 [8]. It was shown to negatively impact on the synthesis of RuBPase and light related phycocyanin-PC involved in Calvin cycle [9]. Indeed, organic carbon supplement have shown to induce metabolic differences in both respiration and photosynthesis in cyanobacteria [10]. Little is known, however, on the differences taking place at the metabolic level of cultivating algal cells under autotrophic, heterotrophic and mixotrophic culture modes. A metabolic flux analysis (MFA) was carried out in *Synechococcus* sp., it was found the glycolysis, TCA cycle, and oxidative phosphorylation fluxes were affected when glucose was added in the autotrophic culture [11]. However, for the microalgae *C. protothecoides*, which shows a high industrial potential for producing lipids and fatty acids at high yield, only sparse and incomplete datasets are available in literature on the effect of feeding concurrently glucose to autotrophic.

In the present study, we have thus focused describing how *C. protothecoides* metabolism adapts while varying the carbon source. The microalgae was cultivated under autotrophic, mixotrophic and heterotrophic conditions. A metabolomics strategy was applied to investigate the effect of the carbon source on the central carbon metabolism, integrating lipids synthesis as well as the cell energetic state, for the three culture modes. Therefore, this study unravels the metabolic mechanism

of glucose impact on the carbon flux distribution and thus improves the understanding of the links between central carbon fluxes and lipids metabolisms in this microalgae.

4.4 Material and methods

4.4.1 Algal strain and culture conditions

All cultures of *Chlorella protothecoides*, either under autotrophic, mixtrophic or heterotrophic conditions, were performed in 2.8-L glass flasks (PYREX) at 28°C under continuous orbital agitation (150 rpm) in a Multitron II incubator (Infors-HT, Bottmingen, Switzerland). Modified basal medium (MBM) [4] adjusted at an initial pH of 7 was used in all cultures and modified as described below. Glucose was added at 1 % w/v (10g L^{-1}) under mixotrophic and heterotrophic modes. Light was provided for autotrophic and mixotrophic cultures with the intense of 60 µmol m^{-2} s^{-1}. CO_2 was controlled at 5 % in all cultures. Heterotrophic cultures were kept under dark conditions in the same CO_2 incubator; the body of flasks being covered with double layer aluminum foil to avoid light penetration. Exponentially growing cells were inoculated in fresh media at $1x10^6$ cells mL^{-1}. Each flask was sampled every 24 h in a sterile biological hood.

4.4.2 Cell density and biomass estimation

Cell density of culture samples was determined in triplicates by cell counting using an hemocytometer. Culture medium was centrifuged at 4,000 *g* for 10 min, and the collected biomass were vacuumed (remove extra water) and weighed for fresh weight; fresh cell pallets were further freezed dry (VirTis, Advantage Plus EL-85) to determine the dry weight.

4.4.3 Intracellular metabolites extraction and analysis

Cell extraction and analysis of metabolites was developed based on the cold methanol method previously described by Ghorbaniaghdam et al. [12] on the UPLC MS/MS system (Agilent Technologies, Santa Clara, CA, USA). Only modificatons are mentioned here: 10^9 cells pellets were used here for each analysis. Extraction was performed by ultrasonication in ice water for 30 mins and centrifugation at 4℃ for 10 min at 21,000 *g*. The supernatants were filtered by 0.2 µm milipore filter and stored at -80 ºC for nucleotides, sugar phosphates and organic acids analysis [12]. The cell residue was used to do the starch analyis (see below).

4.4.4 Amino acids analysis

Culture media suspension was passed through 0.2 μm filter to do amino acids analysis. The analysis was performed on the UPLC MS/MS system as described previously [12].

4.4.5 Ions analysis

Liquid suspension media was passed through 0.2 μm filter before analysis. Dionex ion chromatography system (Dionex Canada Ltd., Oakville, Canada) equipped with a 4mm×250mm IONPAC AS14A-SC analytical column was used to separate and quantify the anions as previously described [13].

4.4.6 Starch analysis

Starch cell content was analyzed by the starch assay kit (Sigma-Aldrich, St. Louis, MO, USA), as previously described [13]. The hydrolyzed supernatant was collected and detected by a biochemistry analyzer (YSI Life Science, 2700 select, Ohio, USA).

4.4.7 Glucose analysis

1 ml culture media suspension was analyzed by a biochemistry analyzer (YSI Life Science, 2700 select, Ohio, USA) for the glucose concentration.

4.4.8 Total lipids extraction and analysis

The extraction procedure was developed by Gabi [14]. Briefly, 1 mg of dried cells were extracted with 1 mL acetone under ultrasound in ice water for 30 min. 0.1 mL of the supernatant of the mixture was introduced into a micro-centrifuge tube containing 0.9 mL of 1.5 % sulfosalicylic acid; then the absorbance of the mixture was detected at 440 nm by UV-VIS determination (UNICAM 8625, UV/VIS).

4.4.9 Lipids and fatty acids composition analysis

Lipid and fatty acids composition analysis were done in Professor Réjean Tremblay and Jean-Sébastien Deschênes's lab in Rimouski, Quebec, Canada, following the method previously described [15].

4.5 Results and discussion

4.5.1 Growth rate and biomass yield are enhanced in presence of glucose

C. protothecoides was cultivated in autotrophic, mixotrophic and heterotrophic batch cultures (Figure1). As expected, the cell concentration rapidly increased for reaching a plateau of 1.81E+8 ± 7E+6 cell mL^{-1} after 72 h in both cultures with glucose, while the autotrophic culture required more than 2.7 times longer to reach, however, a similar maximum value (Figure 1a). The cells maximum specific growth rate in heterotrophic (0.154 ± 0.007 h^{-1}) and mixtrophic (0.145 ± 0.021 h^{-1}) cultures were similar but significantly higher than that in autotrophic culture (0.104 ± 0.018 h^{-1}) (F_{MH}=3.473, p=0.2033>0.05; F_{AMH}=13.642, p=0.0391<0.05); The sum of this value under heterotrophic and autotrophic modes was not corresponding to that under mixotrophic mode, which differs from the observations reported for *C. regularis* [16] and *C. vulgaris* [17, 18]. The respective metabolisms of photosynthesis and oxidative phosphorylation of glucose are thought to function independently in *C. vulgaris* [17], which may explain a cumulative growth rate in mixtrophic culture. However, according to the growth rate results observed in this work, an interaction between organic and inorganic carbon metabolisms is expected to occur in *C. protothecoides*. Glucose sensing mechanism is known to negatively affect the apparent affinity of CO_2 in *Chlorella* sp. VJ79 [7]. Free glucose in the culture medium was shown to negatively impact on the synthesis of RuBPase and light related phycocyanin-PC involved in Calvin cycle in the alga *Cyanidium caldarium* [9]. Our results showing final biomass yields of 9.54 ± 0.72 g L^{-1} and 10.32 ± 0.83 g L^{-1}, respectively for mixtrophic and heterotrophic conditions and 1.89 and 2.05 folds that obtained in autotrophic (5.04 ± 0.37 g L^{-1}) culture, clearly supports the hypothesis of a strong synergistic interaction between photosynthetic and oxidative phosphorylation metabolisms in *C. protothecoides*.

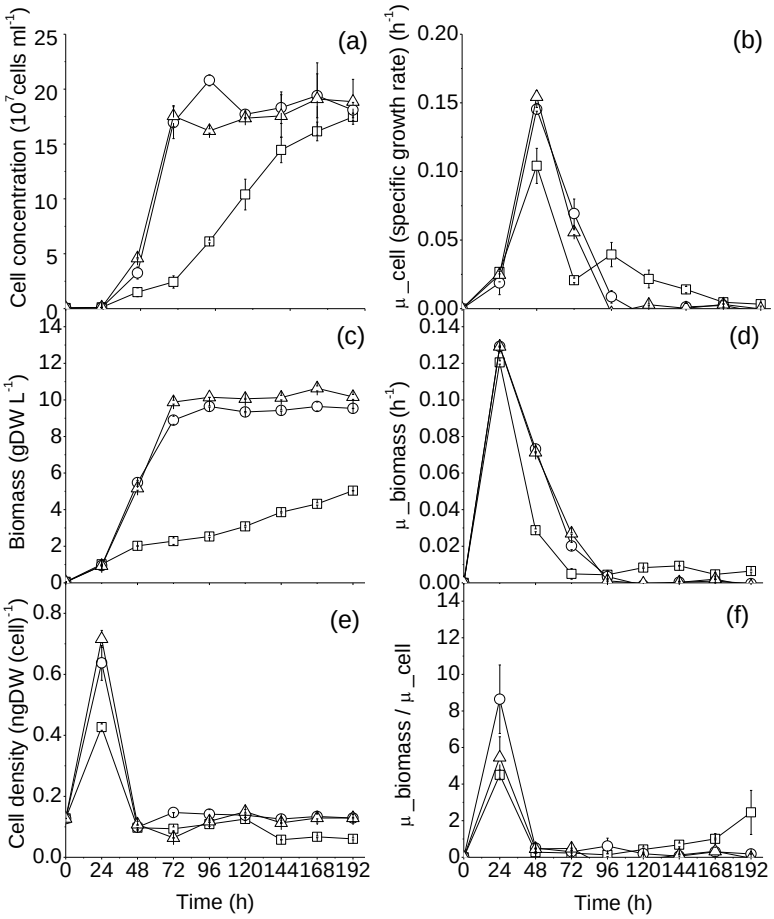

Figure 4.1 Culture growth under autotrophic (Square), mixotrophic (Circle) and heterotrophic (Triangle) conditions. (a) Cell concentration; (b) Cell specific growth rate; (c) Biomass; (d) Biomass specific growth rate; (e) Cell density; (f) Raito of specific growth rate between biomass and cell concentration. Error bars represent the standard deviation of triplicate data.

Interestingly, the final cell concentration (in cells per mL) was not depending on the carbon source, and similar values were reached in all three cultures (1.81E+8 ± 7E+6 cell mL^{-1}). Therefore, lighter cells were thus obtained in the autotrophic culture with 0.427 ± 0.010 ng $cell^{-1}$, compared to 0.638 ± 0.050 ng $cell^{-1}$ and 0.716 ± 0.027 ng $cell^{-1}$ respectively under mixtrophic and heterotrophic conditions. So the evolvation of biomass is not following the same pace with cell concentration; when observed under the microscope, cells in mixtrophic and heterotrophic cultures, after 72 h were larger than those in autotrophic culture; From the ratio of the specific growth rate between biomass and cell concentration (Figure 4.1f), we see that biomass is accumulating faster than the cell number (cell concentration) in mixtrophic and heterotrophic cultures than in autotrophic culture. It seems that the cell divison is affected under mixotrophic and heterotrophic conditions.

Here, nutrients limitation (Figure 4.2) may have affected cell division under these two conditions, which may explain higher specific cell weights. Glucose (Figure 4.2a) was below the detection limit at 96 and 72 h in mixtrophic and heterotrophic culutures, respectively; even in the mixotrophic culture where CO_2 was expected to support a continous growth. However, the amino acids were also depleted (Figure 4.2b) concurrently at 48 h. As observed in Deschenes' work [19], the algae *Scenedesmus obliquus* has shown an intrinsic ability to internalize nitrate much faster than its effective use for growth. Since the cell concentration and the biomass were both still increasing after 48 h, it is assumed that nitrogen is accumulated as intracellular storages [19]. Then a difference occurred from 72 h, while this nitrogenous intracellular pool is probably depleted thus causing growth to stop in mixotrophic and heterophic cultures. However, growth was maintained in autotrophic culture, which may be due to slower growth as well as consumption rate of intracellular nitrogen.

4.5.2 Glucose feeding favors lipids accumulation and improves fatty acids composition

Carbon feeding mode and lipids accumulation dynamic were closely related (Figure 4.2i). Glucose specific consumption rate (Figure 4.2a) in heterotrophic culture (0.910 ± 0.004 mmol L-1d-1) was similar to that in mixotrophic culture (0.828 ± 0.034 mmol L-1d-1) ($F=5.533$, $p=0.1429>0.05$). Haass and Tanner reported an inducible hexose transport system in Chlorella with glucose as an inducer [20], a system that can be significantly inhibited under light condition. However, there was no evidence in our work of this inhibition phenomenon since glucose uptake rate was not reduced in mixotrophic culture.

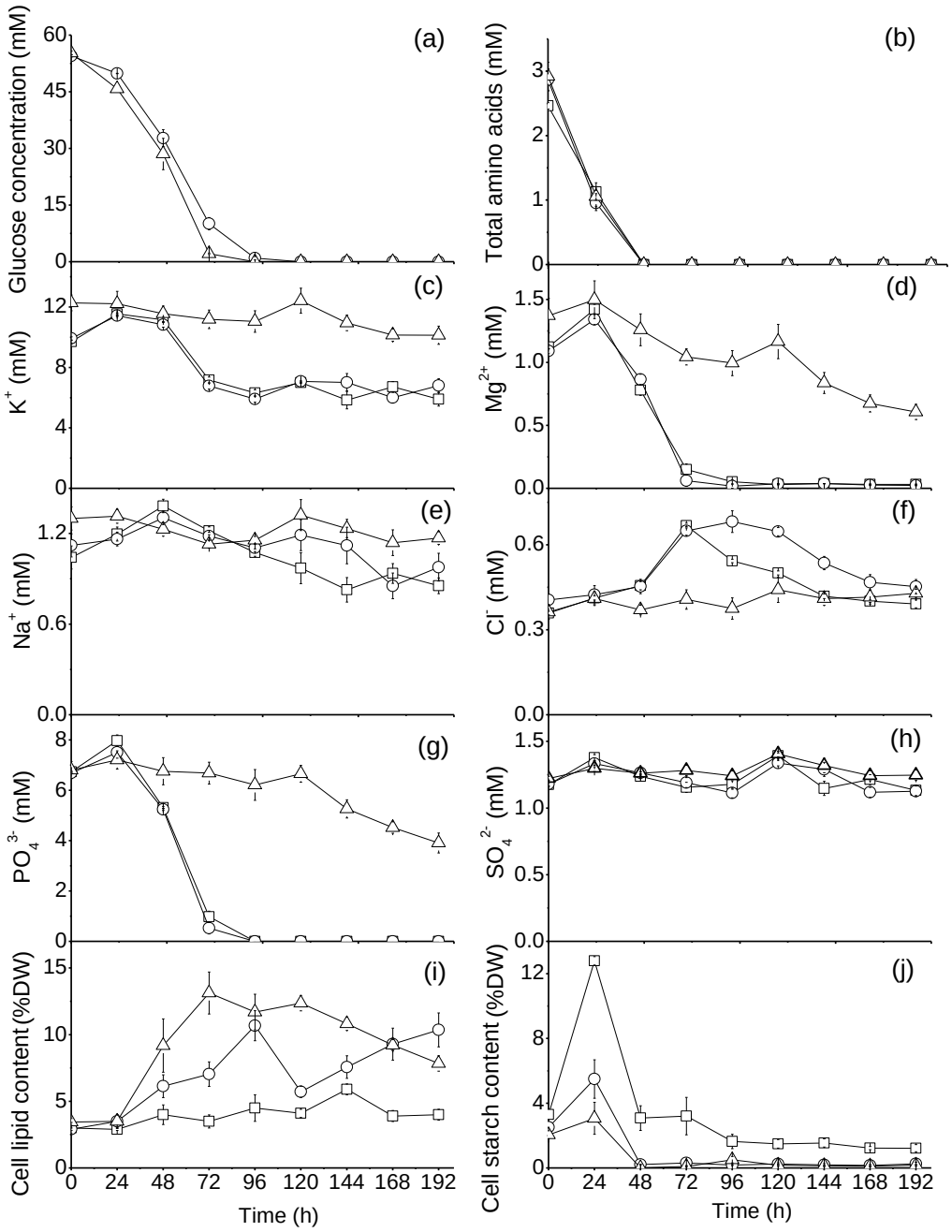

Figure 4. 2 (a) Carbon source (here only glucose was quantified, CO_2 as is always maintained as 5% in the culture incubator, and because of the limitation of monitor we didn't detect it in the culture medium); (b) nitrogen source; (c-h) ions; and (i) cell lipid, (j) starch accumulation under autotrophic (Square), mixotrophic (Circle) and heterotrophic (Triangle) conditions. Error bars represent the standard deviation of triplicate data.

Lipids (Figure 4.2i) start to accumulate rapidly from 24 h in heterotrophic and mixtrophic cultures. It has been reported that most microalgae strains do accumulate lipids under nitrogen limitation stress conditions while carbon source are still available [1]; However, in our results, the availability in amino acids cannot explain the difference observed in the lipids patterns for the three culture modes assessed; the cell consumption of the nitrogenous sources (12 amino acids) was similar among all culture modes and depletion occurred at 48 h (Figure 4.2b). Total amino acids quantity is given here because they all behaved the same.

The cell ionic environment is a crucial parameter of cell behavior, and the evolution of the media ions content was analysed together with intermediates of the carbon storage routes (Figure 4.2c-h). Interestingly, both concentrations in Mg^{2+} (Figure 4.2d) and PO_4^{3-} (Figure 4.2g) decreased below the detection limit at 96 h only for autotrophic and mixotrophic, which may suggest their importance under light and mixed energetic conditions involving CO_2 uptake. As it is well known, Mg^{2+} is essential for photosynthesis, and PO_4^{3-} is involved in the transformation of intermediate products of the photosynthesis energy transfer pathway [21]. It is interesting to see that K^+ decreases concurrently to biomass growth in autotrophic and mixotrophic cultures and stayed non-limiting (Figure 4.2c), since this ion normally remain at a stable concentration in plant cells [22]. However, K^+ is involved in the carbohydrates metabolism as it can promote the transport of sugars into the storage organelle, and promote the synthesis of other storage materials [23]. Particularly for the stored carbohydrates, higher levels of starch (Figure 4.2j) are found in autotrophic and mixtrophic conditions compared to that in heterotrophic condition. Na^+, which is normally involved to balance the transmembrane ions exchange and for keeping the cell membrane electronegativity, was kept at a quasi steady-state concentration during the whole culture (Figure 4.2e). In addition, stable SO_4^{2-} level (Figure 4.2h) suggests there was no protein degradation problem, a phenomenon normally attributed to cell death.

Cell lipid content accumulated at a lower rate (0.046 ± 0.006g DW^{-1} h^{-1}) and at a lower level (5.9 ± 0.4 % DW) in autotrophic culture compared to mixotrophic and heterotrophic cultures. Mixotrophic and heterotrophic cultures accumulated lipids at a similar initial rate (respectively 0.133 ± 0.034g DW^{-1} h^{-1} and 0.202 ± 0.051g DW^{-1} h^{-1}; $F=3.741$, $p=0.1927>0.05$), and reached similar lipids content (respectively 10.3 ± 1.2 % DW and 13.2 ± 2.1 % DW; $F=0.674$, $p=0.4980>0.05$). However, in mixotrophic, a two-step increase/decrease cycle was observed while a peak in cell lipid content was reached in heterotrophic at 72 h. Clear differences arose later (> 72

h) in heterotrophic culture with a constant decrease of the cell lipid content (0.204 ± 0.017 % DW h^{-1}) following glucose depletion. Under mixotrophy, although the cell lipid content also showed to decrease after glucose depletion, lipids started re-accumulating under the subsequent autotrophic mode using CO_2, and interestingly at a similar rate than earlier in the culture when glucose and CO_2 were both present. Reaching free glucose depletion thus lead, in heterotrophic and mixotrophic cultures, to a similar behaviour with the re-mobilisation of stored lipids. However, the mixtrophic culture can still capture CO_2 with light supply, after re-organization of cell metabolism and promoting lipids accumulation. Moreover, it is interesting and looks intriguing that the second lipids accumulation phase from glucose depletion was at a similar rate (0.064 ± 0.003 % DW h^{-1}; $F=4.596$, $p=0.16>0.05$) but reached a higher level (10.3 ± 1.2 % DW; $F=89.811$, $p=0.011<0.05$) compared to pure autotrophic culture (0.075 ± 0.006 % DW h^{-1} and 5.9 ± 0.4 % DW, respectively). Therefore, adding glucose as a complementary organic carbon source in mixotrophic culture may have triggered an enhanced cell ability to accumulate lipids. Another but not contradictory possibility is that some metabolites may have been released in the culture medium while glucose was present, metabolites that have been re-uptaked concurrently to CO_2 from glucose depletion. It should be noted that cell respiration under a glucose metabolism is releasing CO_2 that dissolves in the liquid medium both in heterotrophic and mixtrophic cultures that cannot be re-uptaken in heterotrophic culture since it was performed at dark. However, mixotrophic culture could have still reuse this dissolved CO_2, which is adding to using exogenous CO_2.

To better understand the results on lipids accumulation, we also measured starch accumulation (Figure 4.2d), since it has been reported that starch is the main storage carbohydrate competing with lipids synthesis in algae cells [24]. Interestingly, starch showed to accumulate in all culture modes, with clear peaks after 24 h for then reaching similar initial basal values from 50 h. The maximum level was reached in autotrophic culture (12.79 ± 0.367 % DW), and lower but significantly similar values were observed in mixotrophic and heterotrophic cultures (5.5 ± 1.19 % DW and 3.07 ± 0.98 % DW respectively; $F_{AMH}=31.238$, $p=0.009<0.01$; $F_{MH}=2.464$, $p=0.257>0.05$). This global trend thus suggests that the enzymatic machinery for starch accumulation can rapidly be activated, but that the cell priority is to convert this storage into lipids, since lipids start accumulating from 24 h when starch catabolism is initiated. However, the starch content reached an higher level in autotrophic culture compared to mixtrophic and heterotrophic cultures, a result that may reveal that starch is stored at a lower metabolic cost than lipids; lipids are reported as a

form of storage componds with 2.25 times higher stored enregy than starch for the same weight [25]. Cells growing under the autotrophic mode are carbon-limited and maintain a strictly efficient nutritional behavior to maintain a balanced growth, which limits either lipids and starch accumulation along exponential growth. This result is also similar to that reported in *C. reinhardtii*, in which starch accumulation was observed earlier than lipids, where lipids catabolism showed to start after starch degradation [26]. The phenomenon that starch is accumulated and degraded faster than lipids is also consistent with results reported for *Chlamydomonas* [26]. It is thus clear that starch and lipids in *Chlorella prototehcoides* have different metabolic functions; starch serves as the cell preferential storage and re-mobilize compound, and lipids serves as long term storage under nutritional shortage or culture stresses.

Lipids mainly include polar lipids (PL, structural lipids, mainly phospholipids) and neutral lipids (NL, reserve lipids, mainly TAG), in which neutral lipids are the preferential source for biodiesel production. However, the fatty acids composition and structure such as unsaturated degree and carbon chain length can affect the properties of the resulting biodiesel [27]. Therefore, polar and neutral lipids were first separated (see Material and methods) and then characterized independently for their fatty acids profile. The heterotrophic culture shows a higher NL-to-PL ratio (steady state of 13.48± 2.45) compared to that in autotrophic culture (steady state of 0.32 ± 0.11) (Figure 4.3a), while averaged values are observed under mixtrophic conditions (steady state of 3.49 ± 1.93). So with glucose supplementation, cells are more prone to accumulate storage lipids, which favours the downstream biodiesel production.

Fatty acids composition of NL and PL classes were also analyzed and differences were observed among culture conditions. In the NL class (Figure 4.3d), the 16:0, 16:1, 18:1, 18:2, and 18:3 fatty acids were dominant with the percentage of each fatty acids depending on the culture mode, for example, in the autotrophic culture, 16:1, 18:2 and 18:3 together are more than 70 % of total NL fatty acids at steady state, while in mixotrophic and heterotrophic cultures the 16:0 and 18:1 mostly dominated (around 65 % of total NL fatty acids). In PL class (Figure 4.3c), the 16:0, 18:1, 18:2, and 18:3 fatty acids were dominant, in which 18:2 and 18:3 are more than 80 % of total fatty acids in autotrophic culture at steady state. However, in mixotrophic and heterotrophic cultures, 16:0 and 18:1 are more than 70 % of total PL fatty acids.

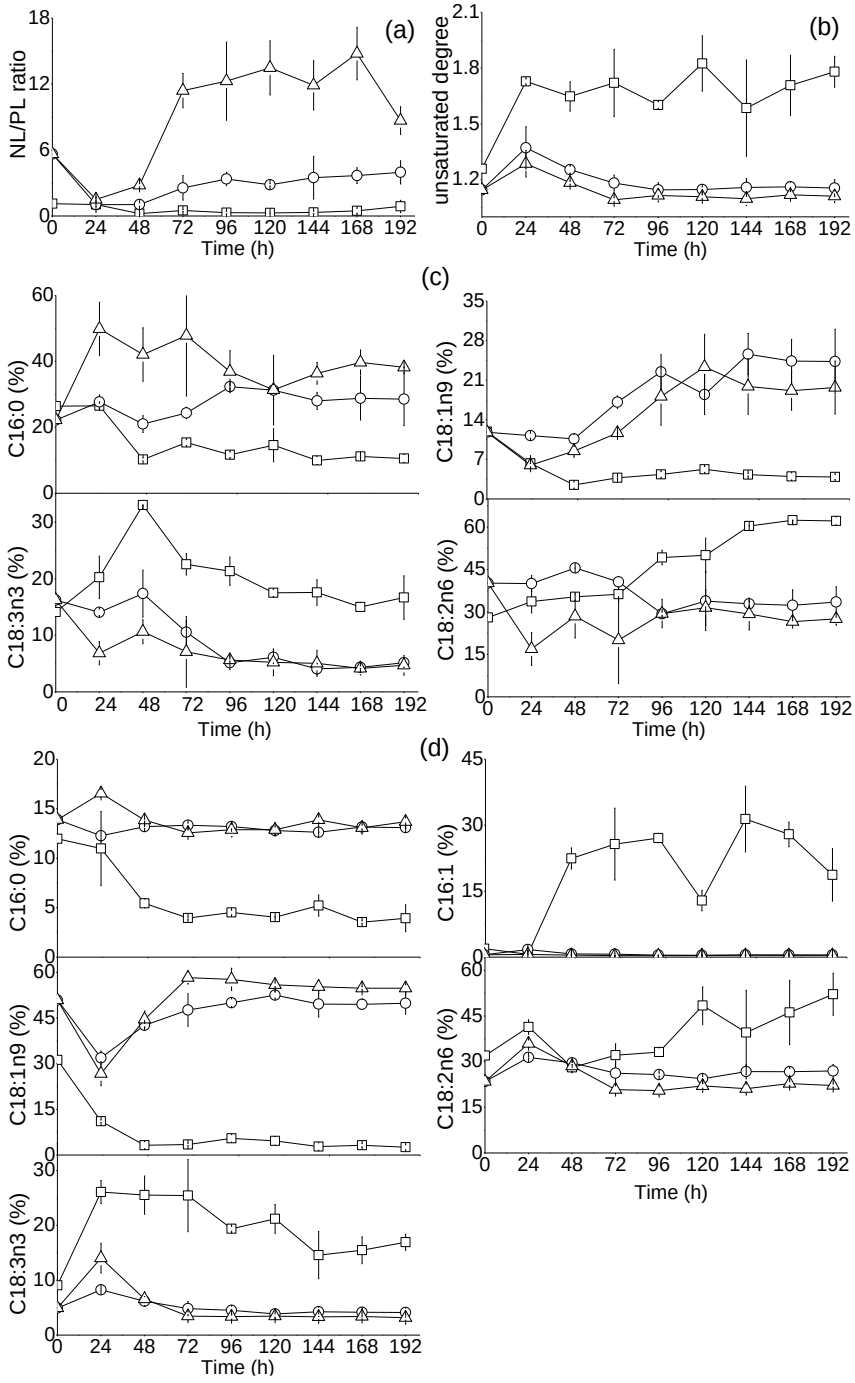

Figure 4. 3 Fatty acids compositon under autotrophic (Square), mixotrophic (Circle) and heterotrophic (Triangle) conditions. (a) Neutral lipids (NL) and polar lipids (PL) ratio; (b) Fatty acids unsaturated degree; (c) Fatty acids main composition in polar lipid class; (d) Fatty acids main composition in neutral lipid class. % represent each independent fatty acid percentage of total fatty acids (weight/weight). Error bars represent the standard deviation of triplicate data.

As noted previously, biodiesel properties are defined by the fatty acids unsatured degree and carbon chain length, such as the higher cetane number, which can offer a better engine performance, leading to less white smoke at start up, less noise and lower emissions. Fatty acids carbon chain length of 16-18 could mean a high cetane number, but higher carbon chain lengths can affect the cold flow properties of biodiesel [28]. In this work, glucose addition showed no significant effect on the carbon chain length (i.e. cells fatty acids), while, the fatty acids unsaturated degree (Figure 4.3b) decreased from 1.63 ± 0.37 ∇/mol in autotrophic culture to 1.18 ± 0.19 ∇/mol in mixtrophic culture and 1.14 ± 0.14 ∇/mol in heterotrophic culture. Highly unsaturated fatty acids have a very low cetane number, and when heated, they easily produce polymers and form colloids [28]. Thus, the fatty acids carbon chain should preferably contains only one double bonds [29]. Our results revealed that glucose supplement could increase the ratio of neutral lipids to polar lipids and decrease the unsaturated degree of fatty acids. Therefore, mixtrophic and heterotrophic cultures showed to favour obtaining desired fatty acids composition for biodiesel production.

4.5.3 Glucose feeding recalibrates the cell metabolism for downstream intermediates and lipids accumulation rather than upstream metabolites

In order to further unravel the metabolic differences from adding free glucose in the medium, which led to different cell lipid content as previously discussed, we extended our study analyzing intracellular metabolites concentration with culture time. Glucose-1-P (G1P), glucose-6-P (G6P) and fructose-6-P (F6P) rapidly increased after inoculation (0-24 h) in autotrophic and in mixotrophic (to a lower extent), while these metabolites stayed constant in the heterotrophic culture (except for G6P, which increased as for the mixotrophic culture). Upstream (glycolysis / gluconeogenesis pathways) intracellular intermediate metabolites concentrations in G1P, G6P, F6P and phosphoenolpyruvate (PEP) (Fig.4a-c,f) under autotrophic conditions were 2-5 folds those in mixtrophic and heterotrophic cultures at the maximum peak observed before glucose depletion (24-72 h). However, similar levels and trends with time were measured thereafter in all culture modes, except for PEP in autotrophic where a punctual but significant increase was observed at 144 h. Intermediate metabolites of the upstream glycolysis (G1P, G6P, F1P) all showed to temporarily increase after glucose depletion (72-120 h), for increasing again from 144 h in both heterotrophic and mixtrophic cultures. These early increases in G1P, G6P, F1P (72-120 h) were concomitant to decreases of cell lipid content in both heterotrophic and mixtophic cultures, but at distinct extents

for the different culture modes. The late increase trend was, however, only concomitant for the autotrophic and heterotrophic cultures. The mixotrophic culture showed a different behavior with an increase of cell lipids (Figure 4.2i) that may be attributed to a continuous efficient carbon source (i.e. CO2) uptake (described in the previous section). Therefore, lipids degradation at 96-120 h in mixtrophic and at 72-192 h in heterotrophic culture is thought to have occurred to support the cell metabolism at stationary phase (i.e. maintenance and other anabolic reactions) after the depletion of the exogenous carbon source.

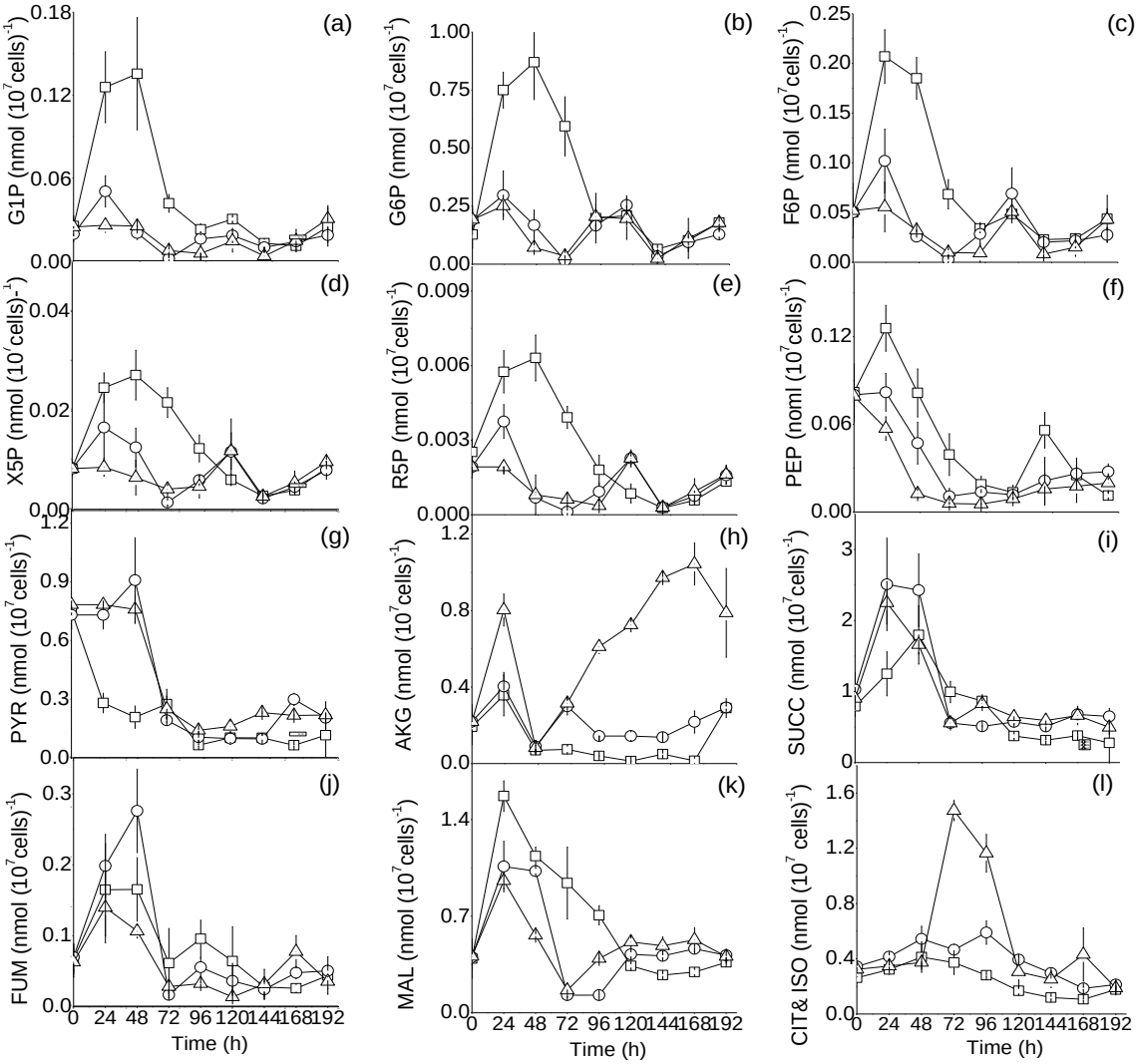

Figure 4. 4 Intracellular metabolites concentrations in glycolysis / gluconeogenesis pathway and PPP/ Calvin-RuBP regeneration pathway as well as TCA cycle organic acids concentrations under autotrophic (Square), mixotrophic (Circle) and heterotrophic (Triangle) conditions. (a) G1P: glucose 1-phosphate; (b) G6P: glucose 1-phosphate; (c) F6P: fructose 6-phosphate; (d) X5P:

xylulose 5-phosphate; (e) R5P: ribose 5-phosphate; (f) PEP: phosphoenolpyruvate; (g) PYR: pyruvic acid; (h) AKG: α-Ketoglutaric acid; (i) SUCC: succinic acid; (j) FUM: fumaric acid; (k) MAL: malic acid; (l) CIT: citric acid; ISO: isocitrate. Error bars represent the standard deviation of triplicate data.

Of interest, intermediate metabolites of pentose phosphate pathway (PPP) and of Calvin-RuBP regeneration pathway (R5P and X5P) showed similar behaviors to those of G1P, G6P, F6P and PEP, for all culture modes (Figure 4.4d-e), except again for the autotrophic culture where no punctual increases were observed at 72-120 h. These results thus clearly confirm, from this intimate relationship between the cell concentrations in G1P, G6P, F6P and R5P and X5P, PPP is continuously fed from upstream metabolites of glycolysis in presence of glucose. And oppositely, the Calvin-RuBP regeneration pathway is continuously feeding glycolysis in the autotrophic culture. It is thus clear that in the autotrophic culture, which is fuelled by the inorganic carbon CO_2 entering the Calvin cycle under light condition, R5P and X5P are maintained at higher levels than in the other culture modes with free glucose in culture medium. These intermediate metabolites are critical for photosynthesis as precursors of RuBP, which is needed for CO_2 fixation. The high level of R5P and X5P as well as of upstream metabolites of glycolysis in autotrophic culture confirm that Calvin cycle is more intense than in mixtrophic culture. Rapid starch accumulation in autotrophic culture concurrently to a low cell growth rate (and division rate) before 24 h thus revealed a higher carbon fixation rate than for the cell demand (Figure 4.1b). Moreover, lower upstream intermediates level in mixtrophic as well as in heterotrophic cultures, are thought to be due to higher metabolic activities, and thus of the metabolic demand for anabolic biochemical reactions as well as for energy production (see next section), as observed from higher specific growth rates in these cultures. The inhibition of Calvin cycle when using free glucose may also explain the results in the mixtrophic culture. In mixtrophic and heterotrophic cultures, organic carbon catabolism leads to pyruvate (PYR) (4 folds intracellular concentration than in autotrophic culture) and acetyl coenzyme A, an intermediate metabolites which activates downstream lipids synthesis from sugar-phosphates [30].

We further tracked the downstream metabolism of TCA cycle, which is another main branch pathway parallel to lipids synthesis. The results show that metabolites in mixtrophic and heterotrophic cultures are mainly concentrated in TCA cycle and previous steps entering TCA such as PYR (Figure 4.4g-i). However, the evolution trends for the metabolites in TCA cycle are quite

different. Concentrations of CIT, ISO and AKG are higher in heterotrophic, with only FUM and MAL that are slightly higher in autotrophic and mixtrophic cultures as compared to that in the heterotrophic culture. AKG is one of the precursors for chlorophyll synthesis, which suggests a lower outlet flow from this point in the heterotrophic culture compared to the mixtrotrophic and autotrophic cultures, in which AKG is maintained in a stable level. Also in TCA cycle, the reaction from AKG to SUCC is known to be a rate limiting step and also to be irreversible [31]. So CIT, ISO AKG are accumulated while not SUCC. In autotrophic and mixtrophic cultures, MAL could be supplemented from PEP (higher levels were observed under these two culture modes), since this is a reversible reaction in gluconeogenesis helping to maintain MAL at relatively higher levels in autotrophic and mixtrophic cultures.

Combining our results altogether for upstream and downstream metabolites, we could conclude that feeding glucose to *Chlorella protothecoides* recalibrates the cell metabolism towards downstream intermediates and lipids accumulation rather than to upstream metabolites.

4.5.4 Cell energetic state drives carbon metabolism and reflects lipids accumulation

Cell energetics is directly involved in metabolic regulation [32]. Indeed, the ATP-to-ADP ratio, a biomarker of cell energetic state, was significantly higher in heterotrophic and mixtrophic (to a lesser extent) cultures than that in autotrophic culture specifically at 48 h (F_{AH}=143.257, p=0.0069<0.01; F_{AM}=37.948, p=0.0253<0.05; F_{AMH}=86.246, p=0.0021<0.01) (Figure 4.5). With a ATP-to-ADP ratio of 64.8 ± 6.9 at 48 h, the cell energetics was particularly high in the heterotrophic culture grown on glucose, while a maximum value of 22.8 ± 4.3 was measured in the mixotrophic culture, and only a value of 5.1 ± 1.5 in the autotrophic culture. Interestingly, all cultures showed converging to a similar ultimate value of 2.3 ± 0.42 from 72 h, therefore before and after glucose depletion. These maxima values of the ATP-to-ADP ratio coincided with the maximal cell growth rate observed in all culture modes (Figure 4.1b), thus using glucose and/or CO_2 as the carbon source. Glucose catabolism, combined to respiration metabolism, provides a high energetic turnover capacity in the heterotrophic and the mixtrophic cultures, compared to autotrophic growth. These results are consistent with TCA cycle metabolites that were significantly higher in heterotrophic and mixtrophic cultures compared to that in autotrophic. Under autotrophic mode, light provided the energy required in the CO_2 fixation process, but hexoses synthesis requires

energy, which thus reduces the global energy output that can be available for anabolic reactions of the central metabolism. Our results also suggest that the CO_2 fixation process limits cell metabolism, which explains a quite stable energetic state in autotrophic cells during the whole culture period.

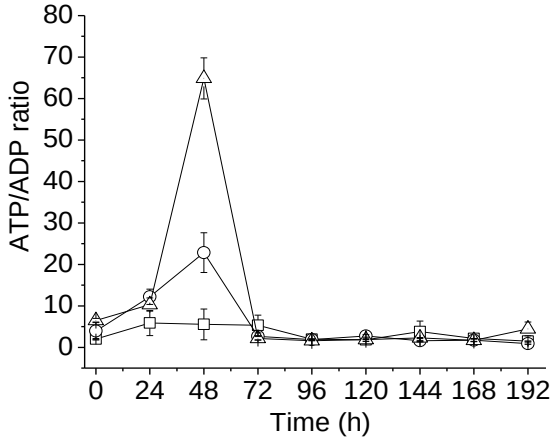

Figure 4. 5 Cell energetic level under autotrophic (Square), mixotrophic (Circle) and heterotrophic (Triangle) conditions. Error bars represent the standard deviation of triplicate data.

Except for the autotrophic culture, two distinct phases can be observed: before (phase I) and after (phase II) glucose depletion. In phase I, glucose uptake suffices to the cell energetic load as well as momently (0 – 24 h) accumulating starch and then lipids (24– 100 h). This phenomenon occurred in both heterotrophic and in mixotrophic cultures; the use of exogenous glucose being the common condition between these two culture modes. At glucose depletion, in tracellular carbon and energy storage pools is degraded and re-mobilized to maintain cellular metabolic activity and biomass viability. However, unlike glucose high energetic metabolism, lipids seem to feed energy at a rate following cell demand with an energetic state maintained at a quasi steady-state level. However, the intermediates issued from lipids degradation fluctuate, which may suggest alternate metabolic demands.

4.6 **Conclusion**

In this study, *Chlorella protothecoides* dynamic metabolic profile and cell behavior showed being highly affected from environmental culture condition, especially with or without feeding glucose. Comparing three typical culture modes, namely the heterotrophic, the mixotrophic and the autotrophic, we clearly showed that glucose addition, as the main or a complementary organic

carbon source to CO_2, stimulates algae metabolism towards lipids production rather than to carbohydrates accumulation, the highest lipid content was reached as 13% DCW in heterotrophic culture compared that of 6% in autotrophic culture. Furthermore, it showed to improve lipids and fatty acids composition in regards to biodiesel production, neutral to polar lipids ratio were greatly improved from 0.32 ± 0.11 to 13.48 ± 2.45 while fatty acids unsatarated degree were reduced from 1.63 ± 0.37 ∇/mol to 1.18 ± 0.19 ∇/mol with glucose supplement. The carbon flux direction preference is thought being regulated by the cell energetic state, which depends on the cell carbon source management.

4.7 Acknowledgements

The authors are grateful to the "Ressources Aquatiques Québec (RAQ)" and the "Fonds de recherche du Québec – Nature et technologies (FQRNT)" for a scholarship to X. Ren, and to the National Science and Engineering Council of Canada for a financial support (MJ). Also, the authors give their thanks to François Turcotte from the "Université du Québec à Rimouski (UQAR)" for his contribution on the analysis of fatty acids.

4.8 References

[1] Georgianna, D. Ryan. and Mayfield, Stephen P., 2012. Exploiting diversity and synthetic biology for the production of algal biofuels. Nature 488(7411): 329-335.

[2] Yang Chen, Qiang Hua, Kazuyuki Shimizu, 2000. Energetics and carbon metabolism during growth of microalgal cells under photoautotrophic, mixotrophic and cyclic light-autotrophic/dark-heterotrophic conditions. Biochemical Engineering Journal 6: 87-102.

[3] Tamarys Heredia-Arroyo, Wei Wei, Hu Bo, 2010. Oil accumulation via heterotrophic/mixotrophic Chlorella protothecoides. Appl Biochem Biotechnol. 162(7): 1978-1995.

[4] Xiong Wei, Xiufeng Li, Jinyi Xiang, Qingyu Wu, 2008. High-density fermentation of microalga Chlorella protothecoides in bioreactor for microbio-diesel production. Appl Microbiol Biotechnol 78(1): 29-36.

[5] Kong Wei-Bao, Yang Hong, Xia Chun-Gu et al., 2013. Effect of glycerol and glucose on the enhancement of biomass, lipid and soluble carbohydrate production by *Chlorella vulgaris* in

mixotrophic culture. Food Technol. Biotechnol. 51 (1) 62–69.

[6] Chandra Rashmi, M.V. Rohit, Swamy YV., Venkata Mohan, 2014. Regulatory function of organic carbon supplementation on biodiesel production during growth and nutrient stress phases of mixotrophic microalgae cultivation. Bioresource Technology 165: 279–287.

[7] Lalucat Jorge, Juan Imperial, Ramón Parés, 1984. Utilization of light for the assimilation of organic matter in Chlorella sp. VJ79." Biotechnology and Bioengineering 26(7): 677-681.

[8] Orus M. Isabel, Eduardo Marco, Flor Martinez, 1991. Suitability of Chlorella vulgaris UAM 101 for heterotrophic biomass production. Bioresource technology. 38: 179-184.

[9] Steinmuller Klaus and Zetsche Klaus, 1984. Photo- and metabolite regulation of synthesis of Ribulose bisphosphate carboxylase/oxygenase and the phycobiliproteins in the alga Cyanidium caldarium. Plant Physiology 76: 935-939.

[10] Vonshak Avigad, Suk Man Cheung and Feng Chen, 2000. Mixotrophic growth modifies the response of *Spirulina (Arthrospira) platensis* (cyanobacteria) cells to light, J. Phycol. 36: 675–679.

[11] Yan Riming, Zhu Du, Zhang Zhibin, 2012. Carbon metabolism and energy conversion of *Synechococcus* sp. PCC 7942 under mixotrophic conditions. J. Appl. Phycol. 24:657-668.

[12] Ghorbaniaghdam Atefeh, Jingkui Chen, Olivier Henry, Mario Jolicoeur, 2014. Analyzing clonal variation of monoclonal antibody-producing CHO cell lines using an in silico metabolomic platform. PloS one 9 (3): e90832.

[13] Lamboursain Laurence and Jolicoeur Mario, 2005. Critical influence of *Eschscholzia californica* cells nutritional state on secondary metabolite production. Biotechnol. Bioeng. 91(7):827-37.

[14] Gabi Drochiou, 2005. Turbidimetric lipid assay in seed flours. Journal of food lipids. 12: 12-22.

[15] Jean-Michel Girard, Marie-Laine Roy, Mhammed Ben Hafsa et.al., Mixotrophic cultivation of green microalgae Scenedesmus obliquus on cheese whey permeate for biodiesel production. Algal research. 5: 241-248.

[16] Hiroshi Endo, Hiroshi Sansawa, Kei Nakajima, 1977. Studies on Chlorella regularis, heterotrophic fastgrowing strain. II. Mixotrophic growth in relation to light intensity and acetate

concentration. Plant and cell physiology 18(1): 199-205.

[17] Ogawa Takahira and Aiba Shuichi, 1981. Bioenergetic analysis of mixotrophic growth in Chlorella vulgaris and Scenedesmus acutus. Biotechnology and bioengineering. 23(5): 1121-1132.

[18] Bataah Mohamed G., El-sayed and El-sayed E.w, 2013. Growth of the green alga Chlorella vulgaris as affected by different carbon sources. Life Science Journal 10(1): 2075-2081.

[19] Deschênes J-S, Boudreau A, Tremblay R, 2015. Mixotrophic production of microalgae in pilot-scale photobioreactors: Practicability and process considerations. Algal Research 10: 80-86.

[20] Haass D. and Tanner W., 1974. Regulation of Hexose transport in *Chlorella vulgaris*: characteristics of induction and turnover. Plant Physiol. 53(1):14-20.

[21] Whitmarsh John and Govindjee, 1995. Photosynthesis. Encyclopedia of Applied Physics, VCH Publishers, Inc. 13: 513-532.

[22] Kant, S. and U. Kafkafi. 2002. Potassium and Abiotic Stresses in Plants. Pasricha, N. S., Bansal, S.K. (Eds.), Role of potassium in nutrient management for sustainable crop production in India, Potash Research Institute of India, Gurgaon, Haryana.

[23] Fageria Nand Kumar. 2012. The Role of Plant Roots in Crop Production. CRC Press- Science. p63.

[24] Wang Ziteng, Ullrich Nico, Joo Sunjoo, Waffenschmidt Sabine and Goodenough Ursula, 2009. Algal lipid bodies: stress induction, purification, and biochemical characterization in wild-type and starchless Chlamydomonas reinhardtii. Eukaryot Cell 8(12): 1856-1868.

[25] Han Y, Parsons CM, Alexander DE., 1987. Nutritive-value of high oil corn for poultry. Poultry Sci. 66(1):103-111.

[26] Siaut Magali, Stéphan Cuiné, Yonghua Li-Beisson et al., 2011. Oil accumulation in the model green alga Chlamydomonas reinhardtii: characterization, variability between common laboratory strains and relationship with starch reserves. BMC Biotechnology 11(7):1-15.

[27] Wang Yan, Chen Tao, Qin Song, 2013. Differential fatty acid profiles of Chlorellakessleri grown with organic materials. Journal of Chemical Technology and Biotechnology 88: 651-657.

[28] Luo Wen, Yuan Zhenhong, Tan Tianwei, Lv Pengmei, 2008. Study on the relationship between the fuel properties and components of biodiesel. Acta Energiae Solaris Sinica. 7: 878-882.

[29] Knothe Gerhard, 2011. A technical evaluation of biodiesel from vegetable oils vs. algae. Will algae-derived biodiesel perform? Green Chemistry 13: 3048-3065.

[30] García M.C. Cerón, A. Sánchez Mirón, F. García Camacho et al., 2005. Mixtrophic growth of the microalga *phaeodactylum tricornutum* influence of different nitrogen and organic carbon sources on productivity and biomass composition. Process Biochemistry. 40 (1): 297–305.

[31] Wang Jingyan, 2002. Biochemistry Third Edition 2. Higher Education Press.

[32] Cardol Pierre, Giorgio Forti, Giovanni Finazzi, 2011. Regulation of electron transport in microalgae. Biochimica et Biophysica Acta (BBA) – Bioenergetics 1807 (8): 912–918.

CHAPTER 5 A KINETIC METABOLIC MODEL DESCRIBING LIPID PRODUCTION IN CHLORELLA PROTOTHECOIDES UNDER HETEROTROPHIC CONDITION

5.1 Presentation of this chapter

In this chapter, a kinetic metabolic model was first applied in microalgae platform in *Chlorella protothecoides* under heterotrophic condition. Unlike most dynamic models coping with algae physiology or steady-state metabolic level models, the current model combines both physiology and flux information in a kinetic approach. Cell growth, lipid production and almost 30 metabolic intermediates covering glycolysis, pentose phosphate pathway and TCA cycle and energetic metabolism were included and simulated. Multiple Michaelis–Menten type kinetics were used to describe biochemical reaction rates and the Monod equation was used to describe the cell growth state. Weighted sum of squared residues between experimental data and simulated values was used as the objective function to help convergence during model structuring and for parameter calibration. Parameter sensitivity and confidence interval were carried out to verify model reliability. It is shown that the model can simulate well the experimental data for all available data. Flux analysis results are also in high accordance with the literature, except for a higher lipid synthesis metabolic activity, with higher lipid flux and lower TCA activity, were revealed in our model.

5.2 Introduction

1970's oil crises and the more recent global warming problem have vigorously stimulated the scientific community to identify sustainable alternative energy sources, and microalgae are among the top priority candidates for obvious reasons (Georgianna & Mayfield, 2012; Mayfield; Quintana et al., 2011b). Microalgae can normally accumulate lipid from 20-50 % of their cell dry weight, with some species that can even reach up to 70 %. Fatty acid compositions in microalgae are mainly C_{16} and C_{18}; most of them are saturated or mono-unsaturated fatty acids, which can be used to obtain biodiesel. Indeed, microalgae lipid production has now become one of the most promising platform to replace fossil fuels (Bollinger, 2011; Greenwell et al., 2010a; Maia, 2010; Senne, 2012; Thurman, 1997; Yu et al., 2011b). However, the culture of microalgae presents specific issues as

an industrial production platform. For instance, lipid content is quite unstable along with the growth stages and culture conditions such as light and nutritional status. Among candidate microalgae, *Chlorella protothecoides*, an oleaginous specie, can be cultured under heterotrophic growth using acetate, glucose, or other organic compounds as carbon source, and result in higher biomass as well as lipid content than for autotrophic growth condition (Miao & Wu, 2006a). *C. protothecoides* has been studied optimizing culture medium composition and bioprocess management strategies (Xiong et al., 2008b). Genetic modifications were also assessed targeting lipid synthesis pathways, such as with the overexpression of acyltransferases (ACCase) and fatty acid synthase (FAS) (Radakovits et al., 2010).

With the aim of elucidating key environmental factors involved in microalgae behavior, various mathematical models have been proposed, and the work of Droop (Droop, 1968) describing major nutrients (e.g. inorganic phosphate) management has demonstrated being widely applicable to various microalgae species. For instance, Droop based models (Bernard & Rémond, 2012; Droop, 1983a; Droop, 1968a; Mairet, 2011; Mairet et al., 2011a) did emerge from the Droop original work and have largely contributed to describing the effect of macronutrients, light and temperature on cell growth and product, as well as to identify strategies to maximize lipid production. However, although these models demonstrated being highly efficient at describing global phenomena, they stay at macroscopic level and do not consider detailed carbon fluxes from substrates to lipid synthesis. Knowledge on the intracellular carbon flow distribution may enable refining culture management protocols to maximizing cell productivity in lipid. The flux balance analysis (FBA) approach, which is based on pseudo steady-state approximation, has been applied to microalgae biosystems such as *Arghrospia platensis, Synechocystis sp*. PCC 6803 (Fu, 2009), *Chlamydomonas reinhardtii* (Boyle, 2009; Kliphuis et al., 2012) and *Chlorella protothecoides* (Muthuraj, 2013). For instance, in *Chlorella* sp., a shift in intracellular flux distribution was hypothesized during transition from nutrient sufficient phase to nutrient starvation phase of growth (Muthuraj, 2013). Another appealing modeling approach, which allows simulating a culture's dynamics, is based on a transient-type approach with each flux kinetic described (Ghorbaniaghdam et al., 2013; Shinto et al., 2008). Such kinetic metabolic models can describe cell behavior dynamics, while opening the black box-type usual approach allowing closely look at intracellular metabolic flux rates (Cloutier et al., 2008; Cloutier et al., 2009; Cloutier et al., 2007). An underestimated potential output of these kinetic metabolic models relies in their capacity to perform dynamic metabolic flux

analysis from which key metabolic processes can be examined while assessing *in silico* hypothesis of genetic engineering and/or culture conditions management strategies (Cloutier et al., 2009). However, to the best of our knowledge, there are very few studies reporting metabolomics data of microalgae and even less on the development of mathematical models to describe cell metabolic dynamics (Muthuraj et al., 2013), and this is maybe due to the fact that only few algal genome have been sequenced and annotated so far (Curtis et al., 2012). Moreover, dynamic metabolic models require defining numerical values of numerous kinetic parameters, while only limited data sets are available, a reason that could also explain the limited work in that field so far (Surendhiran & Sirajunnisa, 2015).

In the present work, a kinetic metabolic model describing *Chlorella protothecoides* growth and nutrition was developed to describe heterotrophic culture mode. It included glycolysis, TCA (tricarboxylic acid) cycle, pentose phosphate pathway, global lipid synthesis, starch synthesis, amino acids metabolism, energy synthesis and biomass build up pathway. In this model, cell growth, lipid production and almost 30 metabolic intermediates are simulated. Multiple Michaelis–Menten type kinetics are used to describe biochemical reaction rates and the Monod equation is used to describe the cell specific growth state. The model was successfully calibrated on previously published experimental data. A sensitivity analysis was performed on kinetic parameters and their confidence intervals were determined. The model was then used to perform a dynamic metabolic flux analysis. To the best of our knowledge, this is the first kinetic metabolic model developed for the microalgae platform.

5.3 Material and methods

5.3.1 Algae stain and culture conditions

Details about algae species and culture conditions can be found in a previous work (Ren et al., 2016). Briefly, *Chlorella protothecoides* culture in the dark was carried out in 2.8-L glass flasks with 10 g L^{-1} glucose as the carbon source and the modified basal medium (MBM), thus imposing a strict heterotrophic metabolism. Glucose concentration in the medium was analyzed by a biochemistry analyzer (YSI Life Science, 2700 select, Ohio, USA). Intracellular metabolites extraction was performed as described in (Ren et al., 2016) and their quantification was carried out by UPLC/MS/MS system (1290 model, Agilent Technologies, Santa Clara, CA, USA) also detailed

in (Ren et al., 2016), starch analysis was performed using a starch assay kit (Sigma-Aldrich, St. Louis, MO, USA). Total lipid quantification was done according to Drochiou's method and described in previous work (Ren et al., 2016).

5.3.2 Model development

A kinetic metabolic model was developed to describe the central carbon metabolism of a microalgae platform, including glycolysis, TCA (tricarboxylic acid) cycle, pentose phosphate pathway, total lipid synthesis, starch synthesis, amino acids metabolism, energy metabolism and biomass synthesis. The metabolic network (Figure 5.1) was first built according to databases such as KEGG, MetaCyc, DiatomCyc, BioCyc as well as from literature (Boyle & Morgan, 2009; Kliphuis et al., 2011; Muthuraj et al., 2013). In this work, for simplification purposes, *Chlorella* cells were considered as a unique compartment with no specific intracellular compartments such as mitochondria, chloroplast, vacuoles, vesicles and nucleus. Energy metabolism was considered as a global reaction where *de novo* synthesis and substrate level phosphorylation were combined in a unique pathway. Reversible reactions involving storage carbon such as starch and lipid catabolism were described. As a first attempt, the various lipids found in microalgae cells were taken as a global lipid pool. The stoichiometry of the biochemical reactions of the network is based on a flux balance analysis on *Chlorella protochecoides* (Muthuraj et al., 2013). A full list of the model reactions and reactions stoichiometry is listed in Table 5.1. The Michaelis-Menten kinetic equation is used to describe each flux rate (Table 5.2).

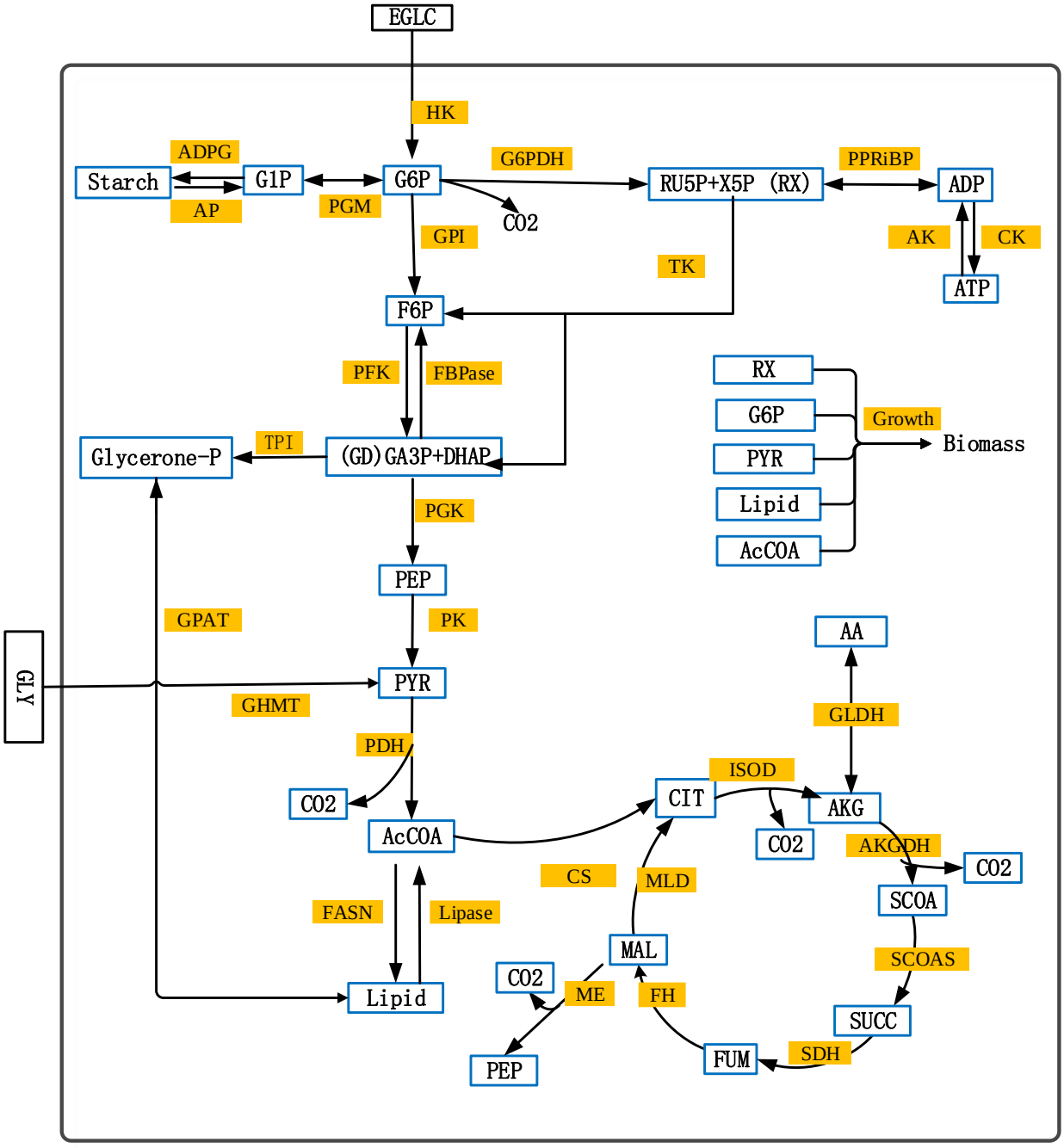

Figure 5. 1 The model metabolic network for heterotrophic *Chlorella protothecoides*

The cells specific growth rate (equation no. 30 in Table 5.2) was defined as in previous works (Cloutier et al., 2009; Leduc et al., 2006), accounting for biomass synthesis from precursors of the major cell constituents such as RX (R5P and X5P), G6P, PYR, AcCOA and total lipid. RX is normally used to synthesize nucleotides, DNA and RNA; G6P leads to organic phosphates providing energy for maintenance and metabolism; PYR is feeding amino acids metabolism which

leads to protein formation; AcCOA is the precursor of fatty acids; while the lipid pool is the main contributor to cell mass accumulation in the algae platform. The specific consumption of precursors to cell mass synthesis was considered in the mass balances. For each metabolite, a mass balance equation (Equation 5.1) included the sum of all the input and output fluxes minus cell dilution effect from the cell division phenomenon (Table 5. 3 with all ordinary differential equations).

$$\frac{d[C_{S_i}]}{dt} = \left(\sum_{i=1}^{M} V_{input_i} - \sum_{j=1}^{N} V_{output_j} - [C_{S_i}] \times V_{growth}\right) \quad \text{Equation 5.1}$$

Where C_{si} is the concentration of each metabolite at time t, M is the input flux number, N is the output flux number, V_{input} and V_{output} are the flux rates at each metabolite node. V_{growth} is the growth rate.

5.3.3 **Model parameters estimation**

The model has 77 parameters, which include 34 maximum flux rates, 38 enzyme half-saturated constants, and 5 growth coefficients for the 5 growth precursors contributing to biomass synthesis. Initial metabolite concentrations (i.e. at t = 0) were taken from experimental data, which include 25 intracellular metabolites distributed in 8 pathways covering 30 metabolic reactions (Ren et al., 2015), or from literature otherwise (Table 5.4). Model simulations were performed using Matlab (the MathWorks Inc., Natick, MA, USA) with the "ode23" solver of the ordinary differential equations system. Initial kinetic parameter values (V_{max}, K_m) for each flux and enzymes in the model were taken within ranges found in the enzyme database BRENDA (http://www.brenda-enzymes.org), and the respective units (mmol/L) were converted to comply with the model (mmol/gDW) by dividing 10 gDW/L biomass obtained in our culture. First estimates of maximal flux rates (V_{max}) have been calculated from experimental data (Ren et al., 2015), or from BRENDA. Model parameter values were determined following the method proposed in Rizzi et al. (Rizzi et al., 1997). Briefly, the time course of each metabolite with experimental concentration data were defined as fixed mathematical functions, enabling the procedure for parameter values optimization to focus first on non-measured metabolites. In the present case of a high number of parameters, this approach allows accelerating parameter values identification. An objective function (Equation 5.2), defined as the weighted sum of squared residues between experimental data and simulated values for each metabolites *m* at time *k*, where the weight is the experimental data for each state variable, was used to quantify simulation error.

$$\min\left(\sum_{n=1}^{N}\sum_{t=1}^{T}\left(\frac{X_{n,t}^{exp}-X_{n,t}^{sim}}{X_{n,t}^{exp}}\right)^2\right)$$ Equation 5.2

Based on this objective function, a sensitivity analysis of model parameters was performed to identify the sensitive ones in order to avoid over-parameterization, by then keeping constant non-sensitive parameters. Sensitivity analysis was performed by changing each parameter from -70 % to +150 % one at a time while holding others constant. From the Matlab optimization toolbox, the "linsqurfit" sub-routine was used to identify model parameter values. This process of parameter calibration was continued until minimizing the objective function, i.e. the simulated results closely following experimental data. Final parameter values of the model are shown in Table 5.5. Confidence intervals of estimated parameters were evaluated using the Matlab sub-routine "nlparci.m" (Table 5.5). It is clear there is no unique solution for parameter values in such an underdetermined system, as well as the values are averaged ones differing from that for each enzyme since a simplified model deals with lumped reactions. However, although a simplified metabolic model only partially describes the biological reality, it remains a valuable tool to assess hypotheses on modeling structure which biological relevancy can be validated comparing model simulations to experimental data.

Table 5. 1 Reactions of a metabolic network

No.	Enzyme	Description	Reaction
1	HK	Hexokinase	EGLC => G6P
2	GPI	Glucose 6 phosphate isomerase	G6P => F6P
3	PFK	6 phosphofructokinase	F6P => 2 GD
4	FBPase	Fructose biphosphate aldolase	2 GD => F6P
5	PGK	Phosphoglycerate kinase	GD => PEP
6	PK	Pyruvate kinase	PEP => PYR
7	PDH	Pyruvate dehydrogenase	PYR => AcCOA + CO_2
8	FASN	Fatty acid synthase	12 AcCOA => Lipid
9	Lipase	Lipase	Lipid => 12 AcCOA
10	GPAT	Glycerol-3-phosphate acyltransferases	GlyP = Lipid
11	TPI	Triosephosphate isomerase	GD => GlyP
12	G6PDH	Glucose 6 phosphate 1 dehydrogenase	G6P => RX + CO_2
13	TK	Transketolase	3 RX => 2 F6P + GD
14	PPRiBP	Phosphoribosyl-diphosphate synthetase	RX = ADP
15	CK	Creatine kinase	ADP => ATP
16	AK	Adenylate kinase	ATP => ADP
17	PGM	Phosphoglucomutase	G6P = G1P
18	ADPG	Adenosine diphosphate glucose-starch glucosyltransferase	25 G1P => Starch
19	AP	Amylase	Starch => 25 G1P
20	GHMT	Glycine hydroxymethyltransferase	GLY => PYR
21	CS	Citrate synthase	AcCOA => CIT
22	MLD	Malate dehydrogenase	MAL => CIT
23	ISOD	Isocitrate dehydrogenase	CIT => AKG + CO_2
24	AKGDH	Oxoglutarate dehydrogenase	AKG => SCOA + CO_2
25	GLDH	Glutamate dehydrogenase	AKG = AA
26	SCOAS	Succinyl CoA ligase	SCOA => SUCC
27	SDH	Succinate dehydrogenase	SUCC => FUM
28	FH	Fumarate hydratase	FUM => MAL
29	ME	Malic Enzyme	MAL => PEP + CO_2
30	growth	Biomass synthesis	G6P + RX + PYR + Lipid + AcCOA => X

Note: '=>' represents unidirectional reactions. '=' represents reversible reactions.

Table 5. 2 Kinetic equations of the metabolites fluxes in the model

No.	Kinetic equations
1	$V_{HK} = V_{\max\_HK} * \frac{EGLC}{K_{m\_HK\_EGLC} + EGLC}$
2	$V_{GPI} = V_{\max\_GPI} * \frac{G6P}{K_{m\_GPI\_G6P} + G6P}$
3	$V_{PFK} = V_{\max\_PFK} * \frac{F6P}{K_{m\_PFK\_F6P} + F6P}$
4	$V_{FBPase} = V_{\max\_FBPase} * \frac{GD}{K_{m\_FBPase\_GD} + GD}$
5	$V_{PGK} = V_{\max\_PGK} * \frac{GD}{K_{m\_PGK\_GD} + GD}$
6	$V_{PK} = V_{\max\_PK} * \frac{PEP}{K_{m\_PK\_PEP} + PEP}$
7	$V_{PDH} = V_{\max\_PDH} * \frac{PYR}{K_{m\_PDH\_PYR} + PYR}$
8	$V_{FASN} = V_{\max\_FASN} * \frac{AcCOA}{K_{m\_FASN\_AcCOA} + AcCOA}$
9	$V_{Lipase} = V_{\max\_Lipase} * \frac{Lipid}{K_{m\_Lipase\_Lipid} + Lipid}$
10	$V_{GPAT} = V_{\max\_GPAT} * \frac{GlyP}{K_{m\_GPAT\_GlyP} + GlyP} - V_{\max r\_GPAT} * \frac{Lipid}{K_{m\_GPAT\_Lipid} + Lipid}$
11	$V_{TPI} = V_{\max\_TPI} * \frac{GD}{K_{m\_TPI\_GD} + GD}$
12	$V_{G6PDH} = V_{\max\_G6PDH} * \frac{G6P}{K_{m\_G6PDH\_G6P} + G6P}$
13	$V_{TK} = V_{\max\_TK} * \frac{RX}{K_{m\_TK\_RX} + RX}$
14	$V_{PPRiBP} = V_{\max\_PPRiBP} * \frac{RX}{K_{m\_PPRiBP\_RX} + RX}$
15	$V_{CK} = V_{\max\_CK} * \frac{ADP}{K_{m\_CK\_ADP} + ADP}$
16	$V_{AK} = V_{\max\_AK} * \frac{ATP}{K_{m\_AK\_ATP} + ATP}$

17 $$V_{PGM} = V_{max\_PGM} * \frac{G6P}{K_{m\_PGM\_G6P} + G6P} - V_{maxr\_PGM} * \frac{G1P}{K_{m\_PGM\_G1P} + G1P}$$

18 $$V_{ADPG} = V_{\max\_ADPG} * \frac{G1P}{K_{m\_ADPG\_G1P} + G1P}$$

19 $$V_{AP} = V_{\max\_AP} * \frac{Starch}{K_{m\_AP\_Starch} + Starch}$$

20 $$V_{GHMT} = V_{\max\_GHMT} * \frac{GLY}{K_{m\_GHMT\_GLY} + GLY}$$

21 $$V_{CS} = V_{max\_CS} * \frac{AcCoA}{K_{m\_CS\_AcCoA} + AcCoA}$$

22 $$V_{MLD} = V_{max\_MLD} * \frac{MAL}{K_{m\_MLD\_MAL} + MAL}$$

23 $$V_{ISOD} = V_{max\_ISOD} * \frac{CIT}{K_{m\_ISOD\_CIT} + CIT}$$

24 $$V_{AKGDH} = V_{\max\_AKGDH} * \frac{AKG}{K_{m\_AKGDH\_AKG} + AKG}$$

25 $$V_{GLDH} = V_{\max\_GLDH} * \frac{AKG}{K_{m\_GLDH\_AKG} + AKG} - V_{\max r\_GLDH} * \frac{AA}{K_{m\_GLDH\_AA} + AA}$$

26 $$V_{SCOAS} = V_{\max\_SCOAS} * \frac{SCOA}{K_{m\_SCOAS\_SCOA} + SCOA}$$

27 $$V_{SDH} = V_{\max\_SDH} * \frac{SUCC}{K_{m\_SDH\_SUCC} + SUCC}$$

28 $$V_{FH} = V_{\max\_FH} * \frac{FUM}{K_{m\_FH\_FUM} + FUM}$$

29 $$V_{ME} = V_{\max\_ME} * \frac{MAL}{K_{m\_ME\_MAL} + MAL}$$

30 $$V_{growth} = V_{\max\_growth} * \frac{G6P}{K_{m\_growth_{G6P}} + G6P} * \frac{RX}{K_{m\_growth_{RX}} + RX} * \frac{PYR}{K_{m\_growth_{PYR}} + PYR} * \frac{AcCOA}{K_{m\_growth\_AcCOA} + AcCOA} * \frac{Lipid}{K_{m\_growth\_Lipid} + Lipid}$$

Table 5. 3 Mass balances of state variables in the model

No.	Mass balances of each metabolite	Unit
1	AA=+ V_GLDH - (V_growth * AA)	mmol/gDW/day
2	ADP =+ V_PPRiBP - V_CK + V_AK - (V_growth * ADP)	mmol/gDW/day
3	AKG =+ V_ISOD - V_AKGDH - V_GLDH - (V_growth * AKG)	mmol/gDW/day
4	ATP =+ V_CK - V_AK - (V_growth * ATP)	mmol/gDW/day
5	AcCOA = + V_PDH - V_CS -(12 * V_FASN) +(12 * V_Lipase) -(V_growth * AcCOA) - (V_growth_AcCOA * V_growth)	mmol/gDW/day
6	CIT = + V_CS + V_MLD - V_ISOD - (V_growth * CIT)	mmol/gDW/day
7	F6P = + V_GPI - V_PFK + V_FBPase +(2 * V_TK) - (V_growth * F6P)	mmol/gDW/day
8	FUM = + V_SDH - V_FH - (V_growth * FUM)	mmol/gDW/day
9	G1P = + V_PGM -(25 * V_ADPG) +(25 * V_AP) - (V_growth * G1P)	mmol/gDW/day
10	G6P = + V_HK - V_GPI - V_G6PDH - V_PGM - (V_growth * G6P) - (V_growth_G6P * V_growth)	mmol/gDW/day
11	GD= +(2 * V_PFK) -(2 * V_FBPase) - V_PGK + V_TK - V_TPI - (V_growth * GD)	mmol/gDW/day
12	GlyP = + V_TPI - V_GPAT - (V_growth * GD)	mmol/gDW/day
13	Lipid = + V_GPAT + V_FASN - V_Lipase - (V_growth * Lipid) - (V_growth_Lipid * V_growth)	mmol/gDW/day
14	MAL = - V_MLD + V_FH - V_ME - (V_growth * MAL)	mmol/gDW/day
15	PEP = + V_PGK - V_PK + V_ME - (V_growth * PEP)	mmol/gDW/day
16	PYR = + V_PK - V_PDH + V_GHMT - (V_growth * PYR) - (V_growth_PYR * V_growth)	mmol/gDW/day
17	RX = + V_G6PDH -(3 * V_TK) - V_PPRiBP - (V_growth * RX) - (V_growth_RX * V_growth)	mmol/gDW/day

18	SCOA = + V_AKGDH - V_SCOAS - (V_growth * SCOA)	mmol/gDW/day
19	SUCC = + V_SCOAS - V_SDH - (V_growth * SUCC)	mmol/gDW/day
20	Starch = + V_ADPG - V_AP - (V_growth * Starch)	mmol/gDW/day
21	EGLC = (- V_HK) * X	mmol/L/day
22	X = V_growth * X	gDW/L/day
23	GLY = (- V_GHMT) *X	mmol/L/day
24	CO_2 = (+ V_PDH + V_G6PDH + V_ISOD + V_AKGDH + V_ME) * X	mmol/L/day

Table 5. 4 State variables description and initial conditions

No.	Metabolites	Description	Values	Units
1	ADP	Adenosine diphosphate	2.22E-03	mmol/gDW
2	AKG	a-Ketoglutarate	5.88E-05	mmol/gDW
3	ATP	Adenosine triphosphate	1.43E-02	mmol/gDW
4	AcCOA	Acetyl–coenzyme A	2.56E-04	mmol/gDW
5	CIT	Citrate	2.00E-04	mmol/gDW
6	F6P	Fructose 6-phosphate	4.72E-05	mmol/gDW
7	FUM	Fumarate	2.42E-05	mmol/gDW
8	G1P	Glucose 1-phosphate	1.05E-05	mmol/gDW
9	G6P	Glucose 6-phosphate	2.36E-04	mmol/gDW
10	GD	Glyceraldehyde 3-phosphate & Dihydroxyacetone phosphate	1.94E-04	mmol/gDW
11	AA	Amino acids	3.80E+01	mmol/gDW
12	GlyP	Glycerone-phosphate	2.00E-04	mmol/gDW
13	Lipid	Lipid	4.76E-01	mmol/gDW
14	MAL	Malate	1.39E-04	mmol/gDW
15	PEP	Phosphoenolpyruvate	2.37E-05	mmol/gDW
16	PYR	Pyruvate	1.10E-04	mmol/gDW
17	RX	Ribose 5-phosphate & Xylose-5-phosphate	2.26E-05	mmol/gDW
18	SCOA	Succinyl–coA	2.00E-05	mmol/gDW
19	SUCC	Succinate	2.00E-05	mmol/gDW
20	Starch	Starch	4.45E-03	mmol/gDW
21	EGLC	Extracellular glucose	5.53E+01	mmol/L
22	X	Biomass	4.21E-02	gDW/L
23	GLY	Glycine	1.32E+00	mmol/L
24	CO_2	Carbon dioxide	1.20E-04	mmol/L

Table 5. 5 Parameter values and 95 % confidence intervals of the highly sensitive parameters

Parameters	Values	Confidence interval	Parameters	Values	Confidence interval
Vmax_HK	20	(19.989, 20.011)	km_HK_EGLC	0.8	
Vmax_GPI	17	(16.998, 17.002)	km_GPI_G6P	0.0001	(8.37E-5, 1.16E-4)
Vmax_PFK	23	(22.998, 23.002)	km_PFK_F6P	0.00003	
Vmax_FBPase	1	(1.000, 1.000)	km_PGK_GD	0.000004	(3.12E-6, 4.88E-6)
Vmax_PK	37	(36.991, 37.009)	km_PK_PEP	0.000007	
Vmax_PDH	40	(39.997, 40.003)	km_PDH_PYR	0.00001	
Vmax_G6PDH	9		km_G6PDH_G6P	0.0009	
Vmax_PGK	30	(29.997, 30.003)	km_TK_RX	0.0001	
Vmax_TK	13	(13.000, 13.000)	km_ADPG_G1P	0.00005	
Vmax_ADPG	10	(9.999, 10.001)	km_AP_Starch	0.008	
Vmax_AP	2	(2.000, 2.000)	km_PGM_G6P	0.00004	
Vmax_PGM	16	(15.992, 16.008)	km_PGM_G1P	0.000005	
Vmaxr_PGM	14	(13.995, 14.005)	km_GHMT_GLY	0.1	
Vmax_GHMT	6	(6.000, 6.000)	km_growth_G6P	0.0000001	(-3.20-E-6, 3.40E-6)
Vmax_growth	2	(2.000, 2.000)	km_growth_PYR	0.0000001	(-2.47E-7, 4.47E-7)
Vmax_PPRiBP	15		km_growth_RX	0.0000006	(4.46E-7, 7.54E-7)
Vmaxr_PPRiBP	7		km_growth_Lipid	0.001	(8.16E-4, 1.18E-3)
Vmax_CK	5		km_growth_AcCOA	0.000001	
Vmax_AK	4.5		km_FBPase_GD	0.0003	(0.0002, 0.0004)
Vmax_TPI	0.01		km_PPRiBP_RX	0.00001	
Vmax_GPAT	0.01		km_PPRiBP_ADP	0.005	
Vmaxr_GPAT	0.06		km_CK_ADP	0.001	
Vmax_FASN	31.3		km_AK_ATP	0.002	
Vmax_Lipase	12.12		km_GPAT_GlyP	0.0001	
Vmax_CS	2		km_GPAT_Lipid	0.01	(0.0098, 0.0102)
Vmax_ISOD	0.3		km_FASN_AcCOA	0.002	
Vmax_AKGDH	0.3		km_Lipase_Lipid	0.01	(0.0099, 0.0101)
Vmax_SCOAS	1		km_TPI_GD	0.002	
Vmax_SDH	13		km_CS_AcCOA	0.2	
Vmax_FH	3		km_GLDH_AA	3	
Vmax_MLD	0.1		km_GLDH_AKG	3	
Vmax_ME	0.1		km_ISOD_CIT	0.7	
Vmax_GLDH	0.01		km_AKGDH_AKG	0.007	
Vmaxr_GLDH	0.02		km_SCOAS_SCOA	0.001	

V_growth_RX	0.001		km_SDH_SUCC	0.00002
V_growth_PYR	0.002		km_FH_FUM	0.008
V_growth_G6P	0.001		km_MLD_MAL	0.003
V_growth_Lipid	0.001	(0.0008, 0.001)	km_ME_MAL	0.001
V_growth_AcCOA	0.008			

Note: Flux rates in mmol gDW^{-1}, except for the maximum specific growth rate *($V_{max,growth}$)* which is in d^{-1}. Enzymes affinity constants in mmol gDW^{-1}, except for HK and GHMT, which affinity constant on substrates are in mmol L^{-1}.

5.4 Results and Discussion

5.4.1 Model structure calibration

Although steady-state approaches such as MFA and FBA seem having virtually no limit at detailing a biosystem metabolic network, with for instance 484 reactions and 458 metabolites in *Chlamydomonas reinharditii* (Boyle & Morgan, 2009), a fully dynamic approach requires limiting overparameterization, and thus network reduction (Jolicoeur, 2014). Our strategy while building-up the model structure consisted in starting from the simplest but minimal network, which included glycolysis, TCA cycle, PPP pathway, and total lipid and starch metabolisms. Then, while progressing calibrating model parameter values evaluating the simulation error from the objective function (equation 5.2), decisions were made to add complexity (i.e. pathways, flux regulation) until simulation trends agreed with experimental data. The final step of parameter values estimation then started from that point. Reactions stoichiometry were taken from a previous FBA study on *Chlorella* sp. in which 158 reactions and 113 metabolites were considered (Muthuraj et al., 2013). The energetic metabolism has been simplified, lumping a series of consumption/regeneration reactions into a single pathway involving the PPRiBP, CK and AK enzymes, and specifically linked to nucleotides pool management.

Lipid synthesis was considered from the major precursor of AcCOA, and fatty acids which are intermediates to lipid were pooled as total lipid for simplification purposes; lipid contain dozens of fatty acids of different lengths and saturated degrees. From the preliminary simulation results while exploring various model structures (not shown), the reaction from AcCOA to lipids showed being mostly unidirectional. Glycerine-phosphate (GlyP), a precursor providing the carbon frame of acyl-glycerol such as triacylglycerol (TAG), a main lipid type in *Chlorella protothecoides*, was

considered. The reaction from GD (GA3P & DHAP) to glycerine-phosphate (GlyP) was also added. TCA cycle is a competing pathway of lipid synthesis pathway while sharing the same precursor AcCOA. Again, in preliminary model simulations (not showed), lipid catabolism could not stimulate TCA fluxes, and any added regulation mechanisms around these enzymes could only increase or decrease fluxes to TCA cycle (e.g. the CS enzyme), and make TCA metabolites level changing but not provide extra carbon flux to make the TCA metabolites rebound. However, interconnecting TCA cycle to amino acids metabolism (AA to AKG) helped simulating TCA cycle metabolites concentration. This then enables the consumption of AA to feed the TCA fluxes.

5.4.2 Calibration of kinetic parameters

A sensitivity analysis on model parameters showed flux maximum rate constants ($V_{max,i}$) to be more sensitive than affinity constants ($K_{m,i}$). For the final calibrated model 21 parameters, 15 maximum flux rates and 6 enzyme affinity constant (Figure 5.2), out of 77 revealed greater sensitivity, defined as affecting the objective function of more than 10 % when applying a -70 % to +150 % parameter value change around its optimized value. Most sensitive parameters are $V_{max,HK}$ and $V_{max,GHMT}$, which are both at the entrance of the major carbon and nitrogen sources; then $V_{max,GPI}$, $V_{max,PGM}$ and $V_{max,PDH}$, which refer to fluxes at the intersection of glycolysis, starch and lipid metabolisms. $V_{max,FASN}$, $V_{max,Lipase}$ and $V_{max,GPAT}$ sensitive suggests lipid metabolism is reactive to variations of connected pathways. Interestingly, the two highly sensitive affinity constants ($km_{,growth\_lipid}$ and $km_{,Lipase\_lipid}$), refer to the importance of lipid for cell biomass growth. Algae cell is a great platform accumulating lipids and biomass, some algae species could accumulate lipids up to 70 % of their biomass. Some reactions or pathways (i.e. their kinetic parameters) such as the maximum specific growth rate, PPP pathway ($V_{max,TK}$) and TCA cycle, showed a low sensitivity level, which suggest these are robust pathways. These sensitivity results were in agreement with published data on plant cell platform, which all reported sensitive parameters being in glycolysis, the specific growth rate and in TCA cycle. Parameters 95 % confidence intervals (Table 5.5) are within ranges found in the BRENDA databank.

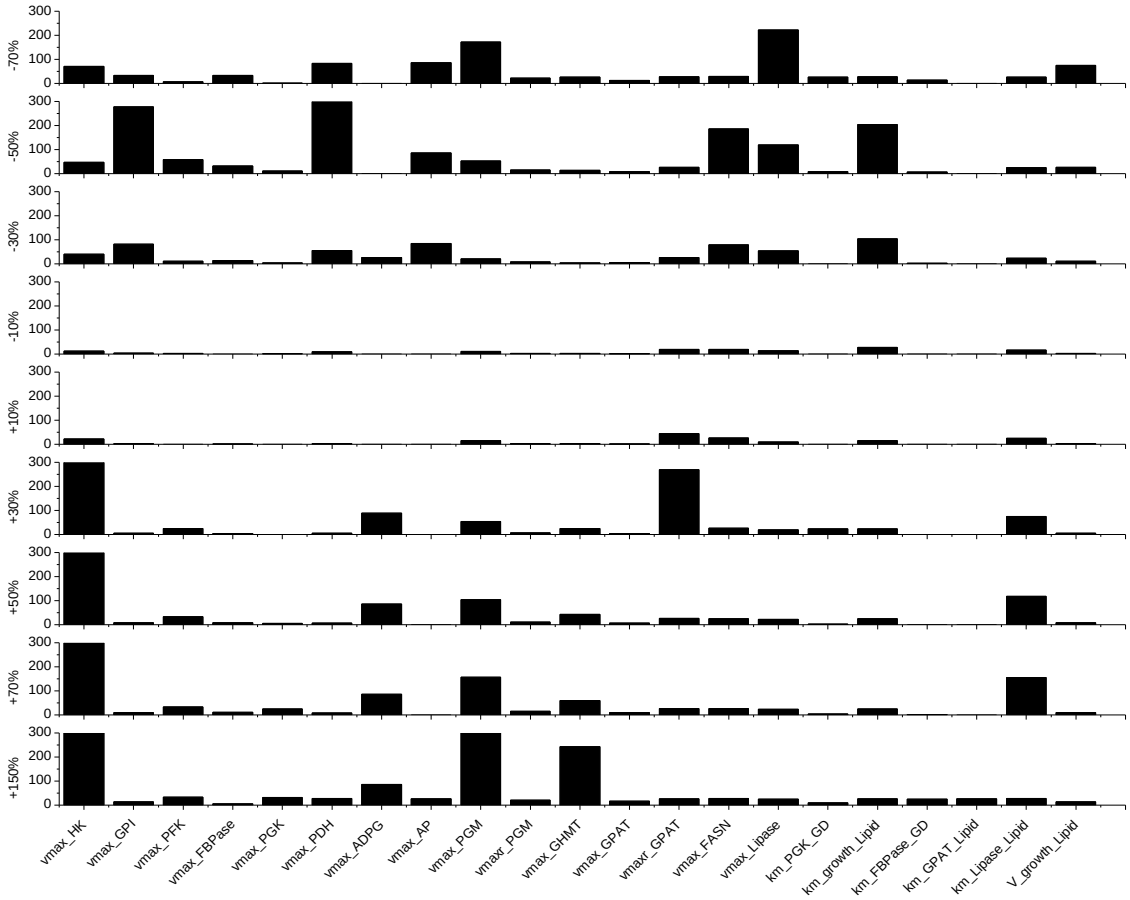

Figure 5. 2 Sensitivity analysis on model parameters. Vertical axis value represents percentage change in the objective function for parameter change from -70 % to +150 % around the optimized value. Parameters not shown have percentage changes less than 10 %.

5.4.3 **Model simulates algae cell behavior under heterotrophic condition**

The final calibrated model cope with the experimental data with adequate fitness (Figure 5.3). Cell growth, as well as extracellular metabolites such as glucose and glycine are closely simulated. More importantly, total lipids and starch as the main products were also simulated adequately. These results thus confirm the model structure as well as its calibrated kinetic parameters to simulate algae cells carbon nutrition and products accumulation dynamics. Many decades ago, the Droop model was developed to represent the effect of B12 vitamin intracellular quota on the growth rate of phytoplankton. The model has been shown appropriate to also represent the effect of intracellular management of nutrients such as nitrogenous compounds and phosphate on growth rate. The model premises were based on observations that cell growth continued after the exhaustion of external nitrogen pool, being then supported by the consumption of intracellular

nitrogen pools such as chlorophyll molecules. This intracellular nutrients management phenomenon has also been modeled for plant cells (Cloutier et al., 2009). In the present work, algae cells biomass still accumulates while glycine and other amino acids pool (AA) reached values under the detection limits. However, this phenomenon was only observed for nitrogen sources since cell biomass growth stopped simultaneously to glucose depletion. Therefore, Droop model philosophy, which is implicit in kinetic metabolic models such as in this work, applies in *C. prototheco*ides. Furthermore, describing metabolic flux kinetics and thus time evolution of the cells enzyme activity in addition to intracellular metabolites concentration, a kinetic metabolic can bring complementary data of high interest, such as for the elucidation of metabolic regulation phenomena, although this type of model is more tedious to build. Indeed, in this work, both the experimental data and model simulations show glycolysis and PPP pathways being more affected by glucose supply while TCA metabolism, which is fed by both carbon and nitrogen metabolisms, seems more robust to perturbations such as extracellular glucose depletion. Although limited to carbon and nitrogen metabolisms, the model led to adequate simulation results when compared to experimental data. Meanwhile, although highly simplified, simulation results showed to cope well with ATP and ADP experimental data, as well as with the ADP-to-ATP ratio. However, the integration of cell energetic status with its known effect on flux regulation (as co-factors and co-substrates) shall, in a further model development step, allow an enhanced simulation capacity under various culture modes.

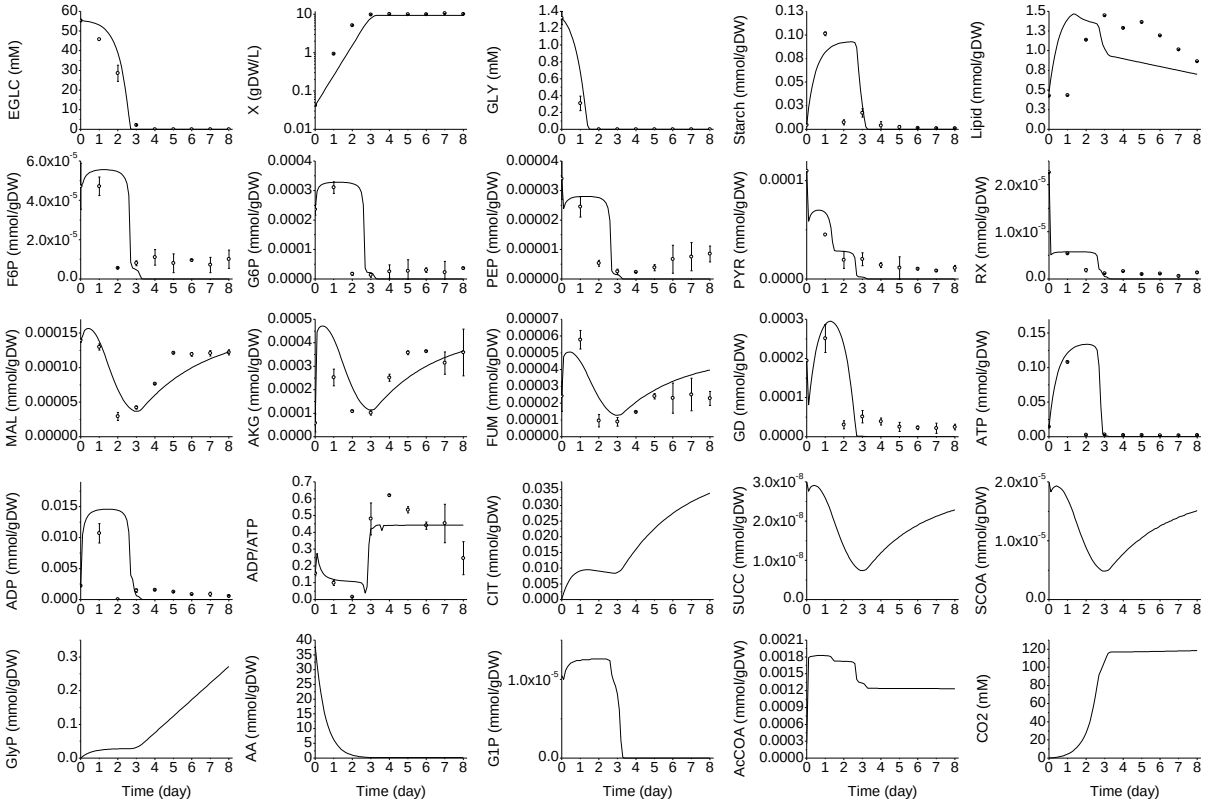

Figure 5. 3 Simulation result versus experimental data for *Chlorella protothecoides* heterotrophic behavior (experimental data: open squares, simulated data: solid line. Experimental data were taken from a previous work (Ren et al., 2016), where the error bars represent the standard error of triplicates data.

5.4.4 **A metabolic flux analysis reveals a high lipid synthesis and low TCA cycle activity**

Considering all the above, it is thus clear that the model structure allows simulating heterotrophic *Chlorella protothecoides* cell behavior. There was then strong confidence turning the model as an *in silico* tool and perform a metabolic flux analysis (MFA) estimating flux distribution. Flux rates were estimated at 48 h before glucose depletion in the exponential growth phase. For comparison purposes, all the flux values were normalized to an uptake flux of 100 mmol $g^{-1}DW\,h^{-1}$ glucose (Figure 5.4). Flux results agree with that reported in (Muthuraj et al., 2013), who performed a flux balance analysis at steady state for *Chlorella protothecoides* under heterotrophic condition, with a GPI flux of 66.28 mmol $g^{-1}DW\,h^{-1}$ (leading to glycolysis), G6PDH of 12.15 (leading to PPP pathway) and PGM of 13.83 (leading to starch), compared to 49.8 mmol $g^{-1}DW\,h^{-1}$, 32.04 and 17.3

respectively. The total flux to G6P obtained from our model is of 92.26 mmol $g^{-1}DW\ h^{-1}$ compared to 99.22 in (Muthuraj et al., 2013). The net flow From F6P to GD (PFK minus FBPase) was of 73.47 mmol $g^{-1}DW\ h^{-1}$ compared to 70.35 (from F6P to GAP) in (Muthuraj et al., 2013), and the flux from GD to PEP was of 150.51 mmol $g^{-1}DW\ h^{-1}$ in our model versus 148.25 (from GAP to PEP) in (Muthuraj et al., 2013). The fluxes of nucleotides synthesis (from RX to ADP) was of 1.36 mmol $g^{-1}DW\ h^{-1}$ compared to 0.67 in (Muthuraj et al., 2013) (from PRPP to DNA and RNA). Biomass synthesis rate was of 9.19 compared to 7.36 in (Muthuraj et al., 2013). Furthermore, downstream fluxes to AcCOA, the sum of the downstream lipid and TCA cycle flux was of 74.01 mmol $g^{-1}DW\ h^{-1}$ compared to 86.14 in (Muthuraj et al., 2013). Although a similar total flux around the TCA cycle was obtained, with 73.93 mmol $g^{-1}DW\ h^{-1}$ at lipid branch and 0.08 at TCA branch, different results were reported in (Muthuraj et al., 2013) with 81.21 mmol $g^{-1}DW\ h^{-1}$ at TCA cycle and 4.82 mmol $g^{-1}DW\ h^{-1}$ at lipid branch. This discrepancy may rely on a high lipid level (13.13 % DW) in our cell culture compared to that in (Muthuraj et al., 2013) (1 % DW). Differences in culture conditions may be involved as well.

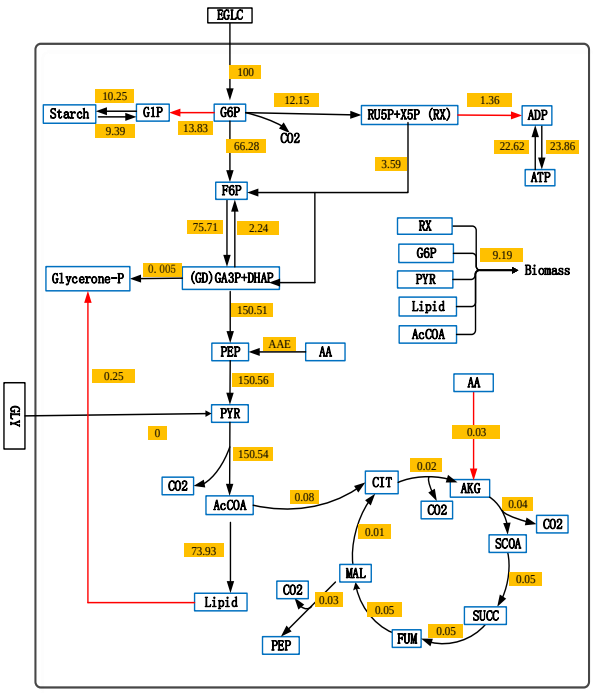

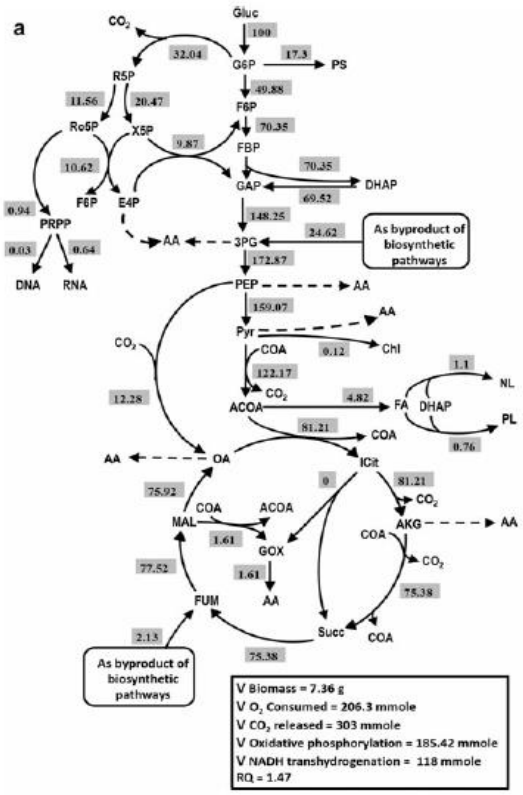

Figure 5. 4 Flux distribution under heterotrophic cultivation at exponential phase (48 h). Note: All the flux values are normalized to 100 mmol glucose assimilated and are measured in mmol/gDW/day. Red arrows represents the flux direction for the four reversible reactions. The figure on the right is screen-cut from the cited article as mentioned in the text.

5.4.5 A dynamic flux analysis suggest a robust and stable metabolism in *Chlorella protothecoides*

A dynamic metabolic flux analysis was performed from model simulation (Figure 5.5). Looking at glucose flux (V_{HK}), glycine flux (V_{GHMT}) as well as cell specific growth rate (V_{growth}) (Figure 5.5a), it is clear that cell growth proceeds simultaneously to carbon source uptake, but not proportionally to nitrogenous source uptake. Interestingly and as previously discussed for glycine concentration, glycine flux (V_{GHMT}) ceased more than 24 h prior to growth cessation.

Fluxes of PPP pathway and starch synthesis (Figure 5.5c, 5.5d) originate from G6P and are partially affected in some extent by glucose flux (Figure 5.5a). For instance, model simulation V_{PGM} flux showed being reversible from accumulation to decomposing at around day 3, where glucose reached depletion. This suggests that starch, which is an intracellular carbon storage pool, rapidly responds to a low carbon source level threshold, contributing providing continuous carbon flow feeding cell metabolism and maintenance. However, as an alternative carbon storage pool, net lipid flux shows a continuous catabolism at a quasi-constant rate, composed of a synthesis flux (V_{FASN}) that was slightly affected at glucose depletion and two catabolic fluxes (V_{Lipase} and V_{GPAT}) which stayed quite constant (11.87-12.04 mmol gDW^{-1} d^{-1} and 0.05 mmol gDW^{-1} d^{-1} respectively) (Figure 5.5e). Interestingly, TCA cycle fluxes (V_{ISOD}, V_{SDH}) (Figure 5.5f) exhibited a minimum value at glucose depletion, for increasing thereafter. As previously mentioned, the TCA cycle is closely related to lipid metabolism, so this result is not surprizing. Moreover, CS flux dynamics also closely follows the lipid synthesis flux.

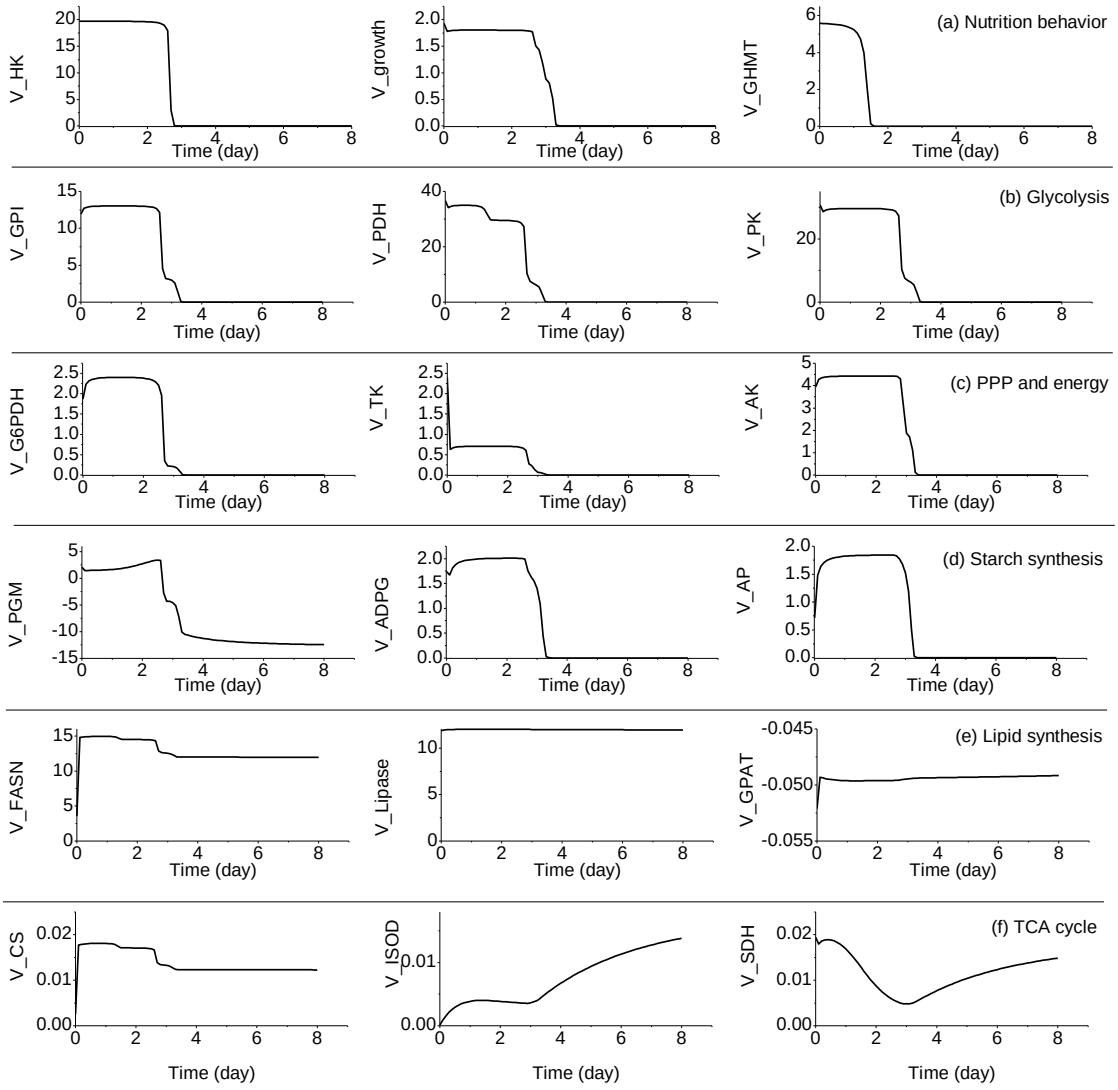

Figure 5. 5 Flux rate of every reaction in the model system. (a) Nutrition fluxes and growth rate; (b) Glycolysis fluxes; (c) PPP pathway fluxes; (d) Starch synthesis fluxes; (e) Lipid synthesis fluxes; (f) TCA cycle fluxes. All flux units were in mmol gDW^{-1} d^{-1}.

We then looked at the major branch points of glycolysis. Model simulations show that the glucose uptake rate (V_{HK}) and the glycolytic fluxes went down to a very low level after day 2.6, we have thus analyzed their related flux ratios only before glucose depletion (< 2.6 d). First, we evaluated that 6 % of the glucose flux contributes to biomass synthesis and growth (V_{growth}-to-V_{PK} ratio) (Figure 5. 6a), a value comparable to the literature with 3.9 % (Follstad et al., 1999). Within the same range, 8 % (8.323-8.325 %) of the glucose flux feed lipid synthesis (Figure 5. 6b). However, as a main product contributing to biomass, the lipid catabolism-to-biomass synthesis and growth

ratio (V_{FASN} -V_{Lipase} - V_{GPAT} to V_{growth}) shows two successive constant values at around 60 % increasing at 80 % at mid-exponential growth phase (1.5 d) (Figure 5. 6e). Model simulations also suggest that around 1 % of the glucose flux goes to starch synthesis (V_{ADPG}-V_{AP} to V_{HK}) (Figure 5.6c), and that 15 % to 7 % of the glucose flux feed nucleotides synthesis (V_{PPRiBP} to V_{G6PDH}). Concerning the PPP pathway activity, around 12 % of the glucose uptake flux flow into the pentose phosphate pathway (V_{G6PDH} to V_{HK}). Therefore, the dynamic metabolic flux analysis using the developed model mostly suggest a robust and stable metabolism.

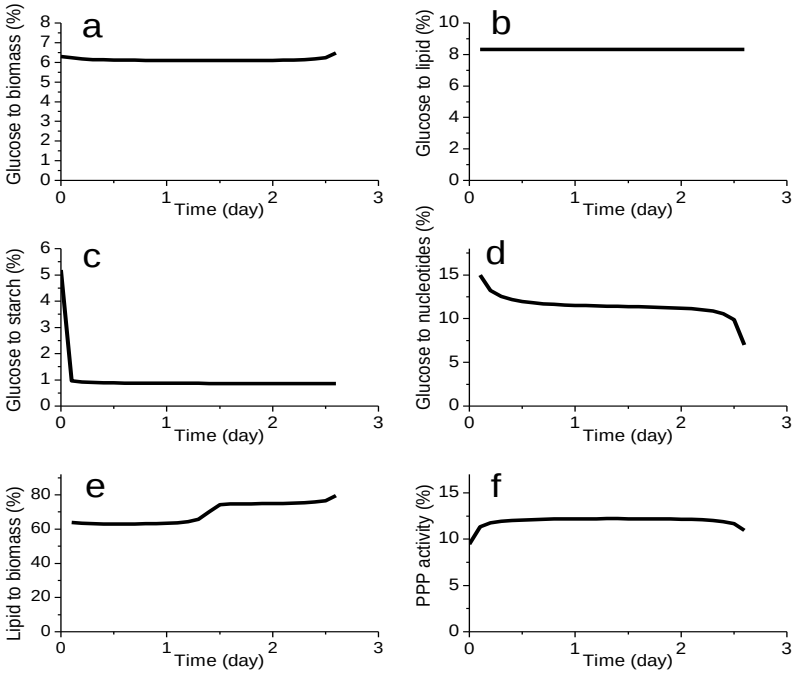

Figure 5. 6 Metabolic flux ratios between different pathways. Glucose contribution ratio to biomass (a), lipids (b), starch (c) and nucleotides (d); Lipid contribution to biomass (e); PPP pathway activity (f); (a) V_{growth} to V_{PK} ratio; (b) V_{FASN} -V_{Lipase} - V_{GPAT} to V_{growth} ratio; (c) (V_{ADPG}-V_{AP}) to V_{HK} ratio; (d) V_{PPRiBP} to V_{G6PDH} ratio; (e) V_{PPRiBP} to V_{G6PDH} ratio; (f) V_{G6PDH} to V_{HK} ratio

5.5 Conclusion

A model simulating *Chlorella protothecoides* cell metabolic behavior under heterotrophic condition and describing metabolic network flux kinetics and energetic states has been developed and calibrated. Simulation results show satisfactory fit with experimental data. Flux analysis is also in high agreement with literature data. A sustained high lipid synthesis metabolic activity was

further confirmed from model simulations with higher lipid flux and lower TCA activity. The model was also used to analyze the dynamic distribution of the carbon source to the main carbon pathways, such as PPP pathway, starch synthesis, lipid synthesis and nucleotides synthesis. In addition, as the model included a high number of parameters, it described not only experimental data, but also most of the metabolic kinetics that showed statistical significance. It can thus be used as an *in silico* platform for characterizing the cell lines as well as to search for ‘‘optimal’’ culture strategy either by management through rational adjustment of the main nutrient concentrations that affect glucose and/or glycine concentration with time or by genetic manipulation of certain predicted critical enzymes. However, much work remains to be done: it would be of interest to add more metabolic reactions from extracellular multiple nutrients, like ions; and separating the lipids pools to more interest classes; get larger data sets including both extra- and intracellular experimental data, to test and validate the platform as a predictive tool.

CHAPTER 6 ATICLE 2: CURRENT LIPID EXTRACTION METHODS ARE SIGNIFICANTLY ENHANCED ADDING A WATER TREATMENT STEP IN CHLORELLA PROTOTHECOIDES

Xiaojie Ren[1], Xinhe Zhao[1], François Turcotte[2], Jean-Sébastien Deschênes[2], Réjean Tremblay[2], Mario Jolicoeur[1]*

[1] Research Laboratory in Applied Metabolic Engineering, Department of Chemical Engineering, École Polytechnique de Montreal.

[2] Université du Québec à Rimouski, 310 allée des Ursulines, Rimouski, Québec, G5L 3A1, Canada.

(Published in Microbial Cell Factories- 2017, Vol. 16, No. 26)

---

*Corresponding author. Address: P.O. Box 6079, Centre-ville Station, Montreal, Quebec, Canada. H3C 3A7; Telephone: 514 340 4711 x4525; fax: 514 340 4159; e-mail: mario.jolicoeur@polymtl.ca

6.1 Abstract

Background

Microalgae have the potential to rapidly accumulate lipids of high interest for the food, cosmetics, pharmaceutical and energy (e.g. biodiesel) industries such as biodiesel production. Triacylglycerols (TAG) is the major lipid class accounting 60-70 % of total lipids. Free fatty acids (FFAs) as well as polar lipids (PL) were not comparable with TAG, that only in a small ratio of total lipids. Meanwhile, TAG has suitable fatty acids composition of C16 and C18 chains with saturated or mono-unsaturated fatty acids, which are the most suitable components for biodiesel production. Transformation of TAG to biodiesel is also with lower cost compare with PL and FFAs. However, current lipid extraction methods show efficiency limitation and until now, extraction protocols have not been fully optimized for specific lipid compounds, such as TAG. The present study presents a novel lipid extraction method, consisting in the addition of a water treatment of biomass between the two-stage solvent extraction steps of current extraction methods. The resulting modified method not only enhances lipid extraction efficiency, but also yields a higher triacylglycerols (TAG) ratio, which is the highest desirable for biodiesel production.

Results

Modification of four existing methods using acetone, chloroform/methanol (Chl/Met), chloroform/methanol/H_2O (Chl/Met/H_2O) and dichloromethane/methanol (Dic/Met) showed respective lipid extraction yield enhancement of 72%, 36%, 60 % and 61 %. The modified acetone method resulted in the highest extraction yield, with 68.9 ± 0.2 % DW total lipids. Extraction of TAG was particularly improved with the water treatment, especially for the Chl/Met/H_2O and Dic/Met methods. The acetone method with the water treatment led to the highest extraction level of TAG with 73.7 ± 7.3 µg/mg DW, which is 130.8 ± 10.6 % higher than the maximum value obtained for the four classical methods (31.9 ± 4.6 µg/mg DW). Interestingly, the water treatment preferentially improved the extraction of intracellular fractions, i.e. TAG, sterols (ST), and free fatty acids (FFA), compared to the lipid fractions of the cell membranes, which are constituted of phospholipids (PL), acetone mobile polar lipids (AMPL) and hydrocarbons (HC). Finally, from the

32 fatty acids analyzed for both neutral lipids (NL) and polar lipids (PL) fractions, it is clear that the water treatment greatly improves NL-to-PL ratio for the four standard methods assessed.

Conclusion

Water treatment of biomass after the first solvent extraction step improved the global lipids extraction yield. In addition, the water treatment positively modifies the intracellular lipid class ratios of the final extract, in which TAG ratio is significantly increased without changes in the fatty acids composition. The novel method thus provides an efficient way to improve lipid extraction yield of existing methods, as well as selectively favoring TAG, a lipid of the upmost interest for biodiesel production. We found that a hypotonic environment generated adding pure water results in the increase of cell volume (Figure 6.5) to equilibrate osmotic pressure. It may greatly affects membrane integrity, which is already highly weakened from the use of solvents in stage one. Solvents access to the cell interior volume is then made easier and thus improved the extraction of lipids, especially for the intracellular lipids release. However, the hypothesis of water disturbing cell membrane after first stage ultrasound and solvent extraction procedure should be further verified to make the mechanism more clear and solid.

6.2 **Key words**

Chlorella protothecoides - lipid extraction - water treatment - two-stage solvent extractions - high extraction yield - high TAG ratio

6.3 **Background**

Microalgae is an attractive platform for lipid production (Perez-Garcia et al., 2011; Yena et al., 2013). Microalgae cells can accumulate lipids at up to 20–50 % of their cell dry weight (Araujo et al., 2013), and which can be used as precursors for biodiesel production after a transesterification step (Cesarini et al., 2014; Liu et al., 2015). Algal lipids include polar lipids, which are normally structural such as phospholipids and glycolipids, and neutral lipids, which are mainly storage lipids such as mono-, di-, tri-acylglycerides (TAG) and sterols (ST) (Greenwell et al., 2010b; Schuhmann et al., 2012). TAGs represent the most preferable lipid class for biodiesel production since they contain fatty acids that can be removed from their glycerol frame, and transformed through transesterification reaction into fatty acid methyl esters (FAMEs) (Islam et al., 2013). Significant efforts have been devoted to identify the genes and signals that regulate microalgae metabolism (Dangoor et al., 2009; Nikkanen et al., 2016; Peled-Zehav & Danon, 2007; Peled-Zehavi et al., 2010), and to optimize the upstream processing steps to generate lipid-rich cellular biomasses (Chen et al., 2013; Guo et al., 2013; Ho et al., 2013; Ho et al., 2015; Maeda et al., 2016; Mendes & Vermelho, 2013; Pereira et al., 2011; Ren et al., 2013; Shih-Hsin Ho, 2014; Xiong et al., 2008a; Yu et al., 2011a). However, although the downstream process normally accounts for the major part of a bioprocess costs, only limited attention has been placed on the amelioration of lipid extraction protocols (Araujo et al., 2013; Li et al., 2014; Ranjan et al., 2010); a step still considered as one of the major bottlenecks for commercial-scale biodiesel production (Guldhe et al., 2016). Significant amounts of lipids are trapped in the cytoplasm by the cell walls and membranes, so lipid extraction efficiency thus greatly depends on cell disruption technique as well as on the polarity of the solvents used to remove lipids from the cell water phase (Burja et al., 2007; Hamilton et al., 1992; Lee et al., 2010; Lewis et al., 2000). For instance, some protocols favor imposing a high mechanical stress such as ultrasound treatment (Araujo et al., 2013), resulting in a high cell disruption efficiency level. For comparison, a low shear stress approach such as using a hydrocyclone only leads to ~10 % cell lipids extraction efficiency but microalgae cells remain viable (Dommange et al., 2015). Overall, the solvents perform lipid extraction, which explains the amount of work dedicated to identify the most efficient solvents combination.

A short series of solvent-based methods have been largely used to perform lipid extraction from various biological materials. The Folch method (Folch et al., 1957) consists in using chloroform-

methanol (Chl/Met), and then the extracted solvent (chloroform) is washed with water to remove non-lipid substances. Bligh & Dyer then proposed a method based on Folch's combining chloroform, methanol and water (Chl/Met/H_2O), for lipid extraction from a wide range of biological materials (Bligh & Dyer, 1959). More recently, because of concerns on biosafety, a less hazardous solvent mixture of dichloromethane/methanol (Dic/Met) has been proposed by Cequier et al. (Cequier-Sanchez et al., 2008) as a substitute for Bligh & Dyer method. In addition, Drochioiu proposed a fast lipid assay with acetone extraction and turbidimetric reaction with sulfosalicylic acid, which requires only few milligrams of dry samples compared to grams for the above-mentioned methods, which limits their application to pilot and large scale production facilities (Drochioiu, 2005). These methods can be considered as references, or classical, in the field.Comparative studies have been done with different microalgae species using different extraction systems. For the microalga *Chlorella vulgaris*, Araujo et al. (Araujo et al., 2013) revealed that using Bligh & Dyer's method (Chl/Met/H_2O) [11,12] is more efficient than Folch's method (Chl/Met) [10], followed by Chen's method using methanol/dichlorometane (Met/Dic) (Chen et al., 1981), while low efficiency levels were obtained for isopropanol/hexane (Hara et al.) (Hara & Radin, 1978) and soxhlet extraction using acetone (F., 1879). Ryckebosch et al. explored seven solvent mixtures at different ratios on *C. vulgaris*, and showed that extraction efficiency level was higher using chloroform/methanol 1:1, then for chloroform/methanol 2:1, followed by dichloromethane/ethanol 1:1, hexane/isopropanol 3:2, acetone, diethyl ether, and methyl-tert-butyl ether/methanol 10:3 (Ryckebosch et al., 2012a). For the marine microalgae *Tetraselmis sp.*, Li et al. (Li et al., 2014) revealed that Dic/Met (Cequier-Sanchez et al., 2008) was the most efficient method, followed by propan/hexane (Pro/Hex) (Ch. Schlechtriem 2010), Chl/Met/H_2O, supercritical CO_2 (Andrich et al., 2005) and finally ethanol/KOH (Burja et al., 2007). For *Isochrysis galbana*, Grima et al. have also compared seven solvent mixtures and found that the extraction efficiency level was higher for chloroform/methanol/H_2O 1:2:0.8, followed by hexane/ethanol 1:2.5, hexane/ethanol 1:0.9, butanol, ethanol, ethanol/H_2O 1:1, and hexane/isopropanol 1:1.5 (Grima et al., 1994). As it can be seen, lipid extraction efficiency differs with biomass type as well as with the solvent mixture.

In this work, we thus test the hypothesis that a water treatment step added to current extraction protocols, between the two organic solvent extraction steps, increases cell material disruptions with an enhancement of lipid release from the cell. The four different extraction methods largely used

for algal lipid extraction (Folch method with Chl/Met (Folch et al., 1957); Bligh & Dyer method with Chl/Met/H_2O (Araujo et al., 2013; Bligh & Dyer, 1959); Cequier method with Dic/Met (Cequier-Sanchez et al., 2008) and Drochioiu method with acetone (Drochioiu, 2005)) were thus implemented with a water treatment. Results showed a significant improvement of the global lipid extraction efficiency, and especially for TAG, a precursor of biodiesel synthesis.

6.4 Materials and methods

6.4.1 Experimental microalgae

Chlorella protothecoides was cultivated under heterotrophic condition for biomass and lipid accumulation (Ren et al., 2016). The modified basal medium (MBM) (Wei et al., 2008) was used to maintain the inocula and to perform the experiments. Cells were collected at the exponential phase by centrifugation at 4,000 *g* for 10 min, and were vacuumed (remove extra water) and freeze-dried (VirTis, Advantage Plus EL-85) to determine the dry weight. Then the freeze-dried biomass was ground into a fine powder for subsequent extractions.

6.4.2 Current lipid extraction methods

A mass of 35 mg of dried microalgae was used in each experiment. The four non-modified original extraction methods were applied in four control groups as detailed below.

Method A: Acetone (Drochioiu, 2005)

35 mg of dry samples were extracted with 5 mL of acetone under ultrasound (1000 W, 20 kHz) in ice water for 30 min, and centrifuged at 4000 *g* at 4°C for 5 min. Supernatants were transferred to a new test tube for lipid analysis, and the remaining cell pellets were re-extracted repeating the procedure.

Method B: Chl/Met (Folch et al., 1957)

35 mg of dry microalgae samples were extracted with 7.5 mL of a mixture chloroform/methanol (2:1, v/v) under ultrasound (1000 W, 20 kHz) in ice water for 30 min. The mixture was centrifuged at 4000 *g* at 4°C for 5 min. Cell pellets were kept for a re-extraction step and supernatants were transferred to a new test tube with 1.875 mL of H_2O and shaken vigorously following a centrifugation at 4000 *g* at 4°C for 5 min. Then the lower layer of 5 mL chloroform with extracted

lipids were pipetted out for lipid analysis. The remaining cell pellets were re-extracted repeating the procedure.

Method C: Chl/Met/H_2O (Araujo et al., 2013; Bligh & Dyer, 1959)

35 mg of dry microalgae samples were mixed and homogenized with 5 mL of methanol, 2.5 mL of chloroform and 5 mL of water. The mixture was treated under ultrasound (1000 W, 20 kHz) in ice water for 20 min. Another 2.5 mL of chloroform was added to the mixture and sonicated for 10 min. Then the mixture was centrifuged at 4000 *g* at 4°C for 5 min. Then the lower layer of 5 mL chloroform with extracted lipids were pipetted out for lipid analysis. The remaining cell pellets were re-extracted repeating the procedure.

Method D: Dic/Met (Cequier-Sanchez et al., 2008)

This method was the same as the Folch et al. method. However, all extractions used dichloromethane/methanol (2:1, v/v) instead of chloroform/methanol. In order to layering the extracted mixture, 1.625 mL KCL solution (0.88 %) was used instead of 1.875 mL H_2O. Lipids were then within the 5 mL dichloromethane phase. The remaining cell pellets were re-extracted repeating the procedure.

6.4.3 Modified lipid extraction methods

Lipid extraction in the four test groups was carried out according to the four control groups (see above) with the following modifications. The 35 mg of dry microalgae samples were extracted two times as in the above-mentioned methods, but prior to the second solvent extractions, the pre-extracted fresh cell pellets were re-suspended in 5 mL dH_2O (deionized) and vortexed (1000rpm) for 30 s at room temperature, and then centrifuged at 4000 *g* for 5 min at room temperature; the treatment was done only once. After centrifugation, the aqueous phase extractions were also kept for total lipids quantification, but the concentration levels were all around or below the detection limit, thus confirming that no detectable amounts of lipids were released in the water phase. Solvent phases obtained from the first and second extractions are defined as stage 1 and stage 2 respectively in both control and test groups.

6.4.4 Lipid analysis

Fast total lipid assay

Although GC-MS could get more detailed and accurate quantification data of different lipid classes (HC, TAG, FFA, ST, AMPL, PL), there still may be some components missing. Fast total lipid assay was thus used to quantify the total extracted lipid yield.

0.1 mL of extracted solvents were pipetted out from each solvent phase and evaporated under a stream of N_2. Then each sample was re-suspended in 0.1 mL of acetone, and 0.9 mL of 1.5 % sulfosalicylic solution was added. Each sample was shaken vigorously followed by a 30 min standing. The sample absorbance is read at 440 nm by UV–VIS determination (UNICAM 8625, UV/VIS), and then the quantification of the lipids is calculated according to a calibration curve (lipid concentration vs. absorption reading) using lipid extracted from *Chlorella protothecoides* cells harvested at growth steady state. For generating the calibration curve, known weighted lipids were dissolved in acetone to prepare a stock solution (2g/L) and diluted to a series of standard solutions. The lipid concentration vs. absorption reading was taken as a standard curve. Lipid quantification was thus done using this standard curve.

Lipid class analysis

All remaining solvent phases (~4.9 mL) collected in each group were evaporated under a stream of N_2 and each sample was re-suspended in 500 μL dichloromethane to analyze lipid classes. Lipid classes were identified by TLC-FID according to Parrish's method (Parrish, 1987).

Fatty acids profiles analysis

Lipids were separated into polar (structural lipids, mainly phospholipids) and neutral fractions (including wax esters, sterols, free fatty acids and triglycerides) by column chromatography on silica gel micro-columns (30 × 5 mm I.D. Kieselgel 70–230 mesh Merck) as described in Marty's method (Marty et al., 1992). The neutral fraction was purified on an activated silica gel with 1 mL of hexane/ethyl acetate (v/v) to eliminate free sterols. FA composition of the neutral and the polar fractions were determined separately on fatty acid methyl esters (FAMEs) obtained by esterification using sulfuric acid/methanol (2:98, v/v), and then analyzed by GC–MS (Thermo Fisher Scientific Inc., GC model Trace GC Ultra and MS model ITQ900) (Girard et al., 2014; Ren et al., 2016). Standards for 37 fatty acids were used and only 32 fatty acids were detected in this work, listed as: C11:0_Undecanoic, C12:0_Lauric, C13:0_Tridecanoic, C14:0_Myristic, C14:1_Myristoleic, C15:0_Pentadecanoic, C15:1_cis-10-pentadecanoic, C16:0_Palmitic, C16:1_Palmitoleic, C17:0_Heptadecanoic, C17:1_Cis-10-heptadecenoic, C18:0_Stearic,

C18:1n9_Oleic(c)+Elaidic(t), C18:2n6_Linolelaidic(t)+Linoleic(c), C18:3n6_Gamma-linolenic, C18:4n3_semi-quant, C19:0, C18:3n3_Alpha-Linolenic, C20:0_Arachidic, C20:1n9_Cis-11-eicosenoic, C20:2_Cis-11,14-eicosadienoic, C20:3n6_Cis-8,11,14-eicosatrienoic, C21:0_Henicosanoic, C20:4n6_Arachidonic, C20:3n3_Cis-11,14,17-eicosatrienoic, C20:5n3_cis-5,8,11,14,17-eicosapentaenoic, C22:0_Behenic, C22:1n9_Erucic, C22:2_Cis-13,16-docosadienoic, C24:0_Lignoceric, C22:6n_Cis-4,7,10,13,16,19-docosahexaenoic, C24:1n9_Nervonic.

6.4.5 Statistical Analysis

Three replicates were carried out for each experiment samples, and the variation within the replicates were assessed by calculating the standard deviation of the means. Evaluation of differences between the different extraction systems were carried out by analyses of variance (ANOVA) (Cequier-Sanchez et al., 2008).

6.5 Results

6.5.1 H_2O treatment significantly improves total lipid extraction yield

In the present study, we evaluated a modification to current extraction methods for lipids in microalgae, adding a water treatment between two successive solvent extraction stages. The first solvent extraction stage was performed under the same condition in both control and test groups for the four different methods, with total lipids of 26.7 ± 1.1 % DW in control and 26.5 ± 2.6 % DW in test for method A; 17.4 ± 0.6 % DW in control and 16.7 ± 7.9 % DW in test for method B; 28.8 ± 0.1 % DW in control and 28.7 ± 0.6 % DW in test for method C; 26.1 ± 3.9 % DW in control and 24.1 ± 4.0 % DW in test for method D (Figure 6.1). With the water treatment, test groups reached significantly higher total lipid levels compared to control, after the second solvent extraction stage. The total lipids yield in test group (42.3 ± 0.2 % DW) was 3.2-fold that in control group (13.3 ± 1.2 % DW) using acetone, 1.9-fold using Chl/Met (24.1 ± 4.0 % DW in test and 12.6 ± 0.1 % DW in control), 2.9-fold using Chl/Met/H_2O (39.3 ± 13.5 % DW in test and 13.6 ± 1.1 % DW in control) and 3.0-fold using Dic/Met (38.2 ± 0.6 % DW in test and 12.6 ± 0.5 % DW in control). Lipid extraction efficiency thus improved by 72.3 %, 35.8 %, 60.3 % and 60.9 %

respectively for acetone, Chl/Met, Chl/Met/H_2O and Dic/Met by adding a water treatment between the two solvent extraction stages, which usually performed successively.

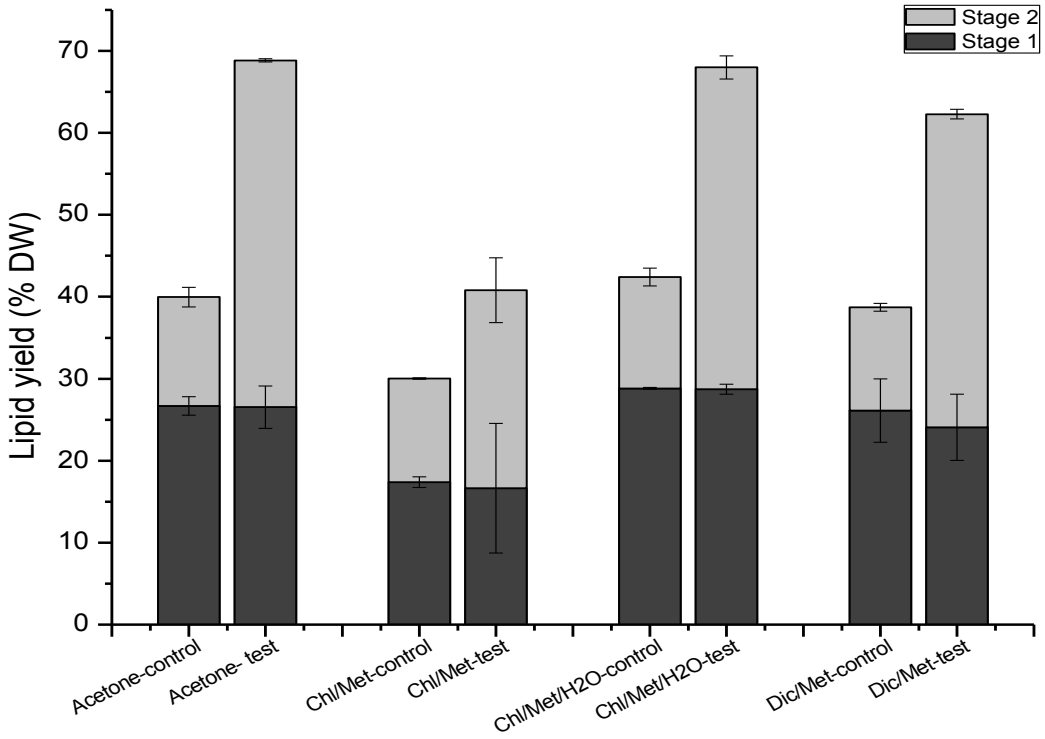

Figure 6. 1 Total lipids extracted in stage 1 (black) and stage 2 (grey) for acetone method, Chl/Met method, Chl/Met/H_2O method and Dic/Met method respectively, without (control) or with a water treatment (test). Error bars represent the standard deviation of triplicate data.

Attempts have been done to enhance lipid extraction yield by adding more solvent to wash the post-extracted biomass, or washing the post-extracted biomass with the extracted mixture (solvent and lipids mixture), but without any improvement (Araujo et al., 2013). Our results also show that in the control group, most of the extraction occurred in the first extraction step, with the second extraction yield only accounting for 31.2 ± 2.9 % (13.3 ± 1.2 % DW), 42.1 ± 1.1 % (12.6 ± 0.1 % DW), 32.0 ± 1.8 % (13.6 ± 1.1 % DW) and 32.5 ± 2.5 % (12.6 ± 0.5 % DW) of total extraction yield for acetone, Chl/Met, Chl/Met/H_2O and Dic/Met methods respectively. However, in the test groups the second extraction stage following the water treatment accounted for 61.4 ± 2.4 % (acetone), 59.2 ± 15.5 % (Chl/Met), 57.7 ± 0.4 % (Chl/Met/H_2O) and 61.3 ± 3.6 % (Dic/Met) of the final lipids yield.

Our data show that the total lipid extraction yield differs among the four original extraction methods. Lipid content in *Chlorella protothecoides* biomass may rely on culture condition but it was reported reaching between 14.6 and 57.8 (%, w/wDW) (Malcata, 2011), a range that is comparable with our data, in control groups. The yield obtained using the Chl/Met was significantly lower than those from Dic/Met ($F_{(1, 4)} = 7.89$, $P < 0.05$) and Chl/Met/H_2O ($F_{(1, 4)} = 249.93$, $P < 0.0001$), which is in agreement with literature (Araujo et al., 2013). The extraction yield using acetone was also significantly higher than that from Chl/Met ($F_{(1, 4)} = 639.15$, $P < 0.0001$), but not statistically different to that from Chl/Met/H_2O and Dic/Met method ($F_{(2, 6)} = 1.08$, $P=0.397$). We then moved further characterizing the effect of the water treatment on extracted lipids composition.

6.5.2 Water treatment promotes TAG-to-total lipid ratio in extraction processes

The major lipid classes identified include HC (hydrocarbons), TAG (triacylglycerols), FFA (free fatty acids), ST (sterols), AMPL (acetone mobile polar lipids) and PL (phospholipids) (Figure 6. 2). HC are mainly integrated in the cell membrane through amino acid residues anchored on it (Lodish et al., 2000), TAG and ST are storage lipids, FFA are precursors of lipid synthesis, PL are the main component of cell membranes, whereas AMPL is a group constituted from glycolipids monoacylglycerols, pigments and degradation products of PLs (Salvo et al., 2015).

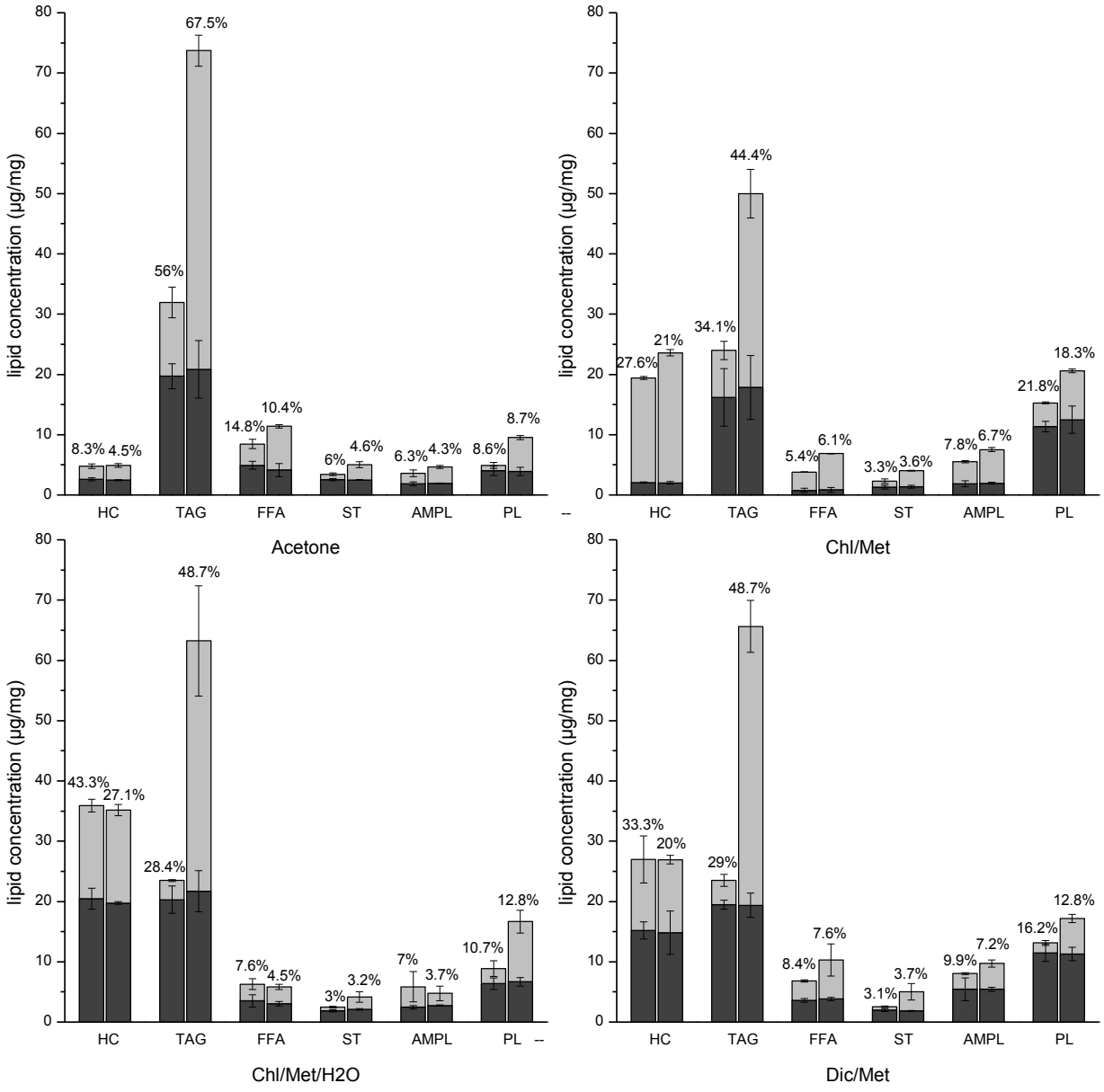

Figure 6. 2 Lipids composition extracted in control (left columns) and test groups (right columns) for acetone method, Chl/Met method, Chl/Met/H2O method and Dic/Met method in the first (black) and second (grey) stage. Error bars represent the standard deviation of triplicate data.

Interestingly, in the first stage TAG was the main component extracted over total lipids, reaching a similar level of 19.4 ± 0.6 µg/mg in all four methods. However, the TAG content in total lipids extracted varied among the four methods with 55.3 ± 2.6 % (acetone), 48.3 ± 5.7 % (Chl/Met), 36.9 ± 0.1 % (Chl/Met/H2O) and 34.0 ± 2.4 % (Dic/Met). Moreover, HC was higher in

Chl/Met/H_2O (36.2 ± 1.0 %) and Dic/Met (26.4 ± 0.2 %), while PL was higher in Chl/Met (34.1 ± 0.2 %) and Dic/Met (20.0 ± 0.1 %). The water treatment affected differently the resulting lipid class distribution profile in the second solvent extraction phase depending on the method, but shows generally increased extraction yields. The second extraction stage led to significantly increased levels of HC in Chl/Met for both control (2.1 ± 0.1 µg/mg in stage 1 and 17.3 ± 0.3 µg/mg in stage 2) and test group (2.0 ± 0.2 µg/mg in stage 1 and 21.6 ± 0.5 µg/mg in stage 2). Using Chl/Met/H_2O and Dic/Met also showed a high extraction efficiency for HC at the second stage with no significant effect of the water treatment, while acetone seems less efficient for HC extraction. Meanwhile, extraction of FFA, ST and AMPL was higher (or comparable) in the second stage for both control and test groups in all four methods. However, comparing control and test groups, HC extraction was only slightly improved in Chl/Met by water treatment (17.3 ± 0.3 µg/mg in control and 21.6 ± 0.5 µg/mg in test respectively), not significantly improved in acetone (2.2 ± 0.1 µg/mg in control and 2.4 ± 0.3 µg/mg in test respectively) and Dic/Met (11.8 ± 3.9 µg/mg in control and 12.1 ± 0.7 µg/mg in test respectively), while it was similar for Chl/Met/H_2O (15.4 ± 1.1 µg/mg in control and 15.4 ± 0.9 µg/mg in test respectively). However, TAG, ST and PL revealed a high sensitivity to water treatment as showed by the significant extraction improvement in test groups compared to control groups in all four methods (Figure 6.2). As the main component, TAG extraction was significantly improved compared to the other components (Table 1), with TAG levels of 4.3 ± 0.7 (acetone), 4.1 ± 0.3 (Chl/Met), 13.0 ± 3.5 (Chl/Met/H_2O) and 11.5 ± 1.9-fold (Dic/Met) for the control groups in stage 2. Our results thus clearly show that the water treatment specifically favored the extraction of intracellular fractions of TAG, ST, and FFA compared to the membrane fractions of AMPL and HC (Table 6.1). Meanwhile, although PL, the main known cell membrane lipid component, reached 4.0 ± 1.9-fold the level in the control group, its extraction improvement was less than for TAG with an average of 8.2 ± 1.5-fold that in control group.

Table 6. 1 Comparative extraction level as test-to-control (T/C) ratio for different lipid classes in stage two

	TAG	**FFA**	**ST**	**AMPL**	**PL**	**HC**
Acetone	**4.3±0.7**	2.1±0.6	2.8±0.2	1.6±0.7	6.3±4.5	1.1±0.4
Chl/Met	**4.1±0.3**	2.0±0.0	2.7±1.1	1.5±0.0	2.1±0.1	1.3±0.1
Chl/Met/H2O	**13.0±3.5**	1.0±0.2	3.3±0.9	0.6±0.2	4.0±0.2	0.8±0.2
Dic/Met	**11.5±1.9**	2.0±0.9	5.8±1.0	1.7±0.3	3.6±1.4	1.0±0.5
Average	**8.2±1.5**	1.8±0.4	3.7±0.8	1.3±0.3	4.0±1.9	1.1±0.3

Results are expressed as the mean ± SD (n = 3).

Overall, combining the two extraction stages, the water treatment resulted in significantly higher TAG-to-total lipids ratios (67.5 ± 0.7 %, 44.4 ± 3.9 %, 48.7 ± 3.7 % and 48.7 ± 0.1 % for acetone, Chl/Met, Chl/Met/H_2O and Dic/Met method respectively) compared to control (56.0 ± 5.0 %, 34.1 ± 5.3 %, 28.4 ± 2.3 % and 29.0 ± 3.8 % for acetone, Chl/Met, Chl/Met/H_2O and Dic/Met method respectively), with reduction of HC-to-total lipids ratio of 3.8 %, 6.6 %, 16.2 % and 13.3 % for acetone, Chl/Met, Chl/Met/H_2O and Dic/Met method respectively (Figure 6.2). Of interest, acetone method with a water treatment resulted in the highest TAG extraction level with 73.7 ± 7.3 µg/mg, which is 130.8 ± 10.6 % higher than the maximum value observed in all control groups (31.9 ± 4.6 µg/mg in acetone method).

Interestingly, when compared in parallel, our results confirm that each extraction method is specific to a lipid class (Figure 6.2). For instance, the highest TAG extraction efficiency is for acetone method, reaching 56.0 ± 5.0 % and 67.5 ± 0.7 % in control and test group respectively, while it only reached 28.4 ± 0.7 % in control and 48.7 ± 2.7 % in test for Chl/Met/H_2O. Acetone showed favoring extraction of ST and FFA, while not PL and HC (8.6 ± 1.7 % and 8.3 ± 1.5 % respectively in control, 8.7 ± 0.2 % and 4.5 ± 0.2 % respectively in test). Chl/Met method led to the highest extraction levels of PL and HC (21.8 ± 0.9 % and 27.6 ± 3.6 % respectively in control group, 18.3 ± 0.2 % and 21.0 ± 1.8 % respectively in test group). However, AMPL extraction level was similar in the four methods (Figure 6.2). Results suggest that the different solvent and extraction procedures studied here have different selectivity for lipid components. Acetone may penetrate

deeply and reach intracellular lipids, while Chl/Met and Dic/Met action may be mostly limited to membrane lipids.

6.5.3 H_2O treatment significantly favors neutral-to-polar lipid ratio extraction

Since fatty acids (FA) composition and structure, such as carbon chain length and unsaturated degree, greatly affect the properties of resulting biodiesel (Tabatabaei et al., 2015; Wang et al., 2013), the FA profile was characterized for neutral (NL) and polar lipids (PL) independently (neutral and polar fractions were first separated as described in material and methods). A total of 32 FA were detected from C11 to C24 (as shown in Material and methods), and similar fatty acids were found in NL and PL fractions with the five most prevalent components being C16:0, C18:0, C18:1n9, C18:2n6 and C18:3n3 in both NL and PL fractions. FAs are known as precursors of both neutral lipids and polar lipids, with no evidence of FAs selection priority during neutral lipid and polar lipid synthesis. Therefore, it was expected that similar FA components were found in both NL and PL.

The same result has also been reported in (Li, 2014), where the most abundant FAs in the lipid extracts accounted for approx. 70 % of total FAs, with C16 hexadecanoic acid, C18:1 (n-9) oleic acid and C18:2 (n-6) octadecadienoic acid. Interestingly, similar components of these dominant FAs were found in the four methods tested here. However, although the FAs in both fractions are quite similar, the quantity of each component differed in NL and PL fraction as shown in Figure 6.3. For instance, the multi-unsaturated fatty acids C18:2n6 and C18:3n3 are clearly more abundant in PL than in NL, which suggests membrane lipids mobility. C16:0 is also more abundant in PL, which is maybe due to the fact that it is the initial FA synthesized and is first used for cell growth as in the structure of cell membrane.

C18:1n9 accounts for the highest content in the NL fraction, followed by C18:2n6 > C18:3n3 > C16:0 > C18:0, and this in all methods (Figure 6.3). A water treatment resulted in a significant enhancement, at stage 2, of C18:1n9 in Chl/Met/H_2O and Dic/Met methods (6.9 ± 1.5 and 4.9 ± 0.5-fold of that in control respectively), followed by acetone (2.4 ± 0.2-fold) and to a lesser extent in Chl/Met method (1.3 ± 0.2-fold). However, C18:1n9 reached a similar final extraction yield of 66.9 ± 1.9 µg/mg in all methods after water treatment. Indeed, C18:2n6, C18:3n3, C16:0 and C18:0 all showed similar trends with a significant improvement using Chl/Met/H_2O and Dic/Met, than acetone and Chl/Met. However, fatty acids in PL fraction differ from that in NL fraction, with

C18:2n6 the predominant component in all methods. With a water treatment, extraction efficiency of all five components were improved in acetone, Chl/Met/H_2O and Dic/Met methods at different extents. However, Chl/Met method resulted in a slightly but significant lower extraction efficiency than the control group (Figure 6.3). Adding a water treatment in Chl/Met method is thus detrimental to polar lipids extraction.

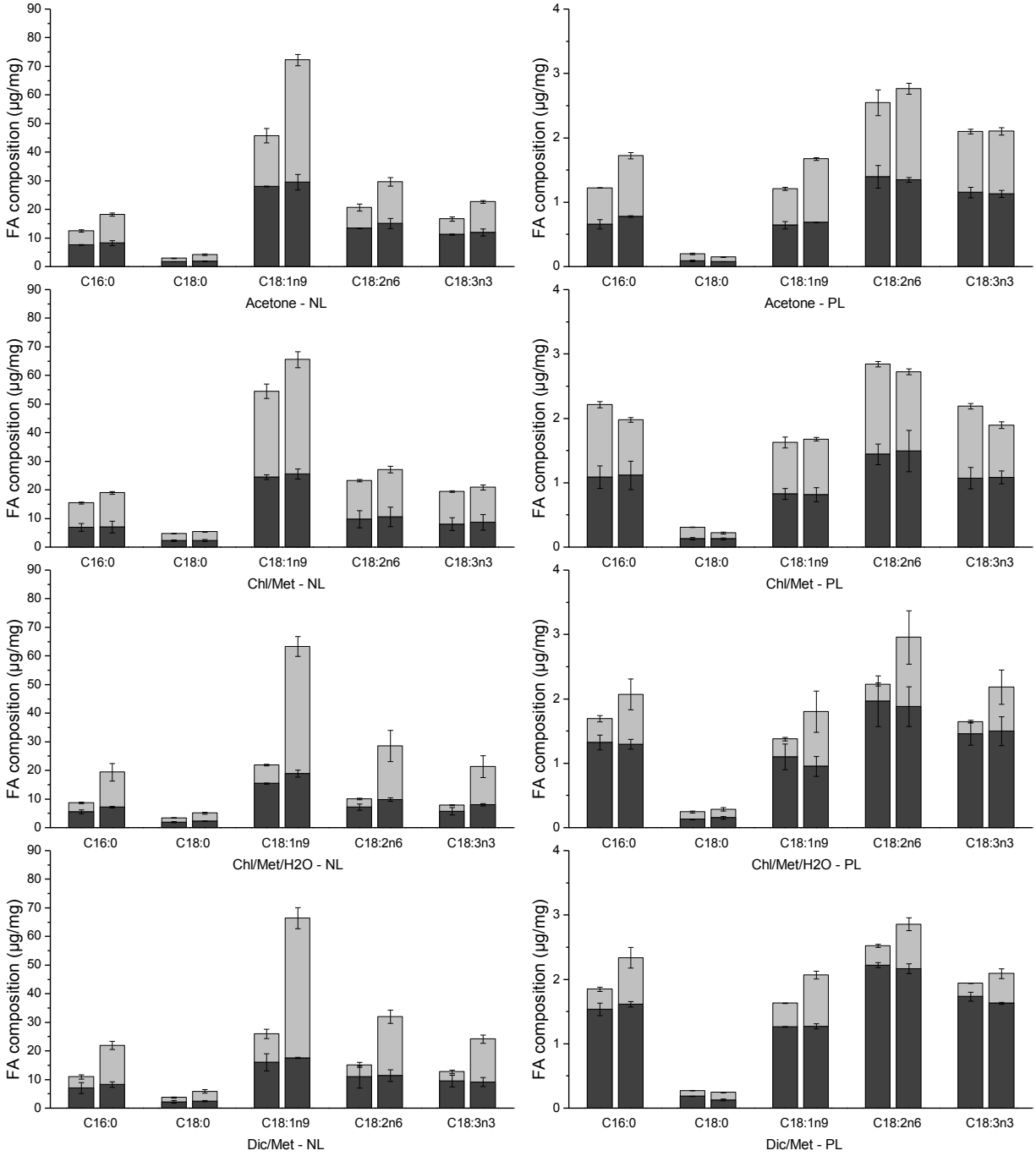

Figure 6. 3 Extraction ratio for each lipid component in different extraction methods. Error bars represent the standard deviation of triplicate data.

We then compared extraction methods analyzing the partition of extracted fatty acids in neutral lipids fraction (FA-NL) and in polar lipids fraction (FA-PL) (Figure 6.4). Before H_2O treatment, averaging the results in control and test samples, acetone method led to FA-NL extraction of 61.6 ± 0.6 µg/mg and FA-PL of 3.9 ± 0.1 µg/mg, corresponding to NL-to-PL ratio of 15.7 ± 0.1. However, in Chl/Met, Chl/Met/H_2O and Dic/Met methods, NL-to-PL ratio is of 11.5 ± 0.2, 7.0 ± 1.0 and 6.9 ± 0.3 respectively, with less NL extracted (53.0 ± 1.8 µg/mg , 41.2 ± 7.3 µg/mg and 47.5 ± 2.2 ug/mg for Chl/Met, Chl/Met/H_2O and Dic/Met methods respectively) but more PL extracted (4.6 ± 0.1 µg/mg , 5.9 ± 0.1 µg/mg and 6.9 ± 0.1 µg/mg for Chl/Met, Chl/Met/H_2O and Dic/Met methods respectively). Acetone method thus shows the highest selectivity level for neutral lipids, with extraction yield ranked as acetone method > Chl/Met method > Dic/Met method > Chl/Met/H_2O method. However, the PL extraction yield in stage one was ranked as Dic/Met method > Chl/Met/H_2O method > Chl/Met method > acetone method (Figure 6.4).

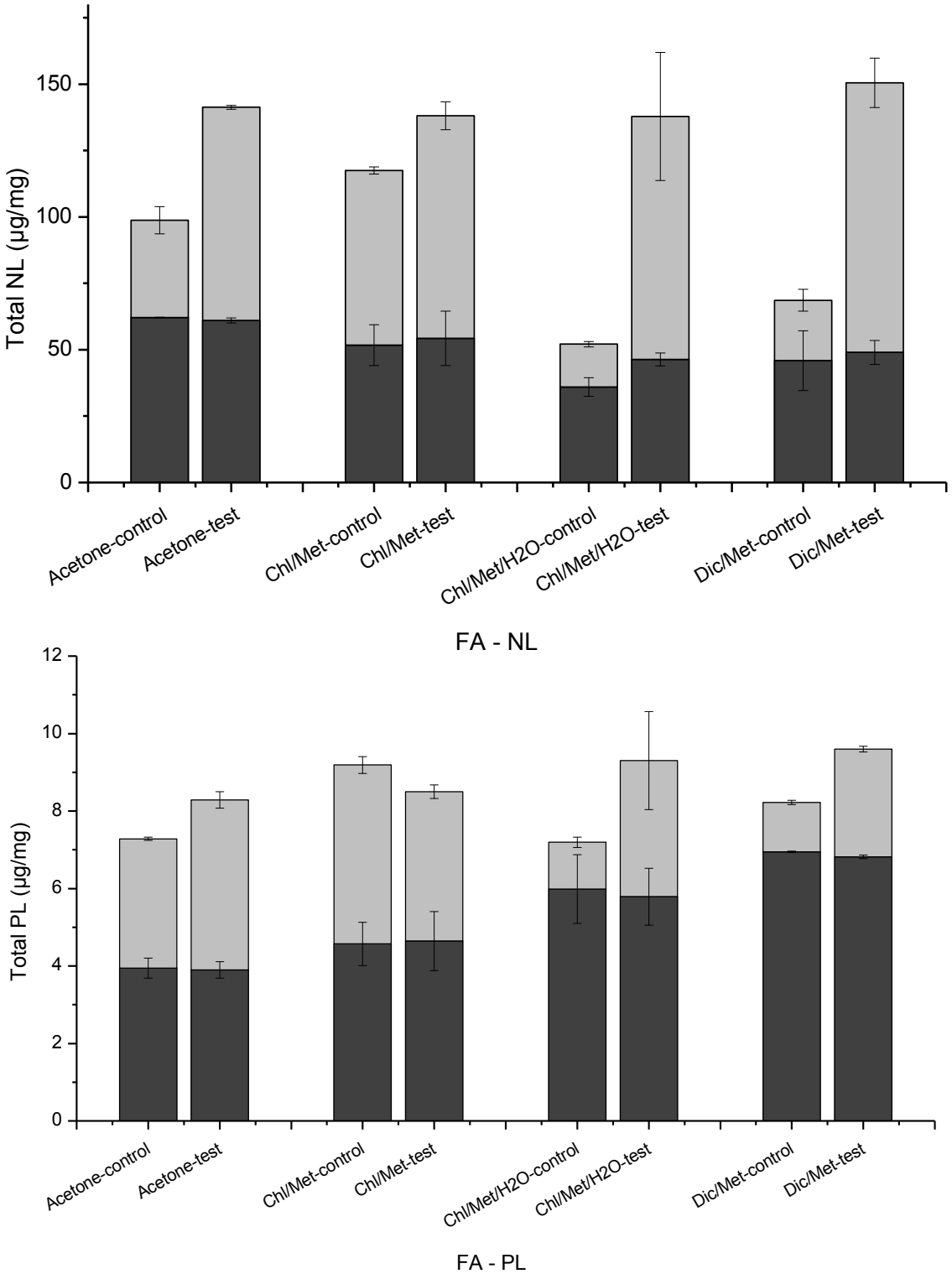

Figure 6. 4 Five main fatty acids composition in neutral lipids fraction and polar lipids fraction respectively. (Control groups: left columns; Test groups: right columns; First stage: black; Second stage: grey). Error bars represent the standard deviation of triplicate data.

For the second stage, results revealed that NL extracted in test groups (80.3 ± 0.7 µg/mg for acetone method, 83.8 ± 5.2 µg/mg for Chl/Met method, 91.5 ± 24.1 µg/mg for Chl/Met/H_2O method and 101.5 ± 9.4 µg/mg for Dic/Met method) were increased compared to that in control groups (36.6 ± 5.1 µg/mg for acetone method, 65.7 ± 1.4 µg/mg for Chl/Met method, 16.1 ± 1.0 µg/mg for Chl/Met/H_2O method and 22.7 ± 4.1 µg/mg for Dic/Met method). Indeed, a water treatment led to 2.1, 1.3, 5.1 and 3.8-fold that in control groups for acetone, Chl/Met, Chl/Met/H_2O and Dic/Met method respectively. However, PL extraction in test groups was only improved in acetone, Chl/Met/H_2O and Dic/Met methods (5.0 ± 0.5, 2.9 ± 0.7 and 2.2 ± 0.2-fold of control group for acetone, Chl/Met/H_2O and Dic/Met methods respectively), and resulted in lower yields than control in Chl/Met method (0.8 ± 0.0 of that in control). Therefore, the NL-to-PL ratio is greatly improved with a water treatment (18.3 ± 1.0 for acetone method, 21.8 ± 0.6 for Chl/Met method, 26.0 ± 4.1 for Chl/Met/H_2O method and 36.4 ± 6.1 for Dic/Met method) compared with control (11.0 ± 2.6 for acetone method, 14.2 ± 1.4 for Chl/Met method, 13.3 ± 1.0 for Chl/Met/H_2O method, 17.8 ± 3.4 for Dic/Met method). Of interest, the neutral lipids fraction is mainly stored in the cell while polar lipids fraction is mainly within the cell membrane, suggesting H_2O treatment favors the release of intracellular storage lipids.

6.6 **Discussion**

The key step in the extraction and recovery of lipids from microalgae relies on their release from intracellular compartment, where stands the major lipid pool (Araujo et al., 2013). Moreover, the extraction process efficiency, which is also a mass transfer operation problem, largely depends on the nature of the solvent as shown in this work as well as in the cited literature. In this work on *Chlorella protothecoides*, lipid extraction yields efficiency is ranked as acetone-based method > Chl/Met/H2O method > Dic/Met method > Chl/Met method. This ranking agrees with the polarity degree of the extraction solvents; acetone and Chl/Met/H_2O polarity being higher than Chl/Met and Dic/Met. It may because the cell membrane mainly contains polar lipids, the use of polar solvents could increase lipids diffusion phenomenon, as suggested by Araujo for acetone (Araujo et al., 2013). It has been already observed that nonpolar solvents have lower extraction levels toward microalgae lipids compared to polar solvents (Araujo et al., 2013). This relationship has also been suggested in other reports. Li (Li et al., 2014) observed that an hexane and ethanol mixture resulted in two times higher lipid yields than hexane in *Tetraselmis sp.*, a result that the

authors explained by the lower polarity of hexane over the hexane & ethanol mixture. Rychecosch et al. (Ryckebosch et al., 2012b) and Lewis et al. (Lewis et al., 2000) also demonstrated that a mixture of polar and non-polar solvents succeeded at extracting higher amounts of lipids compared to non-polar solvents. However, contradictory results have also been reported but for other microalgae species. For instance, Shen et al. (Shen et al., 2009) showed that an hexane and ethanol mixture extracted less lipid than hexane on *Chlorella protothecoides* and *Scenedesmus dimorphus*. Structural and composition differences of algal species may explain differences in extraction protocols efficiencies.

A hypotonic environment generated adding pure water results in the increase of cell volume (Figure 6.5) to equilibrate osmotic pressure, a phenomenon which greatly affects membrane integrity. Solvents access to the cell interior volume is then made easier. All of the above can thus explain that extraction of intracellular TAG, ST and FFA are preferentially increased compared to membrane lipids such as HC, PL and AMPL after water treatment. However, deeper investigation are still needed to find the solid mechanism of water effect on lipid extraction.

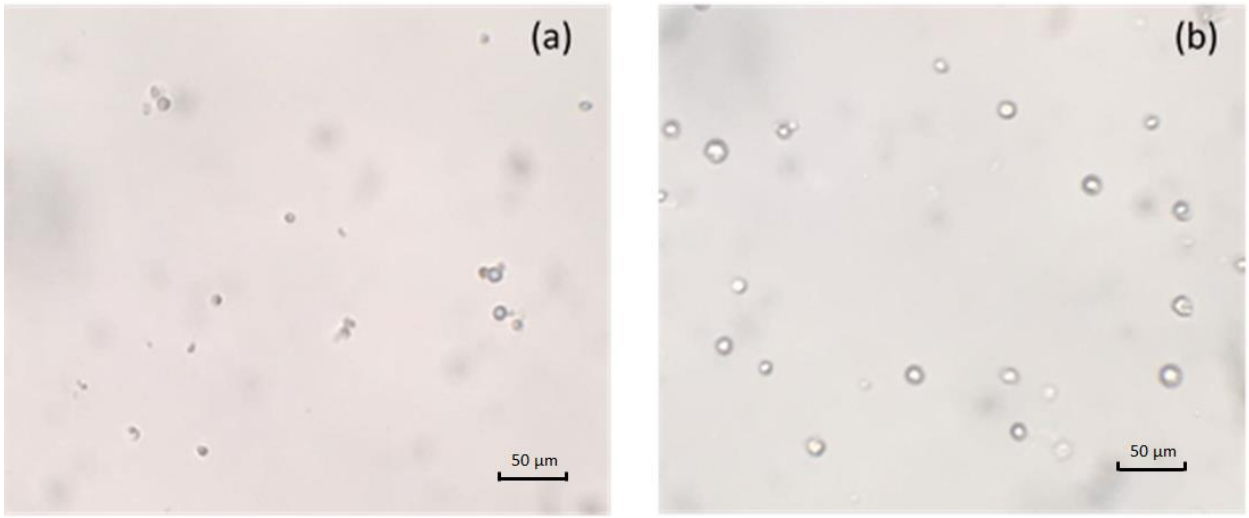

Figure 6. 5 Cells before (a) and after (b) H_2O treatment step, 400X magnification under bright field optical microscopy (Leitz Laborlux S Microscope).

It is also clear from this work (Figure 6.2) as well as from literature that each extraction protocol may differ in its selectivity for the different lipid classes found in microalgae. HC is a non-polar component anchored on the cell membrane by amino acids residues, and should then be more available to the less polar solvent mixtures Chl/Met and Dic/Met. However, although this is the

case for Dic/Met method, results for Chl/Met and Chl/Met/H_2O revealed Chl/Met is quite selective for HC when residual water remains with the cell pellets. This may be due to the fact that the non-polar HC is embedded in the polar phospholipids layers by amino acids residues. The presence of water may thus increase solvent mixture polarity and help weakening the links between polar lipids and proteins anchored into the membrane, hence making HC (neutral) more available to the less-polar solvent mixture Chl/Met. However, two times successive solvent extraction stages shown leading to a similar effect, as shown in Chl/Met and Chl/Met/H_2O with the release of HC from the membrane, no matter whether water treatment is applied or not.

Finally, although H_2O treatment could lead to different lipid class compositions and significantly improve the sum of fatty acids extracted, the effect on the FA composition was less important. The most abundant FAs in the lipid extracts include C16:0, C18:1n9, C18:2n6 and C18:3n3. The FAs composition was not affected by the water treatment, with final FAs composition in each method being similar in control and test groups. For instance, acetone method led to 12.7 % of C16:0 in control group and 12.4 % in test group, 46.4 % of C18:1n9 in control group and 49.1 % in test group, 21.0 % of C18:2n6 in control group and 20.2 % in test group, 16.9 % of C18:3n3 in control group and 15.4 % in test group, and ~3.0 % of other fatty acids in both control and test groups. Moreover, FAs composition was also found similar in the four methods, modified or not, compared stage by stage, which suggests that different extraction methods studied have limited impact on FAs composition selectivity, as proposed by Li (Li et al., 2014). The most abundant FAs extracted in the four methods are fortunately the ones preferred for microalgae biodiesel production (Halim et al., 2011).

In the present work, we have clearly demonstrated that the classical extraction methods can be significantly improved from the addition of a water treatment between the two solvent extraction steps. However, all these methods were historically based on the use of dry microalgae biomass, while recent developments in the field propose the use of fresh biomass. Avoiding the drying process allows reducing process energy and costs, as well as it enables a positive energy balance between the process energy and that extracted from the microalgae biomass (e.g. biodiesel) (Liu, 2013). Therefore, in complement to assessing classical methods which are based on using dry biomass, we have evaluated the effect of adding a water treatment using fresh biomass on a modified acetone-based extraction method, and obtained 1.6-fold total lipid extracted with water treatment (Figure 6.6).

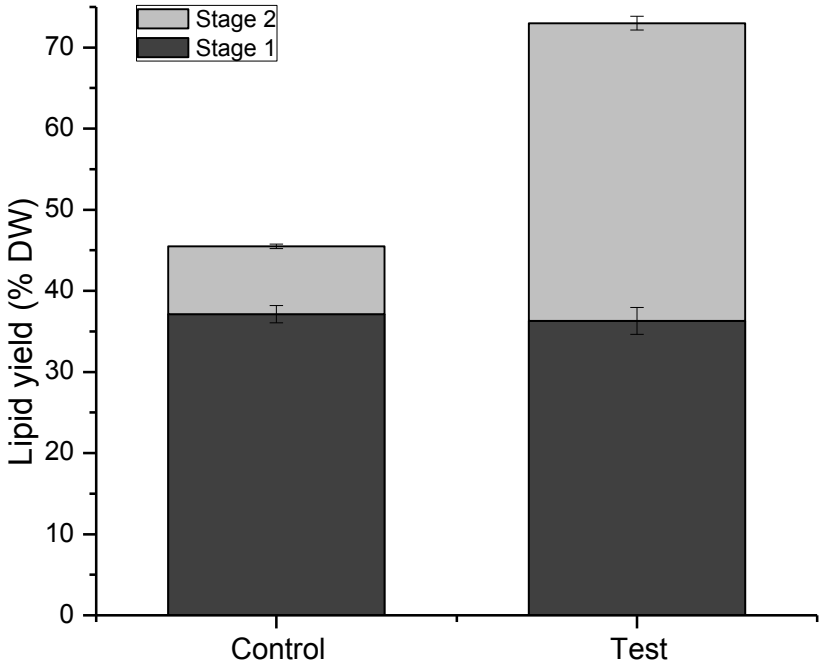

Figure 6. 6 Sum of the fatty acids of neutral lipids fraction (FA-NL) and polar lipids fraction (FA-PL) in different methods. Error bars represent the standard deviation of triplicate data.

Indeed, in addition to significantly improving the lipid extraction efficiency, with over 100 % increase of the harvested TAG, a precursor leading to biodiesel, the addition of a water treatment step is thus expected to enhance significantly the global final energy yield (e.g. of ~100 % estimated from the experimental results in this work) also while avoiding energy consumption for drying the algal cells before the solvents extraction steps. To conclude, the global process may then turn out to be positive energetically speaking, and the energy cost should be greatly lower than for the classical methods. Except for energy, the other part of costs difference between the new protocol proposed here and classical methods rely on equipment investment, from biomass pre-treatment to the extraction process. Adding a water treatment step will specifically require a water deionisation system, which would most likely be already available for other uses in the biological production plant, but will not need a cell dryer equipment such as in classical methods. Therefore, the equipment investment is similar when adding a water treatment step.

Finally, recent approaches propose replacing the use of ultrasounds to perform microalgae cells disruption (Wang et al. 2007; Orr et al. 2016) with “green solvents” such as 1-butyl-3-methylimidazolium chloride (Wang et al. 2007; Orr et al. 2016). These solvents are capable of lysing microalgae cell walls and microalgae vesicle membranes and thus favor the release of the

cell lipids (Wang et al. 2007). In conclusion, it is believed that the addition of a water treatment can allow to enhance lipid extraction efficiency, and thus improve the productivity of a biodiesel production process based on microalgae biomass.

6.7 Conclusion

Through the modification of four classical lipids extraction methods this study clearly demonstrated that water treatment of biomass after the first solvent extraction phase favors the release of intracellular lipids in the second solvent extraction step. Total lipid extraction yield as well as intracellular lipid class ratios in the final extract were thus significantly increased by the water treatment. The neutral-to-polar lipid ratio is also greatly improved after the water treatment, and the preferable lipid component TAG showed being increased up to 130.8 % compared to the original extraction methods. H_2O treatment between two-stage solvent extraction processes thus allows increasing the extraction efficiency, most probably through provide osmotic pressure to the cell membrane, which is already highly weekend from the use of ultrasound and solvents in stage one, thus help the release of especially intracellular lipids. The selection of the proper solvent system is crucial to the extraction process, because it may affect solvent penetration of the cell membrane and therefore lipids extraction.

6.8 List of abbreviations

Chl/Met: chloroform/methanol

Chl/Met/H_2O: chloroform/methanol/H_2O

Dic/Met: dichloromethane/methanol

HC: hydrocarbons

TAG: triacylglycerols

FFA: free fatty acids

ST: sterols

AMPL: acetone mobile polar lipids

PL: phospholipids

FAMEs: fatty acid methyl esters

6.9 Declarations

Ethics approval and consent to participate

Not applicable.

Consent for publication

Not applicable.

Availability of data and material

All data generated or analyzed during this study are included in this published article.

Competing interests

The authors declare that they have no competing interests.

Funding

Fonds de recherche du Québec – Nature et technologies (FQRNT), Grant no. RS-171172.

National Science and Engineering Council of Canada (NSERC) Discovery grant no. 093865 - RGPIN2014-04329.

Acknowledgements

The authors are grateful to the “Ressources Aquatiques Québec (RAQ)” a collaborative grant (RS-171172) from the “Fonds de recherche du Québec – Nature et technologies (FQRNT)” for a financial support (MJ, JSD, RT), and to the National Science and Engineering Council of Canada (NSERC Discovery grant no. 093865 - RGPIN2014-04329) for a financial support (MJ).

Authors' contributions

XR planned and performed the experiments, analyzed the results, and wrote the manuscript. XZ assisted in the design of experiment, on performing the experiment, as well as on results analysis. FT performed lipid analysis and quantification on TLC-FID and GC-MS. Jean-Sébastien Deschênes and Réjean Tremblay participated revising the manuscript and on funding. MJ coordinated the study, participated on the design of experiment, manuscript writing and funding. He has approved the final version.

6.10 References

Andrich, G., Nesti, U., Venturi, F., Zinnai, A., Fiorentini, R. 2005. Supercritical fluid extraction of bioactive lipids from the microalga Nannochloropsis sp. *European Journal of Lipid Science and Technology*, **107**(6), 381-386.

Araujo, G.S., Matos, L.J.B.L., Fernandes, J.O., Cartaxo, S.J.M., Gonçalves, L.R.B., Fernandes, F.A.N., Farias, W.R.L. 2013. Extraction of lipids from microalgae by ultrasound application: Prospection of the optimal extraction method. *Ultrasonics Sonochemistry*, **20**, 95-98.

Bligh, E.G., Dyer, W.J. 1959. A rapid method of total lipid extraction and purification. *Canadian Journal of Biochemistry and Physiology*, **37**, 911-917.

Burja, A.M., Armenta, R.E., Radianingtyas, H., Barrow, C.J. 2007. Evaluation of fatty acid extraction methods for Thraustochytrium sp. ONC-T18. *Journal of Agricultural and Food Chemistry*, **55**, 4795–4801.

Cequier-Sanchez, E., Rodriguez, C., Ravelo, A.G., Zarate, R. 2008. Dichloromethane as a solvent for lipid extraction and assessment of lipid classes and fatty acids from samples of different natures. *J. Agric. Food Chem.*, **56**, 4297-4303.

Cesarini, S., Haller, R.F., Diaz, P., Nielsen, P.M. 2014. Combining phospholipases and a liquid lipase for one-step biodiesel production using crude oils. *Biotechnology for Biofuels*, **7**, 29.

Ch. Schlechtriem , U.F.K.B. 2010. Effect of different lipid extraction methods on δ13 C of lipid and lipid-free fraction of fish and different fish feeds. *Isotopes in Environmental and Health Studies*, **39**(2), 135-140.

Chen, C.-Y., Chang, J.-S., Chang, H.-Y., Chen, T.-Y., Wu, J.-H., Leef, W.-L. 2013. Enhancing microalgal oil/lipid production from *Chlorella sorokiniana* CY1 using deep-sea water supplemented cultivation medium. *Biochemical Engineering Journal*, **77**, 74-81.

Chen, I.S., Shen, C.S.J., Sheppard, A.J. 1981 Comparasion of methylene chloride and chloroform for the extraction of fats from food products. *J. Am. Oil Chem. Soc*, **58**, 599–601.

Dangoor, I., Peled-Zehavi, H., Levitan, A., Pasand, O., Danon, A. 2009. A small family of chloroplast atypical thioredoxins. *Plant Physiology*, **149**(3), 1240-1250.

Dommange, X., Tanguy, P.A., Jolicoeur, M. 2015. Feasibility of lipid mechanical extraction from viable Monoraphidium minutum. *Microalgae Biotechnology*, **1**(1), 12-19.

Drochioiu, G. 2005. Turbidimetric lipid assay in seed flours. *Journal of food lipids*, **12**, 12-22.

F., S. 1879. The weight analytic determination of milk fat. *Polytechnisches J.*, **232**, 461.

Folch, J., Lees, M., Stanley, G.H.S. 1957. A simple method for the isolation and purificatioin of total lipids from animal tissues. *J. Biol. Chem*, **1**, 497-509.

Girard, J.-M., Roy, M.-L., Hafsa, M.B. 2014. Mixotrophic cultivation of green microalgae Scenedesmus obliquus on cheese whey permeate for biodiesel production. *Algal research*, **5** 241-248.

Greenwell, H.C., Laurens, L.M.L., Shields, R.J., Lovitt, R.W., Flynn, K.J. 2010. Placing microalgae on the biofuels priority list: a review of the technological challenges. *Journal of the Royal Socity Interface* **7**, 703–726.

Grima, E.M., Medina, A.R., Giménez, A.G., Pérez, J.A.S., Camacho, F.G., Sánchez, J.L.G. 1994. Comparison between extraction of lipids and fatty aids from microalgal biomass. *Am Oil Chem Sco* **71**, 955–959.

Guldhe, A., Singh, B., Ansari, F.A., Sharma, Y., Bux, F. 2016. Extraction and Conversion of Microalgal Lipids. *Green Energy and Technology*, **Algae Biotechnology**, 91-110.

Guo, S.-L., Zhao, X.-Q., Tang, Y., Wan, C., Alam, M.A., Ho, S.-H., Bai, F.-W., Chang, J.-S. 2013. Establishment of an efficient genetic transformation system in *Scenedesmus obliquus*. *Bioresource Technology*, **163**, 61-68.

Halim, R., Gladman, B., Danquah, M.K., Webley, P.A. 2011. Oil extraction from microalgae for biodiesel production. *Bioresource Technology*, **102**, 178-185.

Hamilton, R.J., Hamilton, S., Sewell, P. 1992. *Extraction of lipids and derivative formation. In Lipid Analysis: a practical approach*. Oxford University Press, New York.

Hara, A., Radin, N.S. 1978. Lipid extraction of tissues with a low-toxicity solvent. *Anal. Biochem*, **90** 420–423.

Ho, S.-H., Huang, S.-W., Chen, C.-Y., Hasunuma, T., Kondo, A., Chang, J.-S. 2013. Characterization and optimization of carbohydrate production from an indigenous microalga *Chlorella vulgaris* FSP-E. *Bioresource Technology*, **135**, 157-165.

Ho, S.H., Nakanishi, A., Ye, X., Chang, J.-S., Chen, C.Y., Hasunuma, T., Kondo, A. 2015. Dynamic metabolic profiling of the marine microalga Chlamydomonas sp. JSC4 and enhancing its oil production by optimizing light intensity. *Biotechnology for Biofuels*, **8**, 48.

Islam, M.A., Magnusson, M., Brown, R.J., Ayoko, G.A., Nabi, M.N., Heimann, K. 2013. Microalgal Species Selection for Biodiesel Production Based on Fuel Properties Derived from Fatty Acid Profiles *Energies*, **6**, 5676-5702.

Lee, J.-Y., Yoo, C., Jun, S.-Y., Ahn, C.-Y., Oh, H.-M. 2010. Comparison of several methods for effective lipid extraction from microalgae *Bioresource Technology*, **101**, S75–S77.

Lewis, T., Nichols, P.D., McMeekin, T.A. 2000. Evaluation of extraction methods for recovery of fatty acids from lipid-producing microheterotrophs. *Journal of Microbiological Methods*, **43**, 107–116.

Li, Y., Naghdi, F.G., Garg, S., Adarme-Vega, T.C., Thurecht, K.J., Ghafor, W.A., Tannock, S., Schenk, P.M. 2014. A comparative study: the impact of different lipid extraction methods on current microalgal lipid research. *Microbial Cell Factories*, **13**.

Liu, J., Chu, Y., Cao, X., Zhao, Y., Xie, H., Xue, S. 2015. Rapid transesterification of micro-amount of lipids from microalgae via a micro-mixer reactor. *Biotechnology for Biofuels*, **8**, 229.

Liu, Z. 2013. Micro algae oil industrialization proceeded to the cost first.

Lodish, H., Berk, A., Zipursky, S.L., Matsudaira, P., Baltimore, D., Darnell., J. 2000. Membrane Proteins. in: *Molecular Cell Biology, 4th edition*, W. H. Freeman. New York.

Maeda, Y., Tateishi, T., Niwa, Y., Muto, M., Yoshino, T., Kisailus, D., Tanaka, T. 2016. Peptide-mediated microalgae harvesting method for efficient biofuel production. *Biotechnology for Biofuels*, **9**, 10.

Malcata, F.X. 2011 Microalgae and biofuels: A promising partnership? *Trends Biotechnol.*, **29**(11), 542-549.

Marty, Y., Delaunay, F., Moal, J., Samain, J.-F. 1992. Changes in the fatty acid composition of *Pecten maximus* (L.) during larval development. *J Exp Mar Biol Ecol*, **163**, 221-234.

Mendes, L.B.B., Vermelho, A.B. 2013. Allelopathy as a potential strategy to improve microalgae cultivation. *Biotechnology for Biofuels*, **6**, 152.

Nikkanen, L., Toivola, J., Rintamäki, E. 2016. Crosstalk between chloroplast thioredoxin systems inregulation of photosynthesis. *Plant, Cell and Environment*.

Parrish, C.C. 1987. Separation of aquatic lipid classes by Chromarod thin-layer chromatography with measurement by latroscan Flame ionization detection. *Can.]. Fish. Aquat. Sci.*, **44**, 722-731.

Peled-Zehav, H., Danon, A. 2007. Translation and translational regulation in chloroplasts in cell and molecular biology of plastids. *Topics in current Genetics*, **19**, 249-281.

Peled-Zehavi, H., Avital, S., Danon, A. 2010. Methods of redox signaling by plant thioredoxins. in: *Methods in redox signaling*, (Ed.) D.K. Das, Mary Ann Liebert, Inc. Publications.

Pereira, H., Barreira, L., Mozes, A., Florindo, C., Polo, C., Duarte, C.V., Custódio, L., Varela, J. 2011. Microplate-based high throughput screening procedure for the isolation of lipid-rich marine microalgae. *Biotechnology for Biofuels*, **4**, 61.

Perez-Garcia, O., Escalante, F.M.E., de-Bashan, L.E., Bashan, Y. 2011. Heterotrophic cultures of microalgae: metabolism and potential products *Water Research*, **45**, 11–36.

Ranjan, A., Patil, C., Vijayan, Moholkar, S. 2010. Mechanistic Assessment of Microalgal Lipid Extraction. *Industrial & Engineering Chemistry Research*, **49**(6), 2979-2985.

Ren, H.-Y., Liu, B.-F., Ma, C., Zhao, L., Ren, N.-Q. 2013. A new lipid-rich microalga *Scenedesmussp*. strain R-16 isolated using Nile red staining: effects of carbon and nitrogen sources and initial pH on the biomass and lipid production. *Biotechnology for Biofuels*, **6**, 143.

Ren, X., Chen, J., Deschênes, J.-S., Tremblay, R., Jolicoeur, M. 2016. Glucose feeding recalibrates carbon flux distribution and favours lipid accumulation in Chlorella protothecoides through cell energetic management. *Algal Research* **14** 83–91.

Ryckebosch, E., Muylaert, K., Foubert, I. 2012a. Optimisation of an analytical procedure for extraction of lipids from microalgae. *J Am Oil Chem Soc*, **89**, 189–198.

Ryckebosch, E., Muylaert, K., Foubert, I. 2012b. Optimisation of an analytical procedure for extraction of lipids frommicroalgae. *J Am Oil Chem Soc*, **89**, 189-198.

Salvo, F., Dufour, S.C., Hamoutene, D., Parrish, C.C. 2015. Lipid classes and fatty Acids in Ophryotrocha cyclops, a dorvilleid from Newfoundland aquaculture sites. *PLoS ONE*, **10**(8).

Schuhmann, H., Lim, D.K., Schenk, P.M. 2012. Perspectives on metabolic engineering for increased lipid contents in microalgae. *Biofuels*, **3**, 71–86.

Shen, Y., Pei, Z.J., Yuan, W., Mao, E. 2009. Effect of nitrogen and extraction method on algae lipid yield. *Int J Agric Biol Eng*, **2**, 51–57.

Shih-Hsin Ho, A.N., Xiaoting Ye, Jo-Shu Chang, Kiyotaka Hara, Tomohisa HasunumaEmail author and Akihiko Kondo. 2014. Optimizing biodiesel production in marine Chlamydomonassp. JSC4 through metabolic profiling and an innovative salinity-gradient strategy. *Biotechnology for Biofuels*, **7**, 97.

Tabatabaei, M., Karimi, K., Kumar, R., Horváth, I.S. 2015. Renewable Energy and Alternative Fuel Technologies. *BioMed Research International*, 2.

Wang, Y., Chen, T., Qin, S. 2013. Differential fatty acid profiles of Chlorella kessleri grown with organic materials. *Chem. Technol. Biotechnol.*, **88**, 651–657.

Wei, X., Li, X., Xiang, J., Wu, Q. 2008. High-density fermentation of microalga *Chlorella protothecoides* in bioreactor for microbio-diesel production. *Appl Microbiol Biotechnol* **78**(1), 29-36.

Xiong, W., Li, X., Xiang, J., Wu, Q. 2008. High-density fermentation of microalga *Chlorella protothecoides* in bioreactor for microbio-diesel production. *Appl Microbiol Biotechnol*, **78**, 29-36.

Yena, H.-W., Hub, I.-C., Chend, C.-Y., Hoe, S.-H., Leef, D.-J., Chang, J.-S. 2013. Microalgae-based biorefinery – From biofuels to natural products. *Bioresource Technology*, **135**, 166-174.

Yu, W.L., Ansari, W., Schoepp, N.G., Hannon, M.J., Mayfield, S.P., Burkart, M.D. 2011. Modifications of the metabolic pathways of lipid and triacylglycerol production in microalgae. *Microbial Cell Factories*, **10**, 91.

Zhongtian L: Micro algae oil industrialization proceeded to the cost first. 2013. http://www.cnpc.com.cn/syzs/lsht/201312/4d27747c39e041af8852b4fed32532c9.shtml

Salvo R: Lipid extraction from microalgae using a single ionic liquid [P]. 2011; US20110130551 A1, Streamline Automation, LLC. US.

Wang X, Miao H, Zhai Y: Study on the methods of alga cells fragmentation. Journal of Tianjin University of Science and technology, 2007; 22: 21-25.

Orr V, Plechkova N, Seddon K, Rehmann L: Disruption and Wet Extraction of the Microalgae Chlorella vulgaris Using Room-Temperature Ionic Liquids. ACS Sustainable Chem. 2016; 4 (2): 591–600.

CHAPTER 7 GENERAL DISCUSSION

This thesis, which focused on the algae platform *Chlorella protothecoides*, presented a metabolomic study, a kinetic metabolic model as well as a new approach increasing the efficiency of current lipid extraction methods. The metabolomic study confirmed the algae cell metabolic flexibility, comparing autotrophic, mixotrophic and heterotrophic culture conditions. The modeling work, the first of this type, which allowed performing a dynamic metabolic flux analysis while drawing the intracellular carbon flow distribution, opens new perspectives for the evaluation of hypotheses and strategies for metabolic engineering work and bioprocess development. Finally, and taking all the above, by ameliorating current lipid extraction methods, this thesis has contributed with fundamental knowledge as well as technologies useful to the improvement of the lipid yield of the algae platform as well as to its commercial feasibility.

1) Understanding metabolic regulation for improving lipid yield

Lipid synthesis in the algae platform is a complex and highly interacting process, and the regulation of lipid synthesis could either favor or inhibit lipid synthesis pathways depending on a multifactorial set of culture and cellular parameters. Previous studies on metabolic regulation mechanisms in algae platform mainly focused on photosynthesis, with the Calvin cycle as the key regulatory pathway. It is regulated by the enzymes Rubisico (RuBisco), GAPDH (glyceraldehyde phosphate dehydrogenase), FBPase (fructose-1,6-bisphosphatase), SBPase (sedoheptulose-1,7-bisphosphatase) and Ru5PK (ribulose-5-phosphate kinase). RuBisco is an important carboxylase that determines carbon assimilation rate. Moreover, it is also an indispensable oxygenase in photorespiration, which leads to carbon loss during carbon fixation thus reducing the carbon flow to carbohydrates (e.g. starch) and lipid accumulation. High concentrations of CO_2 and adequate light intensity can enhance, however, the net carbon storages (i.e. starch, lipid), while also increasing carbon loss from increasing the carboxylase activity of Rubisco.

Indeed, in the recent years, heterotrophic algae culture gained in attention for lipid production, since it presents advantages such as high final biomass concentration and lipid content (55 % of the dry weight) (Miao and Wu 2006). Although it was expected that an organic carbon source can serve as a more direct organic substrate to an algae, it was surprising that literature reports a no increase of lipid production under mixtrophic culture condition, with the two carbon sources CO_2 and glucose available. Therefore, we have conducted a metabolomic study to better understand the

role of adding an organic carbon source on the microalgae metabolism, focusing on lipid accumulation. This work (Ren et al., 2016) was published in Algal Research. It presents an in-depth study of *C. protothecoides* response to glucose supplementation, comparing heterotrophic and mixotrophic modes to autotrophic culture mode. The observed changes in metabolite pools and energy charge demonstrate a clear effect of the carbon sources of the cellular response, which also affect lipid accumulation. We have also observed that the presence of glucose as a carbon source can substantially augment neutral lipid synthesis, while the metabolomic analysis showed that autotrophic growth favored starch synthesis. Glucose also affect the cells energetic state inducing a high ATP-to-ADP ratio, which is hypothesized to recalibrate a metabolic shift from starch to lipids accumulation. Therefore, novel data were thus disseminated on the role of glucose on the regulation of carbon flow and lipid synthesis in microalgae cells.

2) Developing a dynamic *in silico* model as a tool for bioprocess optimization

The previous work on the metabolomics effects of glucose-fed algae cultures stimulated to conduct a study specifically to better understand the heterotrophic culture condition. There are highly performant models in literature, basically macroscopic, dealing with nutrient limitation (mainly nitrogen), light intensity and temperature variation. Only few models considered lipid accumulation as a product. To the best of our knowledge, there is no mention in literature of models that describe the carbon flux distribution at the metabolic level. In fact, such metabolic model that combine both the environmental factor and metabolic information would further provide a unique tool to identify, through model simulations, optimal nutritional strategy to maximize lipid productivity (Cloutier et al., 2009). A model describing a metabolic network on duty (functional timewise) is thought to also provide a precise tool for the identification of key genetic manipulation hypotheses. We have thus developed a dynamic metabolic model adapted from a previous model originally developed for non-photosynthetic plant cells to describe the behaviour of the central carbon metabolism and cell behavior in heterotrophic *Chlorella protothecoides* cells. We here presented a first attempt which was constrained with the objective to limit model complexity. Since in this model type each flux is kinetically described using a Michaelis-Menten type equation, only the major pathways linking the substrate glucose to the global lipid synthesis pathway, such as glycolysis and pentose phosphate pathways and TCA cycle as well as lipid synthesis were considered, which thus limited the number of kinetic parameters. Cell energetics and redox state were thus not described in the model, and flux regulation was limited to that from metabolic

intermediates. The model structure and kinetic parameters were determined based on experimental data for heterotrophic growth obtained in Chapter four (4), minimizing an objective function for the simulation global error. The error minimization step implied performing a parameter sensitivity analysis, enabling to focus on the minimal set of sensitive parameters. Once calibrated, the model showed adequate to simulate experimental data for heterotrophic *C. protothecoides* culture. Then, model simulation output allowed performing a dynamic metabolic flux analysis of the algae biosystem. It was showed that high lipid yield is companied with high lipid flux and low TCA activity. Meanwhile, the dynamic flux distribution also suggest a robust and stable metabolism in *Chlorella protothecoides* with relatively constant ratio of glucose distributed to biomass, lipid, starch, nucleotide as well as pentose phosphate pathway. This work thus presents the first kinetic metabolic model applied to the algae platform, to the best of our knowledge, which provides a biologically relevant model of the cell metabolic dynamics. This model represents a valuable fundamental and bioprocess tool.

3) Improving bioprocess lipid yield enhancing lipid extraction method efficiency

Every step in a production bioprocess is important to reach maximum yield. We have first worked upstream acquiring knowledge and developing tools to enhance algae productivity, then we also put effort at downstream to maximize the efficiency of lipid extraction process. Classical and mostly used extraction methods consist of two successive solvent extractions. Our strategy was then to ameliorate lipid extraction efficiency by further disturbing the cell membranes integrity by adding a water step between the two successive solvent extractions. The new approach allowed over 100 % increase of the harvested lipids, and for the four most popular methods currently widely used. It showed water treatment of biomass after the first solvent extraction phase favors the release of intracellular lipids in the second solvent extraction step. Total lipid extraction yield as well as intracellular lipid class ratios in the final extract were thus significantly increased by the water treatment. The neutral-to-polar lipid ratio is also greatly improved after the water treatment. The addition of a water step also showed to favor TAG lipids, thus favoring the energy level harvested, since TAG is the precursor of final energetic product biodiesel. The highest TAG extraction yield by the modified method was of 73.7 µg/mg, while the highest TAG extraction yield by the classical methods was of 31.9 µg/mg. So, adding a water treatment step multiplies by a factor two the TAG extraction yield. Although we added an extraction step in our proposed method, less solvent is then required with increased yield. Our results can be applied as well using more “environment friendly”

“green” solvents as extractive phase (Salvo, 2011b). The vortex treatment such as the length of the treatment, the power of agitation, as well as its effect on the extracted lipids classes should also be included for further clarity of the single role of water treatment. Different solvents could also be used as substitute of water to verify whether water is the specific one that could help improving the extraction. Meanwhile, literature has recently become abundant proposing extraction procedures using fresh algae biomass oppositely to dry algae biomass in classical methods. This method modification can significantly lower the costs and fasten total required time of the downstream processing step, which are crucial issues to establish commercial feasibility of a bioprocess. Indeed, we have also validated our method modification showing enhanced extraction efficiency using fresh biomass. Therefore, although our new approach adds an extra step, the extra cost is thought counteracted by removing a biomass mechanical cell disruption pre-treatment step, can be applied using either dry or fresh algae biomasses, using less solvent as well as resulting in higher lipid yield. Taking all above-mentioned advantages adding a water treatment step, our method is expected to impact practices at laboratory and industrial scales, enabling to harvest more energy (i.e. that from lipid) that the energy requires in the whole bioprocess, a serious issue for industrials (Liu, 2013).

CHAPTER 8 CONCLUSION

In this thesis, the dynamic metabolic profile and cell behavior of *Chlorella protothecoides* were studied under three typical culture modes, namely the heterotrophic, the mixotrophic and the autotrophic. Results showed the metabolomic status of this algae species was highly affected by the environmental culture condition, especially with or without feeding glucose. Glucose showed playing an important role both as a complementary organic carbon source to CO_2 and as energy source. It induces a high energy gradient (ATP-to-ADP ratio), which directly stimulates algae metabolism towards lipids production rather than to carbohydrates such as starch accumulation. Furthermore, glucose also improved lipids and fatty acids composition in regards to biodiesel production.

Based on such knowledge and conclusion, a model simulating *Chlorella protothecoides* cell metabolic behavior under heterotrophic condition and describing metabolic network flux kinetics was developed. Simulation results show satisfactory fit with experimental data with the minimum objective function value. A sustained high lipid synthesis metabolic activity was further confirmed from model flux analysis with higher lipid flux and lower TCA activity. Such model also provides a platform exploring hypotheses for genetic manipulations improving lipid production by, for instance, looking at re-directing TCA activity. Indeed, this *in silico* platform allows both exploring and questioning fundamental metabolic behavior then guiding experimental plan. Finally, it could be used as a tool to search for ‘‘optimal’’ culture management strategy guiding the management of the main nutrients concentration that affect lipid synthesis.

In complement, we also ameliorated the lipid extraction method based on classical current methods. An intermediate treatment step using water in current lipid extraction methods was confirmed helping the release of intracellular lipids in the second and last extraction, which accordingly can clearly improve the final lipids extraction yield. In addition, the water treatment greatly improves NL-to-PL ratio, and positively modifies the lipid class ratios in the final extract, which favors selective extraction of TAG. The novel method thus provides an efficient way to improve lipid extraction yield of existing methods, as well as selectively favoring TAG, a lipid of the highest interest for biodiesel production.

Therefore, this thesis presents a coherent set of complementary studies showing that a glucose addition strategy, identified using the kinetic metabolic model we developed, combined to the

ameliorated lipid extraction method could result in improved lipids yield and composition; all factors contributing to establish the economic viability of the algae platform to produce biodiesel.

CHAPTER 9 RECOMMENDATION

We believe the metabolic model can become a central tool supporting the development and the management of an economically feasible biodiesel production using the algae platform. However, more work remains to be done for having a predictive model, and we are presenting below some research ideas to reach that ultimate goal.

1. Adapt the heterotrophic model to autotrophic and mixotrophic conditions

Since the specific character of the algae platform relies in its high photosynthesis efficiency, which can fix CO_2 and thus contribute to solve the global warming problem, it would be of interest to adapt our heterotrophic kinetic model to autotrophic and mixotrophic cultures to compare flux distribution profile in different culture modes and get more information of lipid synthesis regulation, and have a clearer view on the specific advantages of the three culture modes.

2. Expand the metabolic reaction network including key nutrients, such as inorganic ions, that are known to have a regulatory role on lipid production

Some ions are known to play various roles in lipid synthesis, for example, from our metabolic study in which Mg^{2+} shows its importance under light and mixed energetic conditions. Mg^{2+} is essential for photosynthesis, so it is expected that the heterotrophic condition leads to less Mg^{2+} requirement. Therefore, the management of Mg^{2+} concentration can be seen as a way in the control of cultures, and a mathematical model may be used for that purpose. In the case of K^+, it normally remains at a stable concentration in plant cells (Kant, 2002). However, K^+ ion is involved in the transport of sugars into the storage organelle, and is promoting the synthesis of other storage materials (Kumar, 2012). Therefore, adding this ion in the model as a nutrient factors could help to design a balanced nutrient strategy favoring lipid production. And there are many other nutrients that can be important, such as inorganic phosphate (Pi).

3. Accounting for lipid classes

There is storage lipid and functional lipid pools. Some lipid greatly accumulates under stressful environmental conditions, such as storage pools (mainly as TAG) that are of interest for biodiesel production, and membrane lipids, which could also be of interest although these require further chemical transformation to be biodiesels. Therefore, modifying the model for describing the specific pathways leading to major lipid classes can definitely enhance the value of the model.

4. Expand data sets of experimental data, both extracellular and intracellular

Although very few studies have been reported with this large number of measurements for the intermediate metabolites of *Chlorella protothecoides* cells, such as in the present study, it would also improve model predictive capacity to include more detailed pathways on, for instance, nitrogen metabolism, and intracellular compartmentalization. However, to this end, there will be no choice to include cell energetics and redox states in the model.

5. Appling the metabolic model in process simulation and control.

To the long term, based on a model further developed as suggested above, using it as a tool, it will be the ultimate interest to evaluate the model capacity to support directed manipulation of the carbon flow favoring lipids and fatty acids synthesis. Such simulation platform would also be useful to design a nutrient fed-batch culture strategy for a balance between microalgae growth and lipids synthesis. Finally, the *in silico* platform may also be helpful guiding work for the identification of potential targets for genetic engineering.

BIBLIOGRAPHY

Andrich, G., Nesti, U., Venturi, F., Zinnai, A., Fiorentini, R. 2005. Supercritical fluid extraction of bioactive lipids from the microalga Nannochloropsis sp. *European Journal of Lipid Science and Technology*, **107**(6), 381-386.

Araujo, G.S., Matos, L.J.B.L., Fernandes, J.O., Cartaxo, S.J.M., Gonçalves, L.R.B., Fernandes, F.A.N., Farias, W.R.L. 2013. Extraction of lipids from microalgae by ultrasound application: Prospection of the optimal extraction method. *Ultrasonics Sonochemistry*, **20**, 95-98.

Armbrust, E.V., J. A. Berges, C.B., Green, B.R., etc., D.M. 2004. The genome of the diatom Thalassio- sira pseudonana: ecology, evolution, and metabolism. *Science*, **306**(79-86).

Armstrong, R. 2006 Optimality-based modeling of nitrogen allocation and photoacclimation in photosynthesis. *Deep Sea Research Part II: Topical Studies in Oceanography*, **53**(5-7), 513–531.

Bao, X., Ohlrogge, J. 1999. Supply of Fatty Acid Is One Limiting Factor in the Accumulation of Triacylglycerol in Developing Embryos. *Plant Physiology*, **120**, 1057-1062.

Bernard, O. 2005. non-liner control for algae growth models in the chemostat. *Bioprocess Biosyst Eng*, **27**, 319–327.

Bernard, O., Gouzé, J.-L. 1999. Nonlinear qualitative signal processing for biological systems: application to the algal growth in bioreactors. *Math. Biosci. ,* **157**, 357–372.

Bernard, O., Rémond, B. 2012. Validation of a simple model accounting for light and temperature effect. *Bioresource Technology* **123** 520–527.

Blatti, J.L., Beld, J., Behnke, C.A., Mendez, M., Mayfield, S.P., Burkart, M.D. 2012. Manipulating fatty acid biosynthesis in microalgae for biofuel through protein-protein interactions. *PLoS ONE*, **7**(9), e42949.

Bligh, E.G., Dyer, W.J. 1959. A rapid method of total lipid extraction and purification. *Canadian Journal of Biochemistry and Physiology*, **37**, 911-917.

Bollinger, J.A. 2011. Combining Biological Knowledge with Sampling Know-How: Kinetic Space Modeling & Control Over Growth in the Chlamydomonas reinhardtii Metabolism, Vol. Ph.D, University of Maryland, Baltimore County.

Borowitzka, M.A. 1988. Microalgae as sources of pharmaceuticals and other biologically active compounds. *Journal of Applied Phycology*, **4**, 267-279.

Bowler, C., Allen, A.E., Badger, J.H., Grimwood, J., Jabbari, K., Kuo, A., et al. 2008. The Phaeodactylum genome reveals the evolutionary history of diatom genomes. *Nature*, **456**(7219), 239-44.

Boyle, N.R., Morgan, J.A. 2009. Flux balance analysis of primary metabolism in Chlamydomonas reinhardtii. *BMC Syst Biol*, **3**, 4.

Boyle, N.R.a.J.A.M. 2009. Flux balance analysis of primary metabolism in Chlamydomonas reinhardtii. *BMC Syst Biol* **3**, 4.

Bumbak, F., Cook, S., Zachleder, V., Hauser, S., Kovar, K. 2011. Best practices in heterotrophic high-cell-density microalgal processes: achievements, potential and possible limitations. *Appl Microbiol Biotechnol*, **91**(1), 31-46.

Burja, A.M., Armenta, R.E., Radianingtyas, H., Barrow, C.J. 2007. Evaluation of fatty acid extraction methods for Thraustochytrium sp. ONC-T18. *Journal of Agricultural and Food Chemistry*, **55**, 4795–4801.

Cequier-Sanchez, E., Rodriguez, C., Ravelo, A.G., Zarate, R. 2008. Dichloromethane as a solvent for lipid extraction and assessment of lipid classes and fatty acids from samples of different natures. *J. Agric. Food Chem.*, **56**, 4297-4303.

Cesarini, S., Haller, R.F., Diaz, P., Nielsen, P.M. 2014. Combining phospholipases and a liquid lipase for one-step biodiesel production using crude oils. *Biotechnology for Biofuels*, **7**, 29.

Ch. Schlechtriem , U.F.K.B. 2010. Effect of different lipid extraction methods on δ13 C of lipid and lipid-free fraction of fish and different fish feeds. *Isotopes in Environmental and Health Studies*, **39**(2), 135-140.

Chen, C.-Y., Chang, J.-S., Chang, H.-Y., Chen, T.-Y., Wu, J.-H., Leef, W.-L. 2013. Enhancing microalgal oil/lipid production from *Chlorella sorokiniana* CY1 using deep-sea water supplemented cultivation medium. *Biochemical Engineering Journal*, **77**, 74-81.

Chen, F. 1996. High cell density culture of microalgae in heterotrophic growth. *Trends in BIotechnology*, **14**(11), 421-426.

Chen, I.S., Shen, C.S.J., Sheppard, A.J. 1981 Comparasion of methylene chloride and chloroform for the extraction of fats from food products. *J. Am. Oil Chem. Soc*, **58**, 599–601.

Cloutier, M., Bouchard-Marchand, E., Perrier, M., Jolicoeur, M. 2008. A predictive nutritional model for plant cells and hairy roots. *Biotechnol Bioeng*, **99**(1), 189-200.

Cloutier, M., Chen, J., Tatge, F., McMurray-Beaulieu, V., Perrier, M., Jolicoeur, M. 2009. Kinetic metabolic modelling for the control of plant cells cytoplasmic phosphate. *J Theor Biol*, **259**(1), 118-31.

Cloutier, M., Perrier, M., Jolicoeur, M. 2007. Dynamic flux cartography of hairy roots primary metabolism. *Phytochemistry*, **68**(16-18), 2393-404.

Cogne, G., Gros, J., Dussap, C. 2003. Identification of a metabolic network structure representative of arthrospira (spirulina) platensis metabolism. *Biotech Bioeng.*, **84**(6), 667-676.

Coleman, L.W., Rosen, B.H., Schwartzbach, S.D. 1988a. Preferential loss of chloroplast proteins in nitrogen deficient Euglena. *Plant cell Physiol*, **29**, 1007-1101.

Curtis, B.A., Tanifuji, G., Burki, F., Gruber, A., Irimia, M., Maruyama, S., Arias, M.C., et al. 2012. Algal genomes reveal evolutionary mosaicism and the fate of nucleomorphs. *Nature*, **492**(7427), 59-65.

Dangoor, I., Peled-Zehavi, H., Levitan, A., Pasand, O., Danon, A. 2009. A small family of chloroplast atypical thioredoxins. *Plant Physiology*, **149**(3), 1240-1250.

Dehesh, K., Tai, H., Edwards, P., Byrne, J., Jaworski, J.G. 2001. Overexpression of 3-ketoacyl-acyl-carrier protein synthase IIIs in plants reduces the aate of lipid synthesis. *Plant Physiology*, **125**, 1103–1114.

Derelle, E., Ferraz, C., Rombauts, S., Rouze, P., Worden, A.Z., Robbens, S., et al. 2006. Genome analysis of the smallest free-living eukaryote Ostreococcus tauri unveils many unique features. *Proc Natl Acad Sci U S A*, **103**(31), 11647-52.

Deschênes, J.-S., Wouwer, A.V. 2015. Dynamic optimization of biomass productivity in continuous cultures of microalgae *Isochrysis galbana* through modulation of the light intensity. *IFAC papers online-Conference paper archive*, **48**(8), 1093-1099.

Dommange, X., Tanguy, P.A., Jolicoeur, M. 2015. Feasibility of lipid mechanical extraction from

viable Monoraphidium minutum. *Microalgae Biotechnology*, **1**(1), 12-19.

Drochioiu, G. 2005. Turbidimetric lipid assay in seed flours. *Journal of food lipids*, **12**, 12-22.

Droop, M.R. 1983a. 25 years of algal growth kinetics, a personal view. *Botan. Marina*, **16** (99–112).

Droop, M.R. 1983b. 25 years of algal growth kinetics, a personal view *Botan. Marina.* **16**, 99–112.

Droop, M.R. 1968a. Vitamin B12 and marine ecology. IV. The kinetics of uptake growth and inhibition in *Monochrysis lutheri*. *J. Mar. Biol. Assoc.*, **48**(3), 689-733.

Droop, M.R. 1968b. Vitamin B12 and marine ecology. IV. The kinetics of uptake growth and inhibition in Monochrysis lutheri. *J. Mar. Biol. Assoc.* , **48** (3), 689–733.

Dunahay, T.G., Jarvis, E.E., Rossler, P.G. 1995. Genetic transformation of the diatoms Cyclotella Cryptica and Navicula Saprophila. *J. Phycol*, **31**, 1004-1012.

Duong, V.T., Thomas-Hall, S.R., Schenk, P.M. 2015. Growth and lipid accumulation of microalgae from fluctuating brackish and sea water locations in South East Queensland—Australia. *Front. Plant Sci.*, **6**, 359.

Erwin, J.A. 1973. Comparative biochemistry of fatty acids in eukaryotic microorganisms. In Lipids and Biomembranes of Eukaryotic Microorganisms. *Academic Press*, 141-143.

F., S. 1879. The weight analytic determination of milk fat. *Polytechnisches J.*, **232**, 461.

Falkowski, P.G., Raven, J.A. 2007 *Aquatic Photosynthesis*. Princeton University Press, Princeton.

Faugeras, B., Bernard, O., Sciandra, A., Levy, M. 2004. A mechanistic modelling and data assimilation approach to estimate the carbon/chlorophyll and carbon/ nitrogen ratios in a coupled hydrodynamical-biological model. *Nonlinear Process. Geophys.*, **11**, 515–533.

Feng Chen, M.R.J. 1991. Effect of C/N ratio and aeration on the fatty acid composition of heterotrophicChlorella sorokiniana. *Journal of Applied Phycology*, **3**(3), 203-209.

Flynn, K.J. 2001. A mechanistic model for describing dynamic multi-nutrient, light, temperature interactions in phytoplankton. *Journal of Plankton Research*, **23**(9), 977.

Folch, J., Lees, M., Stanley, G.H.S. 1957. A simple method for the isolation and purificatioin of total lipids from animal tissues. *J. Biol. Chem*, **1**, 497-509.

Follstad, B., Balcarel, R., Stephanopoulos, G., Wang, D. 1999. Metabolic flux analysis of hybridoma continuous culture steady state multiplicity. *Biotechnol Bioeng*, **63**, 675–683.

Frank, I.B., Dubinsky, Z. 1999. Balanced growth in aquatic plants: myth or reality? *BioScience* **49**, 29–37.

Fu, P. 2009. Genome-scale modeling of synechocystis sp. Pcc 6803 and prediction of pathway insertion. *Chemical Technology and Biotechnology*, **84**(4), 473-483.

Gao, C., Zhai, Y., Ding, Y., Wu, Q. 2009. Application of sweet sorghum for biodiesel production by heterotrophic microalga *Chlorella protothecoides*. *Applied Energy*. 87, 756–761.

Geider, R., MacIntyre, H., Kana, T. 1998. A dynamic regulatory model of phytoplanktonic acclimation to light, nutrients, and temperature. *Limnol. Oceanogr.*, **43**, 679–694.

Georgianna, D.R., Mayfield, S.P. 2012. Exploiting diversity and synthetic biology for the production of algal biofuels. *Nature*, **488**(7411), 329-335.

Ghorbaniaghdam, A., Henry, O., Jolicoeur, M. 2013. A kinetic-metabolic model based on cell energetic state: study of CHO cell behavior under Na-butyrate stimulation. *Bioprocess Biosyst Eng*, **36**(4), 469-87.

Girard, J.-M., Roy, M.-L., Hafsa, M.B. 2014. Mixotrophic cultivation of green microalgae Scenedesmus obliquus on cheese whey permeate for biodiesel production. *Algal research*, **5** 241-248.

Greenwell, H.C., Laurens, L.M., Shields, R.J., Lovitt, R.W., Flynn, K.J. 2010a. Placing microalgae on the biofuels priority list: a review of the technological challenges. *J R Soc Interface*, **7**(46), 703-26.

Greenwell, H.C., Laurens, L.M.L., Shields, R.J., Lovitt, R.W., Flynn, K.J. 2010b. Placing microalgae on the biofuels priority list: a review of the technological challenges. *Journal of the Royal Socity Interface* **7**, 703–726.

Grima, E.M., Medina, A.R., Giménez, A.G., Pérez, J.A.S., Camacho, F.G., Sánchez, J.L.G. 1994. Comparison between extraction of lipids and fatty aids from microalgal biomass. *Am Oil Chem Sco* **71**, 955–959.

Guanqun Chen, Y.J., Feng Chen. 2008. Salt-induced alterations in lipid composition of diatom

Nitzschia laevis(Bacillariophyceae) under heterotrophic culture condition. *Journal of Phycology*, **44**(5), 1309-1314.

Guihéneuf, F., Khan, A., Tran, L.-S.P. 2016. Genetic engineering: a promising tool to engender physiological, biochemical, and molecular stress resilience in green microalgae. *Front. Plant Sci.*, **7**, 400.

Guldhe, A., Singh, B., Ansari, F.A., Sharma, Y., Bux, F. 2016. Extraction and Conversion of Microalgal Lipids. *Green Energy and Technology*, **Algae Biotechnology**, 91-110.

Guo, S.-L., Zhao, X.-Q., Tang, Y., Wan, C., Alam, M.A., Ho, S.-H., Bai, F.-W., Chang, J.-S. 2013. Establishment of an efficient genetic transformation system in *Scenedesmus obliquus*. *Bioresource Technology*, **163**, 61-68.

Halim, R., Gladman, B., Danquah, M.K., Webley, P.A. 2011. Oil extraction from microalgae for biodiesel production. *Bioresource Technology*, **102**, 178-185.

Hamilton, R.J., Hamilton, S., Sewell, P. 1992. *Extraction of lipids and derivative formation. In Lipid Analysis: a practical approach*. Oxford University Press, New York.

Hara, A., Radin, N.S. 1978. Lipid extraction of tissues with a low-toxicity solvent. *Anal. Biochem*, **90** 420–423.

Harris, E.H. 2001. Chlamydomonas as a model organism. *Annual Review of Plant Physiology and Plant Molecular Biology*, **52**, 363-406.

Harris, R.P.D.a.L.M. 1999. Metabolic Flux Analysis Elucidates the Importance of the Acid-Formation Pathways in Regulating Solvent Production by Clostridium acetobutylicum. *Metabolic Engineering*, **1**, 206-213.

Ho, S.-H., Huang, S.-W., Chen, C.-Y., Hasunuma, T., Kondo, A., Chang, J.-S. 2013. Characterization and optimization of carbohydrate production from an indigenous microalga *Chlorella vulgaris* FSP-E. *Bioresource Technology*, **135**, 157-165.

Ho, S.H., Nakanishi, A., Ye, X., Chang, J.-S., Chen, C.Y., Hasunuma, T., Kondo, A. 2015. Dynamic metabolic profiling of the marine microalga Chlamydomonas sp. JSC4 and enhancing its oil production by optimizing light intensity. *Biotechnology for Biofuels*, **8**, 48.

Hu, Q., Sommerfeld, M. 2008. Microalgal triacylglycerols as feedstocks for biofuel production:

Perspec- tives and advances. *The Plant Journal*, **54**, 621-639.

Hu, Q., Sommerfeld, M., Jarvis, E., Ghirardi, M., Posewitz, M., Seibert, M., Darzins, A. 2008. Microalgal triacylglycerols as feedstocks for biofuel production: perspectives and advances. *Plant J*, **54**(4), 621-39.

Islam, M.A., Magnusson, M., Brown, R.J., Ayoko, G.A., Nabi, M.N., Heimann, K. 2013. Microalgal Species Selection for Biodiesel Production Based on Fuel Properties Derived from Fatty Acid Profiles *Energies*, **6**, 5676-5702.

Ito, T., Tanaka, M. 2012. Metabolic and morphological changes of an oil accumulating trebouxiophycean alga in nitrogen-deficient conditions. *Metabolomics*, **9**(178-187).

Jack Myers, G.O.B. 1940. Studies on photosynthesis some effects of light of high intensity on chlorella. *Journal of General Physiology*, **24**(1), 45-67.

Jain, R., Coffey, M., Lai, K., Kumar, A., MacKenzie, S. 2000. Targeting of the Arabidopsis homomeric acetyl-coenzyme A carboxylase to plastids of rapeseeds. *Biochemical Society Transactions* **28**(6), 958-961.

Jianxin, H., Jue, S. 2003. The Utilization of nitrate and phosphate in Dunaliella salina and the accumulative process of carotene *Marine Sciences*, **27**(2), 41-44.

Jolicoeur, M. 2014. Modeling cell behavior: moving beyond intuition *AIMS Bioengineering*, **1**(1), 1-12.

Khan, S.A., Rashmi, H.M.Z. 2009. Prospects of biodiesel production from microalgae in India. *Renewable and Sustainable Energy Reviews*, **13**(9), 2361-2372.

Kliphuis, A.M., Klok, A.J., Martens, D.E., Lamers, P.P., Janssen, M., Wijffels, R.H. 2012. Metabolic modeling of Chlamydomonas reinhardtii: energy requirements for photoautotrophic growth and maintenance. *J Appl Phycol*, **24**(2), 253-266.

Kliphuis, A.M.J., Martens, D.E., Janssen, M., Wijffels, R.H. 2011. Effect of O2-CO2 Ratio on the Primary Metabolism of Chlamydomonas reinhardtii. *Biotechnology and Bioengineering*, **108**, 2390-2402.

Kozaki, A., Karnada, K., Nagano, Y. 2000. Recombinant carboxyltransferase responsive to redox of pea plastidic acety-COA carboxylase. *J.Biol Chem.*, **275**, 10701-10708.

Lamboursain, L., Jolicoeur, M. 2005. Critical influence of Eschscholzia californica cells nutritional state on secondary metabolite production. *Biotechnol Bioeng*, **91**(7), 827-37.

Larkum, A.W.D. 2012. Selection, breeding and engineering of microalgae for bioenergy and biofuel production. *Biotechnology*, **30**(4), 198-205.

Leduc, M., Tikhomiroff, C., M, M.C., Perrier, Jolicoeur, M. 2006. Development of a kinetic metabolic model: application to Catharanthus roseus hairy root. *Bioprocess Biosyst Eng*, **28**, 295-313.

Lee, J.-Y., Yoo, C., Jun, S.-Y., Ahn, C.-Y., Oh, H.-M. 2010. Comparison of several methods for effective lipid extraction from microalgae *Bioresource Technology*, **101**, S75–S77.

Levy, Gantt. 1990. Development of photosynthetic activity in Porphyridium purpureum. *J Phycol*, **26**, 62-68.

Lewis, T., Nichols, P.D., McMeekin, T.A. 2000. Evaluation of extraction methods for recovery of fatty acids from lipid-producing microheterotrophs. *Journal of Microbiological Methods*, **43**, 107–116.

Lewitus, Caron. 1990. Relative effects of nitrogen or phosphorus and light intensity on the pigmentation, chemical composition and volume of Pyrenomonas salina (Cryptophyceae). *M. Eco. Progress Search*, **61**, 171-181.

Li, Y., Horsman, M., Wang, B., Wu, N., Lan, C.Q. 2008. Effects of nitrogen sources on cell growth and lipid accumulation of green alga Neochloris oleoabundans. *Appl Microbiol Biotechnol*, **81**(4), 629-36.

Li, Y., Naghdi, F.G., Garg, S., Adarme-Vega, T.C., Thurecht, K.J., Ghafor, W.A., Tannock, S., Schenk, P.M. 2014. A comparative study: the impact of different lipid extraction methods on current microalgal lipid research. *Microbial Cell Factories*, **13**.

Liu, J., Chu, Y., Cao, X., Zhao, Y., Xie, H., Xue, S. 2015. Rapid transesterification of micro-amount of lipids from microalgae via a micro-mixer reactor. *Biotechnology for Biofuels*, **8**, 229.

Liu, S., Chen, S., Liang, S. 1999. Researches on the heterotrophic culture of Chlorella vulgaris - optimisation of carbon sources, nitrogen sources, inoculum size and initial pH. *J South China Univ Technol*, **27**(111-115).

Lodish, H., Berk, A., Zipursky, S.L., Matsudaira, P., Baltimore, D., Darnell., J. 2000. Membrane Proteins. in: *Molecular Cell Biology, 4th edition*, W. H. Freeman. New York.

Maeda, Y., Tateishi, T., Niwa, Y., Muto, M., Yoshino, T., Kisailus, D., Tanaka, T. 2016. Peptide-mediated microalgae harvesting method for efficient biofuel production. *Biotechnology for Biofuels*, **9**, 10.

Maia, G. 2010. Design of Large Scale Kinetic Metabolic Models: Applications in Mammalian and Algae Metabolism. in: *Biochemical Engineering, PhD thesis*, Vol. Ph.D, University of Maryland Baltimore County.

Mairet, F. 2011. Modelling neutral lipid production by the microalga Isochrysis aff. Galbana under nitrogen limitation. *Bioresource Technology*, **102**(142–149).

Mairet, F., Bernard, O., Lacour, T., Sciandra, A. 2011a. Modelling microalgae growth in nitrogen limited photobiorector for estimating biomass, carbohydrate and neutral lipid productivities. in: *The 18th World Congress: The International Federation of Automatic Control*, (Ed.) Milano. Italy.

Mairet, F., Bernard, O., Masci, P., Lacour, T., Sciandra, A. 2011b. Modelling neutral lipid production by the microalga Isochrysis aff. galbana under nitrogen limitation. *Bioresource Technology*, **102**, 142–149.

Mairet, F., Munoz-Tamayo, R., Bernard, O. 2013. *Adaptive control for optimizing microalgae production*. India. <hal-00921486>, India. <hal-00921486>.

Malcata, F.X. 2011 Microalgae and biofuels: A promising partnership? *Trends Biotechnol.*, **29**(11), 542-549.

Marty, Y., Delaunay, F., Moal, J., Samain, J.-F. 1992. Changes in the fatty acid composition of *Pecten maximus* (L.) during larval development. *J Exp Mar Biol Ecol*, **163**, 221-234.

Mayfield, S. Genetic Engineering of Algae for Biofuel Production. in: *Department of Cell Biology and The Skaggs Institute for Chemical Biology* Vol. PhD, The Scripps Research Institute.

Mendes, L.B.B., Vermelho, A.B. 2013. Allelopathy as a potential strategy to improve microalgae cultivation. *Biotechnology for Biofuels*, **6**, 152.

Merchant, S.S., Prochnik, S.E., Vallon, O., Harris, E.H., Karpowicz, S.J., Witman, G.B., et al. 2007.

The Chlamydomonas genome reveals the evolution of key animal and plant functions. *Science*, **318**(5848), 245-50.

Miao, X., Wu, Q. 2006a. Biodiesel production from heterotrophic microalgal oil. *Bioresour Technol*, **97**(6), 841-6.

Miao, X., Wu, Q. 2006b. Biodiesel production from heterotrophic microalgal oil. *Bioresour Technol*, **97**(6), 841-846.

Monod, J. 1942. Recherches sur la croissance des cultures bacteriennes. *Paris: Herman*.

Murata, N. 2007. Lipids in photosynthesis: an overview, Vol. 6, Advances in Photosynthesis and Respiration, Vol. 6. Siegenthaler, Paul-André, Murata, N. (Eds.) Department of regulation biology, National institute for basic biology, Myodaiji, Okazaki 444 Japan.

Mutanda, T., Ramesh, D., Karthikeyan, S. 2011. Bioprospecting for hyper-lipid producing microalgal strains for sustainable biofuel. *Bioresource Technology*, **102**(1), 57-70.

Muthuraj, M. 2013. Flux balance analysis of Chlorella sp. FC2 IITG under photoautotrophic and heterotrophic growth conditions. *Photosynth Res.*, **118**(167–179).

Muthuraj, M., Palabhanvi, B., Misra, S., Kumar, V., Sivalingavasu, K., Das, D. 2013. Flux balance analysis of *Chlorella* sp. FC2 IITG under photoautotrophic and heterotrophic growth conditions. *Photosynth. Res.*, **118**, 167-179.

Navarro, E., Montagud, A., Co´rdoba, P.F.n.d., Urchueguia, J.F. 2009. Metabolic flux analysis of the hydrogen production potential in *Synechocystis* sp. PCC6803. *International Journal of Hydrogen Energy*, **34**, 8228-8838.

Nan, Y., Liu, JX., Lin, RH., Tavlarides, L. 2015. Production of biodiesel from microalgae oil (*Chlorella protothecoides*) by non-catalytic transesterification in supercritical methanol and ethanol: Process optimization. The Journal of Supercritical Fluids. 97: 174-182.

Nikkanen, L., Toivola, J., Rintamäki, E. 2016. Crosstalk between chloroplast thioredoxin systems inregulation of photosynthesis. *Plant, Cell and Environment*.

Packer, A., Li, Y., Andersen, T., Hu, Q., Kuang, Y., Sommerfeld, M. 2011. Growth and neutral lipid synthesis in green microalgae: a mathematical model. *Bioresour Technol*, **102**(1), 111-7.

Pahlow, M. 2005. Linking chlorophyll nutrient dynamics to the Redfield N:C ratio with a model of

optimal phytoplankton growth. *Mar. Ecol. Prog. Ser.* , **287**, 33–43.

Palenik, B., Grimwood, J., Aerts, A., Rouze, P., Salamov, A., Putnam, N., Dupont, C., et al. 2007. The tiny eukaryote Ostreococcus provides genomic insights into the paradox of plankton speciation. *Proc Natl Acad Sci U S A*, **104**(18), 7705-10.

Parrish, C.C. 1987. Separation of aquatic lipid classes by Chromarod thin-layer chromatography with measurement by latroscan Flame ionization detection. *Can.]. Fish. Aquat. Sci.*, **44**, 722-731.

Peled-Zehav, H., Danon, A. 2007. Translation and translational regulation in chloroplasts in cell and molecular biology of plastids. *Topics in current Genetics*, **19**, 249-281.

Peled-Zehavi, H., Avital, S., Danon, A. 2010. Methods of redox signaling by plant thioredoxins. in: *Methods in redox signaling*, (Ed.) D.K. Das, Mary Ann Liebert, Inc. Publications.

Pereira, H., Barreira, L., Mozes, A., Florindo, C., Polo, C., Duarte, C.V., Custódio, L., Varela, J. 2011. Microplate-based high throughput screening procedure for the isolation of lipid-rich marine microalgae. *Biotechnology for Biofuels*, **4**, 61.

Perez-Garcia, O., Escalante, F.M.E., de-Bashan, L.E., Bashan, Y. 2011. Heterotrophic cultures of microalgae: metabolism and potential products *Water Research*, **45**, 11–36.

Post-Beittenmiller, D., Roughan, G. 1992. <plntphys00710-0384.pdf>. *Regulation of Plant Fatty Acid Biosynthesis*, **100**, 923-930.

Quintana, N., Kooy, F.V.d., Rhee, M.D.V.d., Voshol, G.P., Verpoorte, R. 2011a. Renewable energy from Cyanobacteria: energy production optimization by metabolic pathway engineering. *Appl Microbiol Biotechnol*, **91**(3), 471-90.

Quintana, N., Van der Kooy, F., Van de Rhee, M.D., Voshol, G.P., Verpoorte, R. 2011b. Renewable energy from Cyanobacteria: energy production optimization by metabolic pathway engineering. *Appl Microbiol Biotechnol*, **91**(3), 471-90.

Radakovits, R., Jinkerson, R.E., Darzins, A., Posewitz, M.C. 2010. Genetic engineering of algae for enhanced biofuel production. *Eukaryot Cell*, **9**(4), 486-501.

Ranjan, A., Patil, C., Vijayan, Moholkar, S. 2010. Mechanistic Assessment of Microalgal Lipid Extraction. *Industrial & Engineering Chemistry Research*, **49**(6), 2979-2985.

Ren, H.-Y., Liu, B.-F., Ma, C., Zhao, L., Ren, N.-Q. 2013. A new lipid-rich microalga *Scenedesmussp*. strain R-16 isolated using Nile red staining: effects of carbon and nitrogen sources and initial pH on the biomass and lipid production. *Biotechnology for Biofuels*, **6**, 143.

Ren, X., Chen, J., Deschênes, J.-S., Tremblay, R., Jolicoeur, M. 2016. Glucose feeding recalibrates carbon flux distribution and favours lipid accumulation in Chlorella protothecoides through cell energetic management. *Algal Research* **14** 83–91.

Rizzi, M., Baltes, M., Theobald, U., Reuss, M. 1997. In vivo analysis of metabolic dynamics in *Saccharomyces cerevisiae* - II. Mathematical model. *Biotechnology and Bioengineering*, **55**, 592-608.

Roessler, P.G., Ohlrogge, J.B. 1993. Cloning and characterization of the gene that encodes Acetyl-coenzyme A carboxylase in the alga Cyclotella cryptica. *The Journal of Biological Chemistry*, **288**, 19254-19259.

Ross, O., Geider, R. 2009. New cell-based model of photosynthesis and photoacclimation: accumulation and mobilisation of energy reserves in phytoplankton. *Mar. Ecol. Prog. Ser.* , **383**, 53–71.

Rosso, L., Lobry, J.R., Flandrois, J.P. 1993. An unexpected correlation between cardinal temperatures of microbial growth highlighted by a new model. *Journal of Theoretical Biology*, **162**(4), 447–463.

Ryckebosch, E., Muylaert, K., Foubert, I. 2012a. Optimisation of an analytical procedure for extraction of lipids from microalgae. *J Am Oil Chem Soc*, **89**, 189–198.

Ryckebosch, E., Muylaert, K., Foubert, I. 2012b. Optimisation of an analytical procedure for extraction of lipids frommicroalgae. *J Am Oil Chem Soc*, **89**, 189-198.

Sakthivel, R., Elumalai, S. 2011. Microalgae lipid research, past, present: A critical review for biodiesel production in the future. *Journal of Experimental Science*, **2**(10), 29-49.

Salvo, F., Dufour, S.C., Hamoutene, D., Parrish, C.C. 2015. Lipid classes and fatty Acids in Ophryotrocha cyclops, a dorvilleid from Newfoundland aquaculture sites. *PLoS ONE*, **10**(8).

Salvo, R.D. 2011a. Lipid extraction from microalgae using a single ionic liquid. *Vol. US20110130551 A1, Streamline Automation, LLC. US.*

Salvo, R.D. 2011b. Lipid extraction from microalgae using a single ionic liquid [P]. , Vol. US20110130551 A1, Streamline Automation, LLC. US.

Sandnes, J.M., Källqvist, T., Wenner, D., Gislerød, H.R. 2005. Combined influence of light and temperature on growth rates of *Nannochloropsis oceanica*: linking cellular responses to large-scale biomass production. *Journal of Applied Phycology* **17** (6), 515–525.

Scheible, W.-R., Gonzales, F.A. 1997. Nitrate acts as a signal to induce organic acid metabolism and repress starch metabolism in tobacco. *Plant Cell* **9**, 783-798.

Schuhmann, H., Lim, D.K., Schenk, P.M. 2012. Perspectives on metabolic engineering for increased lipid contents in microalgae. *Biofuels*, **3**, 71–86.

Sciandra, A., Ramani, P. 1994. The limitations of continuous cultures with low rates of medium renewal per cell. *J. Exp. Mar. Biol. Ecol.* , **178**, 1–15.

Senne, S. 2012. A place in the sun - Algae is the crop of the future, according to researchers Geel Flanders Today.

Shah, V. 2010. Emerging Environmental Technologies. **2**, 181.

Sheehan, J., Dunahay, T., Benemann, J. and Roessler, P.G. . 1998. A Look Back at the US Department of Energy's Aquatic Species Program – Biodiesel from Algae. US Department of Energy's Office of Fuels Development.

Shen, Y., Pei, Z.J., Yuan, W., Mao, E. 2009. Effect of nitrogen and extraction method on algae lipid yield. *Int J Agric Biol Eng*, **2**, 51–57.

Shifrin, N.S., Chisholm, S.W. 1981. phytoplankton lipids: Interspecific differences and effects of nitrate, silicate and light-dark cycles. *Journal of Phycology*, **17**, 374-384.

Shih-Hsin Ho, A.N., Xiaoting Ye, Jo-Shu Chang, Kiyotaka Hara, Tomohisa HasunumaEmail author and Akihiko Kondo. 2014. Optimizing biodiesel production in marine Chlamydomonassp. JSC4 through metabolic profiling and an innovative salinity-gradient strategy. *Biotechnology for Biofuels*, **7**, 97.

Shinto, H., Tashiro, Y., Kobayashi, G., Sekiguchi, T., Hanai, T., Kuriya, Y., Okamoto, M.,

Sonomoto, K. 2008. Kinetic study of substrate dependency for higher butanol production in acetone–butanol–ethanol fermentation. *Process Biochemistry*, **43**(12), 1452-1461.

Sivakaminathan, S. 2012. Biomass and lipid production from heterotrophic and mixotrophic fed-batch cultivations of microalgae Chlorella Protothecoides using glycerol. in: *Science Biosystems Engineering.*, Vol. Master, Clemson University.

Stitt, M. 2002. Steps towards an integrated view of nitrogen metabo. *Journal of experimental botany*, **53**(370), 959-970.

Surendhiran, D., Sirajunnisa, A. 2015. Kinetic modeling of microalgal growth and lipid synthesis. *3 Biotech*, **5**, 663–669.

Sweetlove, L.J., Williams, T.C.R., Cheung, C.Y.M., Ratcliffe, R.G. 2013. Modelling metabolic CO2evolution – a fresh perspectiveon respiration. *Plant, Cell and Environment*, **36** (1631–1640).

Tabatabaei, M., Karimi, K., Kumar, R., Horváth, I.S. 2015. Renewable Energy and Alternative Fuel Technologies. *BioMed Research International*, 2.

Thurman, H.V. 1997. Introductory Oceanography, New Jersey, USA: Prentice Hall College. ISBN 0-13-262072-3.

Wang, X., Miao, H., Zhai, Y. 2007. Study on the methods of alga cells fragmentation. *Journal of Tianjin University of Science and technology*, **22**, 21-25.

Wang, Y., Chen, T., Qin, S. 2013. Differential fatty acid profiles of Chlorella kessleri grown with organic materials. *Chem. Technol. Biotechnol.*, **88**, 651–657.

Wei, X., Li, X., Xiang, J., Wu, Q. 2008. High-density fermentation of microalga *Chlorella protothecoides* in bioreactor for microbio-diesel production. *Appl Microbiol Biotechnol* **78**(1), 29-36.

Welter, C., Schwenk, J., Kanani, B., Blargan, V.J., M.J., B. 2013. Minimal Medium for Optimal Growth and Lipid Production of the Microalgae *Scenedesmus dimorphus*. *Wiley Online Library*.

Worden, A.Z., J. H. Lee, T. Mock, P. Rouze, M. P. Simmons, A. L. Aerts, etc. . 2009. Green evolution and dynamic adaptations revealed by genomes of the marine picoeukaryotes

Micromonas. *Science*, **324**, 268-272.

Xiong, W., Li, X., Xiang, J., Wu, Q. 2008a. High-density fermentation of microalga *Chlorella protothecoides* in bioreactor for microbio-diesel production. *Appl Microbiol Biotechnol*, **78**, 29-36.

Xiong, W., Li, X., Xiang, J., Wu, Q. 2008b. High-density fermentation of microalga Chlorella protothecoides in bioreactor for microbio-diesel production. *Appl Microbiol Biotechnol*, **78**(1), 29-36.

Xiong, W., Li, X. F., Xiang, J. Y., & Wu, Q. Y. 2008. High-density fermentation of microalga Chlorella protothecoides in bioreactor for microbio-diesel production. *Applied Microbiology and Biotechnology*, **78**, 29-36.

Xu, H., Miao, X., Wu, Q. 2006. High quality biodiesel production from a microalga Chlorella protothecoides by heterotrophic growth in fermenters. *Journal of Biotechnology*. 126, 499-507.

Yang, J., Rasa, E., Tantayotai, P., Scow, K.M., Yuan, H., Hristova, K.R. 2011. Mathematical model of Chlorella minutissima UTEX2341 growth and lipid production under photoheterotrophic fermentation conditions. *Bioresour Technol*, **102**(3), 3077-82.

Yang, L. 2012. Mixtrophic culture and metabolic flux analysis of Phaeodactylum tricornutum. in: *pharmaceutical engineering*, Vol. Master, Beijing university of chemical.

Yena, H.-W., Hub, I.-C., Chend, C.-Y., Hoe, S.-H., Leef, D.-J., Chang, J.-S. 2013. Microalgae-based biorefinery – From biofuels to natural products. *Bioresource Technology*, **135**, 166-174.

Yu, W.L., Ansari, W., Schoepp, N.G., Hannon, M.J., Mayfield, S.P., Burkart, M.D. 2011a. Modifications of the metabolic pathways of lipid and triacylglycerol production in microalgae. *Microb Cell Fact*, **10**, 91.

Yu, W.L., Ansari, W., Schoepp, N.G., Hannon, M.J., Mayfield, S.P., Burkart, M.D. 2011b. Modifications of the metabolic pathways of lipid and triacylglycerol production in microalgae. *Microbial Cell Factories*, **10**, 91.

Yue Jiang, F.C. 2000. Effects of medium glucose concentration and pH on docosahexaenoic acid

content of heterotrophic Crypthecodinium cohnii. *Process Biochemistry*, **36**(10), 1205-1209.

Zhiyou Wen, F.C. 2003. Heterotrophic production of eicosapentaenoic acid by microalgae. *Biotechnology Advances*, **21**(4), 273-294.

APPENDICE A RECOVERY RATE OF NUCLEOTIDES, REDOX, SUGAR PHOSPHATE AND ORGANIC ACIDS

Recovery rate of nucleotides and redox

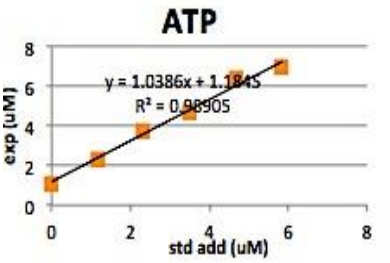

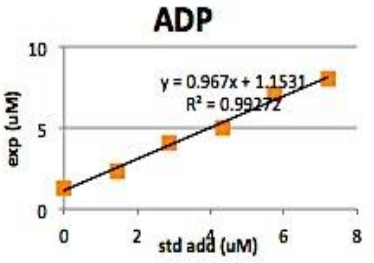

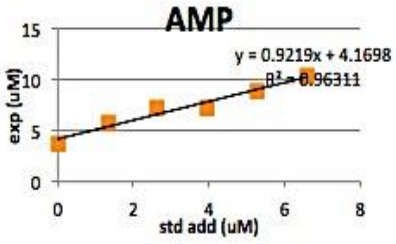

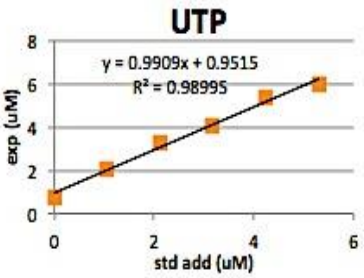

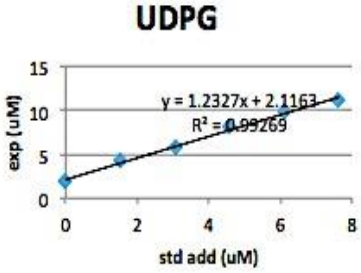

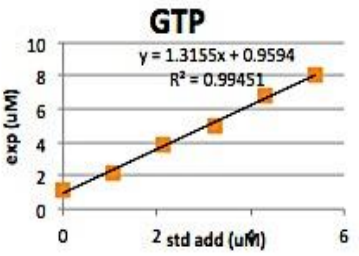

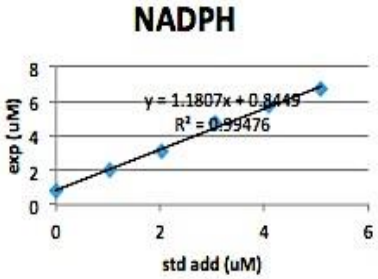

Recovery rate for sugar phosphate and organic acids